TL.114-59/05

SECRET

SPECIAL PROJECTS GROUP

Technical Report No. 267

TEST DATA REPORT FOR THE FULL SCALE 20° WING TIP SEGMENT OF THE AVROCAR

May 1959

Issued by:

Avro Aircraft Limited
Malton, Ontario, Canada.

USAF Contract
AF33(600) 37496

Written by:

D.C. Whittley
Avro Aircraft Limited

E.J. Nemeth
Avro Aircraft Limited

Approved by:

T.D. Earl
Chief Aerodynamicist
Special Projects Group
Avro Aircraft Limited.

The number of pages in this report, including Security Warning sheet, Title page, Table of Contents, List of Illustrations, and List of Symbols is 148.

I.D. No 59RDZ-2891
4298

SUMMARY

Design of the Avrocar wing tip control system was based on tests of small scale models. The twenty degree segment was designed to demonstrate the full scale characteristics of the system, it was also used to carry out development work associated with the transition control. In particular, modifications were introducted to cause the jet to deflect through 180° and adhere to the underside of the test specimen.

Effectiveness of the spoiler type control was demonstrated and small spoiler movements were shown to induce large deflections of the primary jet. Measurements were made of the discharge coefficient of the nozzle and flow patterns were observed by means of a tuft board. It was also possible to obtain an approximate measure of control characteristics.

TABLE OF CONTENTS

		Page Nos.
1.0	Introduction	1
2.0	Principles of Operation. Avrocar I	2
3.0	Description of Test Apparatus.	6
4.0	Instrumentation.	9
5.0	Test Objectives.	11
6.0	Test Procedure and Data Reduction	12
7.0	Discussion of Tests	16
8.0	Analysis of Results	29
9.0	Conclusions	32
10.0	List of Symbols	33
11.0	References	35
12.0	List of Illustration	36
	Appendix 'A' - Photographs and Illustrations	38
	Appendix 'B' - Test Data	66
	Appendix 'C' - Equations Derivations and Sample Calculations	135
	Appendix 'D' - Instrument and Rig Calibrations	140
	Appendix 'E' - Structural Integrity	142

1.0 INTRODUCTION

The Avrocar is a VTOL research aircraft of circular planform with designation VZ-9AV which is under development by Avro Aircraft Limited for the U.S. Army and Air Force.

The aircraft is powered by a ducted fan which is driven by three Continental J-69 engines acting as gas generators. The gas generators transmit power by means of a single stage turbine located at the tip of the fan. Description of the Avrocar program as a whole may be found in Ref. 1, and some of the technical details in Ref. 2. General arrangement of the aircraft is shown in Figure 1.

This report describes the results of tests on a full scale, twenty degree wing tip segment of the Avrocar. The tests form part of a development program aimed at the synthesis of a flying control system suitable for stabilization and control of the vehicle. The system utilizes various methods of jet deflection and some novel control schemes so that a description of the principles of operation is rather necessary for a proper understanding of the test results. Such descriptions are provided in section 2.0.

The tests were carried out at the Nobel Plant of Orenda Engines Ltd. Four phases of testing took place between October 1958 and January 1959 according to a prepared specification (Ref. 3) and an addendum (Ref. 4).

2.0 PRINCIPLES OF OPERATION. AVROCAR I

The fan delivers air in a symmetrical manner to the wing tip by means of radial ducts. The wing planform is circular. The problem remains to deflect the air flow at the periphery in a suitable manner to accomplish vertical take-off, transition and forward flight. Furthermore, the jet must be deflected to provide auto-stabilization and trim control. Various aspects of this problem will now be discussed in detail and this will also provide an opportunity to describe some components of the control system.

The Avrocar exhaust nozzle and control mechanism is shown in Fig.2. Some typical flow patterns are illustrated in Fig. 3.

2.1 Jet Deflection

Use is made of the "Coanda" effect to provide the primary means of jet deflection at the peripheral nozzle. The flow is biased to the upper or lower "cheek" of the nozzle by means of a mechanical spoiler which projects into the stream, furthermore some air is permitted to by-pass the spoiler and provide a small jet of air at right angles to the general flow just downstream of the spoiler, (see diagram below).

4293-802-1

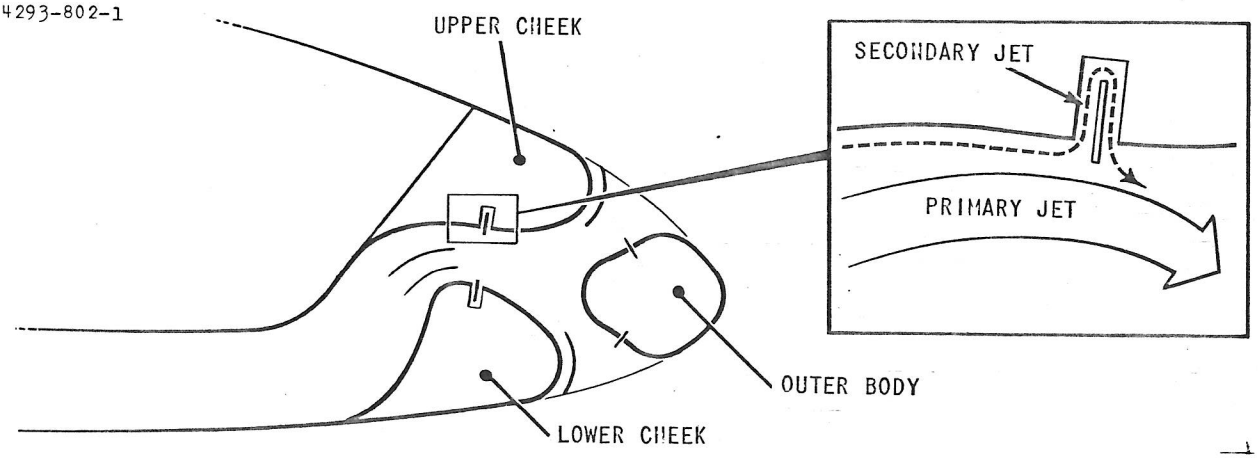

Diagram I. Schematic of Wing Tip and Spoiler

In effect, therefore, we have a combination mechanical/air jet spoiler; this scheme was developed from small scale tests and found to provide more linear characteristics than the simple mechanical spoiler.

This system was found to deflect the flow through $\pm$ 60 degrees above and below the horizontal reference. External guide vanes, the outer-body and transition control rings all help to deflect the jet beyond this amount; these components will be described in more detail later.

It should not be assumed by this that a pure 'Coanda' control is necessarily limited to $\pm$ 60°. We have found, as a general rule, that radius of "cheek" should be approximately twice the jet width and provided this radius is maintained the jet can be made

2.1 Jet Deflection (Continued)

to bend through 180°. On the Avrocar vehicle, however, in order to conform to exterior wing shape, the "cheek" contour was allowed to depart from ideal and guide vanes were substituted to assist the flow from this point onward.

2.2 Hovering Configuration

The Avrocar makes use of the so called "ground cushion" to provide thrust augmentation near the ground. The annular jet, when deflected down all the way round, produces a very strong augmentation close to the ground, but in free air, suction forces appear on the underside which cancel up to 35% of the jet reaction. These suction forces are caused by the jet entrainment of the flow trapped inside the jet curtain. Wind tunnel tests on Avrocar type models have shown, however, that if the jet is deflected through 180° at the periphery and focussed to the centre to form a "tree trunk" type of flow, then these adverse effects mostly disappear.

4294-802-1

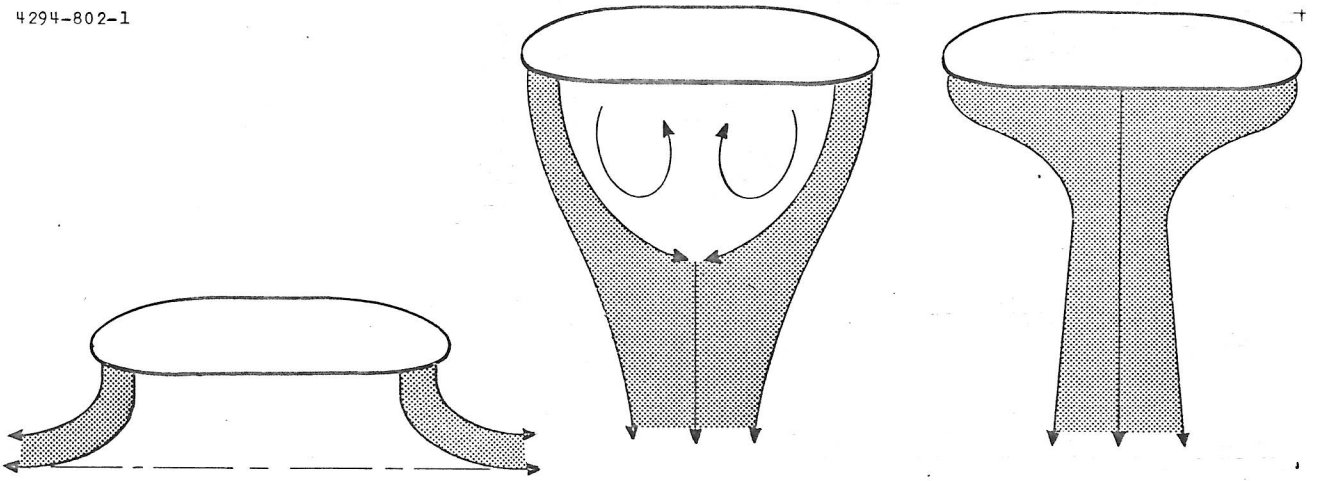

(i) Simple Peripheral Jet Close to the Ground

(ii) Simple Peripheral Jet Distant from the Ground.

(iii) "Tree Trunk" type of Flow With Jet Focussed Toward the Centre

Diagram II. Flow Patterns of Peripheral Jet.

Modifications were therefore introducted into the full scale segment test program to cope with the situation and to find a configuration which would provide the desired "tree trunk" type of flow.

Eventually it might be possible to develop a variable focus system which would provide a "jet curtain" type of flow for hovering close to the ground and also the "tree-trunk" type of flow for hovering in free air - that is, clear of the ground. Tests on both configurations therefore have significance although it is intended to employ only the "tree-trunk" type of flow for the first aircraft which in any event retains a satisfactory ground cushion.

2.2 Hovering Configuration (Continued)

While on the subject of the hovering configuration it might be worthwhile to note that movement of the peripheral nozzle spoiler should provide the desired quantity of flow for control, vertically upwards through the appropriate upper nozzle (pitch or roll) without upsetting the "tree-trunk" flow on the underside.

2.3 Transition

The following diagrams illustrate the various stages in transition from hovering to in-flight state which is here assumed to take place clear of the ground.

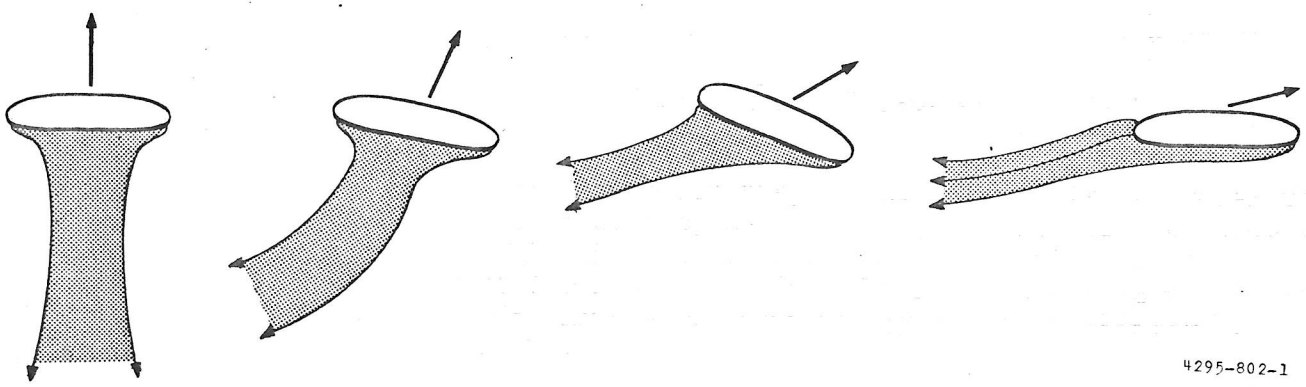

(i) Hovering (ii) Translation (iii) Early stage of transition (iv) Final stage of transition

Diagram III. Mode of Transition

Note the "tree-trunk" type of flow recommended for hovering in free air. The word translation is here used to indicate sideward motion by tilting the lift vector. In the early stages of transition a second spoiler located in the outer wing has been retracted to allow the flow to issue from the nozzle in a rearward direction. (see (iii). In the final stages of transition some gas issues from the top of the rear nozzle and goes round the outer-body to join the lower flow and form a jet flap type of flow pattern. The arrows indicate the approximate direction of jet reaction in each case.

2.4 Transition Control

To focus the jet for the hovering configuration it is necessary to prevent flow from becoming attached to the outer body, whereas for "in-flight" conditions the jet is required to flow round the outer-body, particulary at the rear. The transition control ring is therefore designed to prevent flow around the outer body. There are two schemes for this, one is an air or jet ring the other is a mechanical ring and both act as flow spoilers. The main control is referred to as "the spoiler" and so to avoid confusion the word spoiler is not

2.4 Transition Control (Continued)

used to describe these transition controls - instead they are referred to as "rings" since they cover the entire periphery of the vehicle.

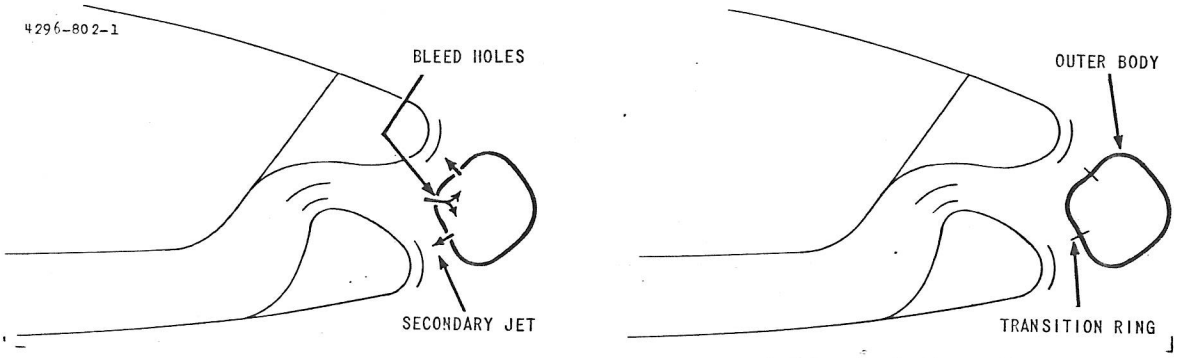

(i) Air or jet transition ring (ii) Mechanical Transition Ring

Diagram IV. Transition Control

The air or jet ring is sometimes referred to as the pneumatic transition scheme, air is bled from the main jet into the outer-body. This air then issues from the transition slot as a secondary jet and prevents the flow from becoming attached to the outer-body. The control is shut off by means of slides which cover the bleed holes.

The other system of control consists simply of a small deflection plate which may be retracted by suitable means.

2.5 Cascades and Guide Vanes

A pair of cascades is fitted in the curved duct just upstream of the control spoiler, these are fixed and simply help the flow to negotiate the bend in a smooth manner.

A guide vane is located in the passage between the outer-body and the "cheek" (both top and bottom). This passage is sometimes referred to as the outer nozzle. The guide vane covers the entire periphery and serves to augment the spoiler control, that is, under certain conditions it supplements the "Coanda" principle to permit jet deflection angles up to 180° whereas without the guide vane, deflections of only ± 60 degrees are possible with the chosen nozzle geometry.

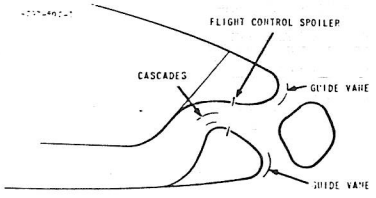

Diagram V. Cascades and Guide Vanes.

3.0 DESCRIPTION OF TEST APPARATUS

The test installation consisted of two major assemblies, the test specimen and the supply mass flow assembly. Pertinent details are evident in Fig. 4 and are elaborated on in the following paragraphs.

3.1 Test Specimen

The model was a full scale 20° segment of the Avrocar outer wing, with only minor departures from the structural features of the actual aircraft. The similarity is apparent in Fig. 5. The main differences, which were introduced to facilitate model construction consisted of the following.

1) Increased gauge metal and the use of steel rather than aluminum for the two enclosing ribs which formed the outer shell of the duct.

2) Approximation of all arcs in the plan view by straight lines.

3) Lighter gauge skin. (0.016" rather than 0.020").

4) A substitute system for operation of flight control spoiler.

5) Provision for only manual adjustment of transition control.

None of these differences were of such nature as to affect the internal or external flow characteristics significantly.

The flight control spoiler installation for the test is given in Fig. 8. A servomotor at each end of the spoiler frame moved the respective ends upward or downward, differentially or in unison through cranks. Movement of about 0.800 in. was possible from top spoiler flush with upper skin to bottom spoiler 0.25 in. below lower skin. Small adjustments to the terminal settings could be readily made.

Two modes of transition control pneumatic and mechanical, involving essentially the same principles were tested. Projections into the main stream above and below the outerbody centre line as in Figs.3 and 7 were to behave as spoilers discouraging flow from attaching to it. In the forward flight regime the transition control ring would be retracted and this would cause flow to be directed axially rearward above and below the outer body. Control is then achieved by changing the jet direction and differential mass flow. In the hovering configuration the transition control ring (mechanical or pneumatic) would extend and prevent flow attaching to the outerbody. The flow would then be directed downward or toward the centre on the under side to provide a lifting force. In this case the jet for control issues vertically upward from a sector of the peripheral nozzle.

The pneumatic system featured a continuously moveable sliding plate

3.0 DESCRIPTION OF TEST APPARATUS (Continued)

3.1 Test Specimen (Continued

to cover the rear 120° segment of peripheral recovery ports located in the outer body. In the open position, small jets of air issued from slits in the outer body to act as flow spoilers.

To minimize complications on the model, two configurations representing terminal control settings were made, with ventsblanked and open respectively. The latter is shown in Fig. 6. No intermediate openings were available, the end conditions being of immediate interest.

The mechanical system employed moveable rings in the place of the pneumatic spoiler slits, as shown in Fig. 7. Projections of 0.25, 0.5, 1.0 and 1.5 inches were tested. Again, these projections were designed to prevent flow attaching to the outer body. Each change necessitated disassembly of the outerbody and in this respect was a configuration change. In the aircraft, transition ring projections would be altered simply by means of an "on-off" switch permitting continuous control of ring position.

In addition to the above variations, outerguide vanes and inner cascades were also modified in the course of the test program. Several changes in the outer vanes were made and key configurations were included in the final test program. These are illustrated in Fig. 10. Both vane position and vane shape were subjects of study. Essentially the same inner cascades were used throughout with a $\frac{3}{4}$" trailing edge addition having a 5° droop for the later stages of the test. (see Fig. 9).

3.2 Supply Mass Flow Assembly

The total mass flow provided by the Nobel Test Establishment amounted to 15 lb./sec. at 105 psig. Since the mass flow requirements were substantially above this (a minimum of 36 lb./sec.) additional provision had to be made. A flow ejector was selected to do the job. In order that flow distribution in the model and at the total mass flow measuring station be unaffected by the ejector, certain precautions as regards length of piping and location of orifice plate had to be taken. The result was an installation of the type shown in Fig. 4 consisting the following:

1) 10" primary mass flow supply.
2) Ejector and silencer.
3) Pipe between ejector and orifice plate
4) Orifice plate
5) Pipe and transition piece between orifice plate and model.

The ejector was designed to supply the test specimen through a 16" diameter pipe with the desired mass flow. The dimensions were arrived at through the application of the momentum equation and using data of Ref. 5. No losses were included. The calculations were conservative however to ensure an adequate supply. The primary

3.0 DESCRIPTION OF TEST APPARATUS (Continued)

3.2 Supply Mass Flow Assembly (Continued)

mass flow was introduced through a Mach 2.4 Laval nozzle with 2.75" throat diameter. The secondary flow was supplied by a contoured annulus between the 16" diameter pipe and the 4.25" diameter exit from the Laval nozzle.

In order that mixing be complete and flow steady and of uniform profile at the orifice plate five sections of pipe totalling 400" were introduced.

Design for the orifice plate to British Standard Specifications was taken from Ref. 6. Both types of instrumentation called for in the specification were installed. An 80" pipe followed by a transition section of 16" diameter on one end and 8.8" x 19.6" at the model end constituted the final supply components. Again the dimensions were established on the basis of uniform steady flow requirements.

4.0 INSTRUMENTATION

The instrumentation employed for the test was concerned with the following:

1) Surface and duct pressures and mass flow measurements.
2) Study of exit flow patterns
3) Movement of control spoiler
4) Regulation of primary mass flow.
5) Photographic records
6) Calibration of instrumentation.

4.1 Surface and Duct Pressure Mass Flow Measurements

A general assembly showing the model pressure stations is given in Fig. 11. Only the numbered stations were actually available. Better views of the outer nozzle pitot and static rakes are given in Figs. 13 and 14. Both the top and bottom nozzle rakes had the same pressure station spacing. The spoiler station rake shown in the general assembly of the instrumentation was replaced by the rake in Fig. 15.

The 16 tube static rake yawmeter assemblies were not employed extensively since no substantial flow angularity was observed and since the sensitivity of the yawmeter to yaw was very small as evident in Fig. 23.

A British Standard orifice plate was used for total mass flow evaluation and is described in Ref. 6. The orifice diameter was 12.4". Both corner taps and D & D/2 taps were included as called for in Ref. 6.

All pressure taps were connected to manometers in the control room. An illustration of the control room layout is given in Fig. 16 and a photograph of the instrumented model is available in Fig. 12. The total of 140 tubes were connected to 12 banks of manometers. These used blue King Fluid with a specific gravity of 1,000,which is particularly well suited for photographing. The differential and upstream pressures for both types of orifice tappings were recorded on individual U tube manometers. The differentials used Meriam 2.95 and the upstream used Mercury.

4.2 Flow Visualization

A wool tufted board shown in Fig. 19 was used for the study of exit flow patterns. Due to the model support structure, tufting of all of the interesting regions was not possible.

4.3 Control Spoiler Instrumentation

The control spoilers were actuated by two electric motors one at each end; similarly, spoiler displacement was sensed by two linear motion potentiometers. The spoiler was actuated by means of two switches located on a panel in the control room. A schematic

4.0 INSTRUMENTATION (Continued)

4.3 Control Spoiler Instrumentation

of the electrical system is given in Fig. 18. It will be observed that limit switches were installed to prevent the control crank from passing top and bottom dead centres. It is also evident that the system resistance has been adjusted to give a full scale reading on the ammeter for the maximum spoiler movement of 0.85" - this enabled spoiler position to be determined very accurately.

4.4 Primary Mass Flow Regulation

The primary mass flow as supplied by five compressors pumping into a collecting gallery. Compressors could be added one at a time to suit the mass flow requirement. Each compressor had four operating levels corresponding to 1/4, 1/2, 3/4 and full capacity. No intermediate adjustment on the compressors themselves was possible. To select intermediate mass flows a servo controlled vernier exhaust bypass was used. A series of 5 orifice plates for mass flow measurement were available, different diameters corresponding to different mass flows to increase sensitivity. These could be selected from the test area through the medium of a servo motor. As far as the test personnel were concerned mass flow was adjustable by finger tip control.

4.5 Photographic Records

Due to the multiplicity of pressure readings, cameras were employed to record the data. Three Bell and Howell Eyemo cameras were installed in the control room as in Fig. 16 to photograph the manometer board. Each was equipped with a relay and motor, for automatic film advance by means of three switches on the control console shown on Fig. 17. The wiring diagram is shown in Fig. 18. The wool tuft photos were taken by means of a Kodak Retina 35 mm. camera.

4.6 Calibration of Instrumentation

See Appendix 'D' for calibration of:

1. Mass flow
2. Yawmeter
3. Control spoiler.

5.0 TEST OBJECTIVES

The primary objectives of the test series may be summarized as follows:

1. Demonstrate feasibility of full scale "Coanda" jet deflection scheme.

2. Demonstrate structural integrity of wing tip segment manufactured from very thin gauge aluminum sheet.

3. Investigate characteristics of spoiler type control scheme.

Secondary objectives, equally important but of a more detailed nature, may be listed as follows:

(a) Evaluation of discharge coefficient of exhaust nozzle

(b) Measurement of pressure loss in duct and nozzle.

(c) To introduce modifications designed to increase jet deflection to 180°. This would correspond to the "tree-trunk" flow pattern on the full scale aircraft as described in section 2.0.

(d) Elimination of flow spillage from upper nozzle with control spoiler in fully down position.

(e) To study both internal and external flow behaviour.

(f) To study affect of end plates on flow characteristics.

(g) To investigate other problems which may arise in the course of testing.

6.0 TEST PROCEDURE AND DATA REDUCTION

6.1 Test Procedure

The rig was set up exactly as described in the specification. - Mass flow controls, spoiler position controls and manometer boards were all located in an enclosure about 25 ft. from the test specimen. Test procedure was similar to that outlined in the specifications (Refs. 3 and 4) except that only pressure ratios of 1.04 and 1.06 were used. The latter value corresponds closely to the sea level design value for hovering flight. Photographic records were taken of flow patterns and pressure data for all configurations and in most cases data were recorded at thirteen different spoiler positions. The fully up position was with upper spoiler slightly retracted below skin. The fully down posiition was with lower spoiler retracted about 0.25". Total spoiler movement was in the order of 0.80". At intermediate control settings, (1, 3, 5 etc.) key pressure data was taken by hand as a precaution against photographic failure. Information such as pressures for mass flow evaluation, upstream total pressures, ammeter readings were taken by hand for all control settings. At the termination of each test a re-run was made for the purpose of photographing the tuft board. A list of the tests and description of the various configurations tested is available in the test logs of Appendix 'B'.

Four periods of testing amounting to about 4 weeks in all were carried out from October 1958 to January 1959. The first two periods covering two weeks involved configurations A to J with no intermediate tests. The final two periods were spent on cursory studies aimed at development of suitable configurations and on testing tentatively acceptable configurations K to X. Development was generally carried out during day shifts with small quantities of air, whereas testing of accepted configurations was done during evening because of the availability of greater air supply. Normally only two complete control runs could be made per shift owing to time lost during configuration changes. The typical control run had a duration of about 1 hr. including tuft photographs. The actual hours and conditions of operation are listed in the test log. A total of about 20 hours was logged for the specimen.

6.2 Data Reduction

Owing to instrumentation limitations, some of the objectives outlined in AVRO/SPG/TR 182/1 were forced to play a subordinate role in the overall study particulary those involving force measurement through surface pressure and duct momentum flux integrations. It is generally agreed that force measurement by means of a balance system would have been of considerable advantage had the installation been simply feasible.

6.0 TEST PROCEDURE AND DATA REDUCTION (Continued)

6.2 Data Reduction (Continued)

Some of the deficiencies of the available instrumentation are listed as follows:

1) Probes located at the model centre line only could not account for transverse non-uniformities in the flow. (Boundary layer irregularity, central rib and support posts effects, etc.)

2) Flow directions required to obtain force through momentum flux evaluation were not exactly known. At the outer nozzle stations, it was only for a few of the runs that the flow direction was sufficiently well known to give an idea of the model forces.

3) Due to limited facilities pressure stations were too sparse. Cascades, spoilers and exit guide vanes did not contain any surface pressure probes.

In view of these difficulties it was not possible to accurately determine the total reactive force nor, therefore, could the thrust efficiency be found. It was however considered worthwhile to evaluate the reactive force normal the axis of nozzle, that is, the control force. This was done for certain simple configurations.

Methods of data reduction for each of the significient parameters are now described one by one.

6.2.1 Control Force

The control force is the component normal to the airplane longitudinal axis. For cases without outer nozzle cascades and small transition spoiler projections surface pressure integration on the cheeks and outer-body proved sufficiently reliable to allow some interesting observations regarding control characteristics. Methods of data reduction may be found in Appendix 'C' and results of calculation are shown in Fig. 53.

6.2.2 Total Mass Flow

The data from the two sets of instrumentation did not concur. Since D and D/2 taps are in first place more susceptible to flow irregularities and further were not considered as good an installation as the corner taps.

6.2.3 Pressure Loss in Ducts

The pressure loss between the upstream and control spoiler

6.0 TEST PROCEDURE AND DATA REDUCTION (Continued)

6.2.3 Pressure Loss in Ducts (Continued)

Stations was evaluated without difficulty as shown in Appendix 'C'. Results of calculation are given in Figs. 69-76.

6.2.4 Effective Exhaust Area and Discharge Coefficient

Evaluation of these parameters entailed the least difficulty since the upstream flow distribution was quite uniform and since mass flows were readily available. The method outlined in the specification and on page 138 was employed.

6.2.5 Control and Differential Mass Flows

Mass flow through upper and lower nozzles (otherwise known as control mass flow) were calculated by performing a duct integration at the respective stations. The differential mass flow is simply the arithmetic difference between these two. These data were introduced as a supplement to force measurements and were intended to show such things as control characteristics, spillover and flow entrainment. The entrainment data was not entirely reliable however since the order of magnitude was small and was obtained by differences between large quantities. Further, exit instrumentation was not extensive enough to provide a clear picture of the flow. Modes of calculation of these parameters are presented on page 139.

6.2.6 Flow Visualization

The wool tuft board gave a fairly satisfactory indication of the general flow picture. Its usefulness was however limited in certain cases where the jet flow was deflected through 180° since supporting structure prevented location of the board in a satisfactory position. A typical flow pattern is shown in Fig. 19.

6.3 Test Parameters

For sake of completeness the test variables are listed below:

1) Nozzle pressure ratio.
2) Control spoiler position.
3) Pneumatic transition spoiler recovery vent opening.
4) Mechanical transition spoiler projections.
5) Outer nozzle guide vane position and configuration.
6) Inner duct cascade configuration.
7) Outer-body configuration.

The basic dependent test variables were:

1) Mass flow

6.3 Test Parameters (Continued)

2) Test specimen duct upstream total and static pressure distribution.
3) Spoiler station total and static pressure distributions.
4) Upper and lower nozzle total and static pressure distributions.
5) Model interior and exterior surface pressure distributions.
6) Exterior flow patterns.

Most of these variables are presented in their original form. However to aid in the study of control characteristics, other forms have also been employed and are listed as follows:

1) Section control force.
2) Section control mass flow.
3) Section differential mass flow.
4) Pressure loss coefficient.
5) Discharge coefficient.

Details of calculation for the above variables along with calculations of additional variables which were considered are covered in Appendix C.

7.0 DISCUSSION OF TESTS

The tests were conducted in four phases, each lasting approximately one week. The first phase was exploratory in nature and following this the time between each test phase was used to 'digest' some of the data and make minor modifications to the test specimen. More time was therefore spent on development than on straight evaluation and for this reason the test program departed in some minor aspects from specification. Each modification, however, revealed new problems and much useful information was obtained concerning the characteristics and limitations of this new type of jet deflection control scheme.

In all 36 runs were made and are described in tabulated form in the test log. (See Appendix 'B')

Before commencement of the test series proper some exploratory tests were conducted to prove the mechanical and structural integrity of the test specimen. The specimen was subjected to a nozzle pressure of 30 in. of water (pressure ratio 1.07) and the thin skin aluminum structure of which it was made showed no signs of failure. In the experience at Avro Aircraft this also gave the first opportunity to demonstrate a full scale jet control scheme based on the 'Coanda' principle - the jet responded nicely to small spoiler movements and it was possible to deflect the jet through $\pm$ 60 degrees.

The nozzle is required to operate in a satisfactory manner in two separate ways. First, in a hovering configuration with transition ring operative, secondly in forward flight with the transition device inoperative or retracted. Development was therefore directed toward a configuration which would satisfy both these demands.

7.1 Phase I - Runs 'A' - 'D'

The purpose of this phase was to determine the characteristics of the test specimen with outer nozzle guide vanes removed; also to use the results to check data reduction techniques so that the most benefit could be obtained from future tests.

7.1.1 Runs 'A' & 'B' (Pressure Ratio 1.04 & 1.06)

The 'in-flight' configuration (runs A & B) exhibited flow deflection angles of $\pm$ 60° relative to the horizontal. It was possible to make the jet sweep the tuft board (see Fig. 19) at any desired angle. In most cases the jet from the upper and lower nozzles flowed round the outer-body to form a single jet although the outer-body formed a strong wake in the flow. The exception to this was for spoiler position close to either extreme when one portion of the jet was much stronger than the other - in such cases there was no tendency for the two jets to coalesce. It must be remembered, however, that the 'in-flight' configuration is not simulated correctly at zero

7.0 DISCUSSION OF TESTS (Continued)

7.1.1 Runs 'A' & 'B' (Pressure Ratio 1.04 & 1.06) (Continued)

forward speed and wind tunnel tests suggest that the jet has a greater tendency to colesce in forward flight. As an in-flight configuration this could then be considered fairly satisfactory. Problems of linearity and control sensitivity will be dealt with in more detail later. (see section 8.0).

7.1.2 Runs C & D (Pressure ratio 1.04 and 1.06)

Runs C & D were then designed to investigate the hovering configuration using the so called pneumatic transition ring. Air is bled from the main jet into the outer-body and then issues from the transition slots; the purpose of this secondary jet is to prevent jet flow from becoming attached to the outer-body.

The system functioned with only partial sucess. Location of bleed holes were such that with spoiler control in extreme positions (up or down) the jet flow missed the bleed holes in the outer-body altogether and consequently there was then no secondary jet flow through the transition slots. For these terminal spoiler psitions, the nozzle operated exactly as in runs A & B with deflections of plus or minus 60 degrees and there was no added incentive for the flow to deflect beyond this. (It will be recalled that the main purpose of the transition control is to provide an overall deflection of the jet of at least 90° to form a flow pattern which gives good ground cushion augmentation).

A small movement of the control from the terminal setting could cause air to strike the bleed holes and provide a secondary jet from the transition ring. Flow direction would then change from say, + 60° to +90°. Upon further movement of the control the jet would gradually transfer from the lower to the upper nozzle and issue in an almost vertical direction. (This provides moment control without sideward force which is also a desirable criterion). Finally the primary jet would miss the bleed holes and the jet would change from -90° to -60° giving once more a final state similar to runs A or B. This final change in direction of the jet corresponds to a condition of control reversal and could not be considered satisfactory.

Operation of the spoiler established two types of flow pattern which were to be the constant aim throughout the test series which followed. For 'in-flight' configurations it was required that control be derived by deflection of the jet as a whole - that is, it is expected to coalesce behind the outer-body and take up some desired deflection angle. For hovering configurations it was required that control be obtained by exchange of mass flow, that is, upon application of the control from the fully down position, part of the jet must issue from the top nozzle in a near vertical direction.

7.0 DISCUSSION OF TESTS (Continued)

7.1.2 Runs C & D (Pressure Ratio 1.04 and 1.06)

Whereas runs A & B proved fairly satisfactory as an in-flight configuration, runs C & D were not so successful. As a pair, for both in-flight and hovering, they were therefore considered unacceptable. It would no doubt have been possible to modify the bleed vents to improve characteristics but it was decided that a mechanical transition ring would be more effective and lend itself more easily to development. Subsequent tests were then all directed toward development of a mechanical system.

One further problem arose. It was noticed that, with spoiler in the fully down position (lower spoiler approximately 0.25 in. below skin surface) some of the jet continued to issue from the upper nozzle. This residual flow we termed 'spill-over'.

Two objectives for future tests were then to increase flow deflection angle in the hovering configuration and to reduce 'spill-over'.

7.1.3 Data Reduction For Runs A to D

Results obtained were then analysed fairly extensively to check data reduction techniques. In general it was concluded that discharge coefficients and duct pressure loss could be determined quite accurately. Mass flow from upper and lower nozzles, although only based on one set of probes on the centre line, provided very useful information. Similarly, the differential mass flow could often be used as an approximate measure of control power. Patterns from the tuft board gave a visual picture of flow characteristics but were not always very clear-cut or precise. Surface pressures gave an insight into the internal and external behaviour of the flow.

It was also realized that surface pressure integrations could not provide an accurate value of the jet reaction - for the same reason it was not possible to evaluate nozzle efficiency.

Further details of data reduction and test results for runs A to D may be found in section 8.0.

7.2 Phase II, Runs E to J

This series of tests was designed to evaluate the mechanical transition ring. The bleed holes in the outer-body were no longer required and the transition ring took the form of a plate which projected into the flow. Plates were made to represent projections of 0.5, 1.0 and 1.5 ins.

It was already known that flow deflection angles of 120° (jet toed in 30° or partly focussed) gave a better ground cushion than flow deflection angles of 90° (jet curtain, flow

7.0 DISCUSSION OF TESTS (Continued)

7.2 Phase II, Runs E to J (Continued)

vertically downward). Furthermore, tunnel tests were beginning to show that it might be more desirable to completely focus the peripheral jet to form a flow pattern resembling a tree trunk. This has already been described in section 2.0 and would correspond to a flow deflection angle of approximately 180°. Since the 'in-flight' configuration was satisfactory without guide vanes it was hoped that the required flow deflection could be obtained in the hovering configuration simply by addition of the mechanical transition ring.

7.2.1 Runs E and F

Runs E and F represented the hovering configuration without guide vanes with $\frac{1}{2}$ and 1 inch transition rings respectively. Both showed similar characteristics. Flow deflection angle for full control was approximately 90° (up or down) and so although we had gained 30° compared to the previous tests we had not caused the jet to attach fully to the bend.

Other points to note were as follows: There was an appreciable amount of 'spill-over' for cases of full control. Also, this residual flow was deflected through 150° to 180° and it was noticed that this flow formed a narrow stream close to the outer-body and was deflected backwards by the transition ring projection. This flow pattern was associated with full control only and did not persist, for, as soon as control spoiler began to move, the flow straightened out giving overall flow deflection angles of approximately 90°. The important thing to note here, is that the residual flow did not deflect through 180° by virtue of the 'Coanda' effect but was simply deflected off the transition ring. As such, therefore, it did not give a clue to means of further development.

7.2.2 Runs G & H

It was realized that the transition ring alone was not enough to deflect the jet inward in the hovering case. Run G, therefore, had a half inch transition ring projection, plus the guide vanes located in the outer nozzle. This gave deflection angles of about 115° (jet toed in 25° on underside) and quite nice response to spoiler movement. In most cases the jet issued vertically from the upper jet as control was applied. Only in the fully down spoiler position did the upper jet depart from this position and then only for the residual flow which bent fully back (180° deflection) in a manner already described in the previous paragraph. In general it could be considered reasonably satisfactory if one were prepared to accept 25° tow-in for the hovering condition. We were therefore interested in studying the characteristics of this same case

7.0 DISCUSSION OF TESTS (Continued)

7.2.2 Runs G & H (Continued

with transition ring projection retracted - this became run H.

Run H was then an 'in-flight' case. With spoiler position fully down the jet deflection angle was approximately 105°, and with control fully up the jet issued vertically upwards (or at -90°). Application of control made the jet sweep the tuft board and it was possible to select almost any desired jet deflection angle between full control limits. In other words, we had shown that the presence of the guide vanes in the outer nozzles did not prevent the jet from flowing round the outer-body and re-uniting behind it. Once again, this flow pattern could not be considered perfect but some improvement, particularly in linearity, can be expected with external flow present. (see also comments in para. 7.1.1).

7.2.3 Runs I & J

A futher attempt was made to deflect the jet through 180° without guide vanes in the outer nozzles; this time with transition ring projections of $1\frac{1}{2}$ ins. (run I). Full control, however, only gave 90° deflection up or down. In the neutral spoiler position the jet from both upper and lower nozzles were deflected through approximately 135°. In addition to this there was a fair amount of 'over-spill' at full control. Altogether, therefore, it was not a very desirable configuration. Run J, the last test in this phase, was with outer-body and cascades removed. The purpose of the test was to determine the characteristics of the jet bending device without any external forms. The jet was seen to respond very nicely to spoiler movement over a range of $\pm$ 60 degrees.

7.3 Phase III - Runs K to P

Structural failure of the lower guide vane during run H prevented further tests using the vane at that time. (see also Appendix E) A short break in the program permitted repairs to be made and tests were resumed on December 17, 1958. The main objective for this phase was to find a configuration which gave a full 180° deflection. Also it was desired to keep 'over-spill' to a minimum and if possible, eliminate it.

There were three proposals for bending the jet:

1. Extension and droop of the cascades located upstream of the control spoiler. It was hoped that this would bias the whole flow downward.

2. Re-location of the guide vane in the lower outer nozzle. There were two ideas here, firstly to move the guide

7.0 DISCUSSION OF TESTS (Continued)

7.3 Phase III - Runs K to P (Continued)

2. vane bodily outward and increase the proportion of flow deflected by the vane, secondly to slightly rotate the guide vane to form a contracting passage between guide vane and lower 'cheek'.

3. To eliminate the possibility of flow breakaway at the leading edge of the guide vane by adding a rounded leading edge.

7.3.1 Run K

The cascades were extended 3/4 in. and this extension was drooped five degrees. The guide vane was kept in its original position since it was desireable to study the effect of one change at a time. The half-inch transition ring projection was installed in order to simulate the hovering condition.

With control spoiler in the fully down position, the jet deflection was approximately 140°. This was more than in any previous test but fell short of the immediate objective, to obtain fully attached flow. There was an indication that the jet was slightly divided by wake from the guide vane and this led to the conclusion that modification to the vane might prevent this and lead to still further improvement. It was also considered that if the inner flow (that is, the flow between the cascade and 'cheek') could be made to adhere then the outer flow would also follow.

7.3.2 Runs L and M

With the foregoing results in mind it was decided to reposition the guide vane. It was rotated about a point approximately one inch from the trailing edge and the gap between leading edge of vane and lower 'cheek' was increased by 0.3 in. All else remained the same.

In this case the guide vane definitely caused the flow to divide, the inner flow turned through about 170°, the outer flow through about 130°. The fact that the inner flow did not adhere fully to the lower 'cheek' suggested that a thick boundary layer might be forming on the inner skin. Subsequent investigation using pressure probes located just downstream of the control spoiler proved this assumption to be incorrect.

At this point it was considered that much could be learned concerning the requirements for flow attachment and optimum setting of guide vane by removing the outer-body altogether. This was done and the configuration arranged otherwise as 'L'. Flow break-away occurred at the leading edge of guide vane which resulted in a sharp division of the jet. The inner flow was exactly as described in the previous paragraph (run L) with de-

7.0 DISCUSSION OF TESTS (Continued)

7.3.2 Runs L and M (Continued)

flection angle of about 170°. It was then noticed that addition of quite small end plates caused the inner flow to adhere completely to the lower 'cheek' and underside of the test specimen. There existed a considerable in-flow towards the jet and this tended to prevent complete attachment of the inner jet - it was sufficient only to hold one's hand flat against the side of the specimen to cause the jet to attach to the skin. On the aircraft there will be no such abrupt end of the jet to cause these edge effects and consequently small end plates were installed on the specimen for all subsequent tests.

The guide vane was then returned to its original position in an attempt to eliminate the flow separation and division of flow. It did just this but now, although the flow was united into a single jet, the deflection angle was only about 135°.

The next most logical step was then to rotate the guide vane (as for run 'L') to cause the inner flow to adhere and add a rounded leading edge to prevent leading edge separation and flow division. This was done but the jet deflection angle was only about 140°, however, the jet did not divide (remember that the outer-body was not installed). The test was, however, sufficiently encouraging to suggest that with outer-body on, complete with transition ring projection and end plates, full deflection might be achieved. This became run 'M'.

Before replacing the outer-body however, further ad hoc tests were carried out. A strip of aluminum was hand held or clipped to simulate a leading edge extension to the guide vane. Similarly, an extension to the trailing edge of vane was simulated. It was found that, whereas both modifications caused the jet to adhere completely to the underside of the specimen, much smaller extensions were required at the trailing edge than at the leading edge. This proved to be very significant in our search for a configuration to bend the jet through 180° and cause it to adhere to the underside of the vehicle.

As mentioned already, run M was simply a repeat of run L with rounded leading edge on the guide vane and with small end plates added. It however showed little change to the characteristics described for the similar case without outer-body, that is, flow deflection angle of about 140°, jet not divided. Apparently, presence of the outer-body and transition ring projection, is not very effective as a primary means of turning the flow.

7.3.3 Runs N and O

Preliminary tests had already suggested that a small extension to the guide vane would cause the jet to adhere to the underside of the test specimen (see para 7.3.2). Configuration for run 'N' was then as follows:

7.0 DISCUSSION OF TEST (Continued)

7.3.3 Runs N and O (Continued)

Guide vanes in original position
3/4 in. extension to trailing edge of guide vane
1/2 in. transition ring projection.
End plates fitted.

The guide vane extension was made of flat aluminum plate clamped and bolted to the existing vane. At first it did not give the required result. The plate was then deflected inward (the part extending beyond existing vane remained straight) to follow more closely the contour of the lower 'cheek'. This achieved the desired result and with the spoiler in the fully down position the jet adhered completely to the surface to give the required deflection of 180°. Flow from both sides of the guide vane joined solidly to form one jet with no apparent wake.

Modification was made to the lower guide vane only and so application of control from the fully down position caused flow to issue vertically from the upper nozzle as before. When the spoiler began to project from the lower surface of the nozzle the jet on the underside became detached. Exchange of mass flow continued until, with control in fully up position, most of the jet issued vertically from the upper nozzle. We had therefore found a case which could form the basis of a hovering configuration. It was now necessary to investigate its characteristics with the transition ring retracted.

Run 'O' was then an in-flight case, exactly as run N except that the 1/2 in. projection was removed from the outer-body. With spoiler fully down deflection angle was about 150° with a slight wake noticable between the two flows. Spill-over from the upper nozzle had been elimated. Upon application of control, from the fully down position, first the jet detached from the lower cheekand adhered to the outer-body. At neutral control the jet divided round the outer-body and re-united to give jet deflection angle of zero. Further application of control followed patterns similar to other in-flight configurations with most of the jet issuing vertically upward. (There was always some "over-spill" from the lower nozzle for full up control). The rounded leading edge was removed from the guide vane and the vane returned to its original position. A check run with fully down spoiler position showed that the flow did not attach even though end plates and guide vane extension were included. It was in effect, a repeat of run 'K' with these two additions.

7.3.4 Run P

It was still desirable to achieve fully attached flow with as few modifications as possible to the existing design and so a final attempt was therefore made to manage without an addition to the leading edge of guide vane, this time with the vane once more in the 'new' location. There was also a secondary purpose in mind;

7.0 DISCUSSION OF TEST (Continued)

7.3.4 Run P (Continued)

the rounded leading edge as tested (e.g. run 'N') involved also an extension of the vane. It was felt that any leading edge extension of the vane would be detrimental to smooth control action for the in-flight case when the flow is required to by-pass the vane and flow round the outer-body. For these reasons, then, the guide vane without rounded leading edge was repositioned to provide a contracting flow passage (as e.g. run 'L') and testing was resumed. The test was quite successful, flow completely adhered to the underside of the test specimen and control characteristics were similar, to run 'N'. There was however still an appreciable amount of spill-over in the fully down spoiler position. Time did not, permit this run to be checked for in-flight characteristics and it became the final test of the Phase III program.

In view of the importance of this final test, the configuration is described once more as follows:

1. Extension and droop of the cascades located upstream of the control spoiler.

2. Re-location of guide vane in lower, outer nozzle to form a contracting passage for the flow captured by the vane.

3. 3/4 in. extension to trailing edge of guide vane in lower nozzle.

4. 1/2 in. transition ring extension.

In the light of these tests, and particularly considering run P and the corresponding run with guide vane in the original setting, we were now quite convinced that it was essential to cant the guide vane outward to obtain fully attached flow. This conviction, was however, proved to be incorrect by the final phase of tests.

7.4 Phase IV - Runs Q to X

Although primary objectives had been achieved some problems still remained. For example spill-over had not been eliminated in the hovering configuration. We were, however, quite confident that a 1/4 in. extension of the transition ring would be sufficient to prevent attachment of flow to the outer-body and also that this modification would reduce spill from the upper nozzle. Again, although the flow had been made to adhere fully to the underside of nozzle segment, three modifications were required to do this: namely, extension of internal cascades, re-location of guide vane in lower outer nozzle and extension of trailing edge of this guide vane. The purpose of Phase IV tests was to investigate these matters and testing re-commenced on 5 January 1959.

7.0 DISCUSSION OF TEST (Continued)

7.4.1 Run "Q"

This test was carried out to finish off the Phase III test program, that is, it was the 'in-flight' counterpart of run P with transition ring projection removed. At full down control the jet deflection angle was roughly 130° with a definite tendency for the flow to be separated by the guide vane into two separate jets. Spill from the upper nozzle was negligible, otherwise the configuration operated in ways typical of other in-flight cases.

First attempt at reducing the number of modifications required was to revert the guide vane in the lower nozzle to its original position. To compensate for this, the trailing edge extension to the guide vane was increased from 3/4 in. to 1 in., furthermore it was curved to follow the same contour as the guide vane itself. The vane was then 1.25 in. from the surface of the lower 'cheek' at all points.

With full down control the jet deflection was only about 140° and the flow was very stable. Attempts were made to deflect the flow further by means of hand held deflector plates but the jet remained firmly in its position.

The guide vane extension was then modified to give more of a curl at the trailing edge. This brought the trailing edge to within 1.10 in. of the lower 'cheek' surface (compared to 1.25 in. at the leading edge) and provided quite a change in the trailing edge angle as well as a convergent passage for the flow. Once again success was achieved; the jet completely adhered to the underside of the model. Spill from the upper nozzle was reduced slightly and control characteristics were similar to other hovering configurations with maximum jet deflection of 180°. Such cases have an inherent discontinuity when the flow detaches from the underside; on the aircraft with a complete peripheral jet this effect would not, however, be so pronounced because of the circular shape of the jet in planform.

Run S was a repeat of this previous configuration with 1/2 in. transition ring projection replaced with projections of only 1/4 in. As expected, the flow characteristics were unchanged except that now spill from the upper nozzle had been still further reduced, this time to almost negligible proportions.

7.4.3 Run T

The extension to the ccascades upstream of the control spoiler (first introduced for run 'K') were then removed. This was again with the object of reducing modifications to a minimum. Further it was realized that the presence of the outer portion of the outer-body made little or no difference when fitted with transition ring projections. This was particularly true of the full down control case and since this component required almost an hour

7.0 DISCUSSION OF TEST (Continued)

7.4.3 Run T (Continued)

to instal it was left off for these exploratory tests.

To recapitulate, the configuration for run T was as follows:

1. Lower nozzle guide vane in original location.
2. 1 in. contoured extension of guide vane.
3. Extension to cascades removed.
4. 1/4 in. transition ring projection.
5. Outer part of outer-body removed. The presence or otherwise of this component made no difference to the results.

Flow characteristics were identical to run S so now we had reduced the required modifications from three to one. Only the extension of the guide vanes was required to permit flow to adhere to the underside of the model provided this extension was of the correct shape. Spill from the upper nozzle was again small and all that remained was to study the characteristics of this configuration more fully and check the in-flight characteristics (see run V).

Without a new designation some further development tests were then made. First the lower transition ring projection was removed, this left a sharp edge to which the flow could hardly adhere and once again the configuration performed equally well, with or without transition ring projection.

This led to consideration of a possible shape of outer-body which would not require a transition control at all. One possible shape is shown in Fig. 27 in which the upper flow would be free to flow round the outer-body for the in-flight case. The sharp edge at the bottom is sufficient to prevent attachment of flow in the hovering case. Transition would then be taken care of entirely by means of the collective jet control. It was not possible to test this configuration but it might form a basis for future development.

Once more with a view to simplification, the curved extension to lower guide vane was replaced by a straight one, it extended one inch beyond the existing vane and was bent in towards the lower 'cheek' to give approximately the same type of contracting passage. The idea here was to try and determine whether the important parameter to achieve fully attached flow was the contracting passage or the trailing edge angle of the vane.

The flow did not attach and we concluded that the fairly severe curl at the end of the previous vane extension was essential if we were to obtain the required flow pattern.

7.0 DISCUSSION OF TEST (Continued)

7.4.4 Runs U, V and W.

In the hovering condition it was considered essential to maintain fully attached flow and yet obtain a reasonable amount of control from the upper nozzle for control purposes. Configurations with the outer portion of outer-body removed and without transition ring projection were poor in this respect. It was thought that addition of a small rounded leading edge which did not involve an appreciable extension might be beneficial in this respect. A small 0.125 in. radius was added to the specimen which was in other respects as detailed in paragraph 7.4.3 (run T) except that item (4) the transition ring projection was missing. No significant improvement in characteristics was noticeable.

Run V was, as mentioned already, the in-flight counterpart of run T. The outer-body was of course replaced for this run and there were no projections. It represented one of the more successful in-flight configurations, flow deflection angles range from about + 80° (full down control) to about -60° (full up control).

Run W was simply a repeat of run T with outer part of outer-body in place. This was a check to make sure that our assumption that this component made no difference was in fact true. Also the opportunity was taken to run the test at the higher pressure ratio (25 in. of water). The test was quite satisfactory and control characteristics may be found in figure 38.

The small end plates were removed and the flow became quite ragged and did not fully adhere at the edges. This was merely a confirmation of our previous findings.

7.4.5 Run X

A configuration had now been found which satisfied most of the required characteristics. A small amount of test time was still available and so a final attempt was made to obtain more air from the upper nozzle for control before the flow separated from the underside of the model. We felt that, if the cascade captured more air the jet would have a greater tendency to hold to the underside and so the guide vane was repositioned to increase the flow passage by 0.3 in. The test was then as run T except for the new position of the guide vane. The flow fully adhered to the underside of the model for full down control and did provide some increase in the control flow available before separation took place. As such, it provided useful information but time did not permit further evaluation.

Finally, the transition ring projection was removed and since the outer part of outer-body was also missing, this also represented a hovering configuration and was of the form found to be most sensitive to flow separation from the underside of model.

7.0 DISCUSSION OF TEST (Continued)

7.4.5 Run X (Continued)

The flow tended to be slightly unsteady for fully down spoiler position, the jet was found, however, to attach fully to the underside. Upon application of spoiler control the jet separated from the underside fairly soon. This test represented a configuration similar to one proposed earlier (see Fig. 27) which would not need a separate transition control and in view of this tendency to separate it was found to require further development.

Testing was terminated on Thursday, January 8, 1959.

8.0 ANALYSIS OF RESULTS

Results have been presented in Fig. 28 - 93. These contain data relating to the subjects listed below which shall be discussed in turn in the paragraphs which follow:

1.	Differential mass flow	Figs. 28 - 39
2.	Upper & lower nozzle mass flow	Figs. 40 - 52
3.	Control force	Fig. 53
4.	Pressure Distribution	Figs. 54 - 60
5.	Discharge coefficient	Figs. 61 - 68
6.	Pressure loss coefficient	Figs. 69 - 76
7.	Flow distribution	Figs. 77 - 93

8.1 Differential Mass Flow

Differential mass flow is defined as the difference between flow from upper and lower nozzles and it provides an approximate measure of control power for hovering configurations. It has already been explained that, for most cases, we were unable to obtain an accurate measure of control force by pressure integration and consequently the differential mass flow became of considerable interest.

Data from most of the runs are presented in Figs. 28 - 39 and it can be seen that they all form a similar pattern. Variation of control power with spoiler position is not linear but follows more closely a sinusoidal shape. In the absence of external flow we cannot expect differential mass flow for the in-flight configuration to give an accurate measure of control power, and care must be taken in interpretation. For the hovering configurations we are mostly concerned with the characteristics of control with the spoiler close to the bottom of its travel. This means we are concerned primarily with the lower right hand portion of these curves.

Individual cases may be studied at will, we are however, particularly interested in configuration 'T' which represents our final choice. In this case, with spoiler in the fully down position the jet adheres to the underside of the aircraft to form the so-called 'tree-trunk' flow pattern. It is desireable that movement of the peripheral nozzle spoiler should provide the required quantity of flow through the upper nozzle without upsetting the 'tree-trunk' flow pattern on the underside. As the spoiler moves up a position is reached at which the jet detaches from the underside. The amount of control corresponding to this point was investigated for run 'X' (see Figs. 39 & 93) and particular note was made of the spoiler position. It was found that the flow separated from the underside soon after the spoiler began to project above the surface of the skin. Note also that shape of the curve in this region for runs 'T' and 'X' are very similar.

In the fully down position the spoiler was approximately 0.25 inches below the surface and as a result the primary nozzle area is correspondingly reduced. In these final configurations also the amount

8.0 ANALYSIS OF RESULTS

8.1 Differential Mass Flow

of spill from the upper nozzle had been reduced to almost negligible proportions. Upward movement of the spoiler then gradually increased the primary nozzle area and spill from the upper nozzle increased accordingly. It was realized then, that control in this region was not dependent upon action of the spoiler control as a spoiler but as a means of changing the relative sizes of the primary and secondary nozzle areas.

It is considered that the tendency for the complete peripheral jet to adhere and coalesce on the underside of the vehicle is quite strong. It is felt, therefore, that indications of separation obtained from the 20° segment form a lower limit for attached flow, and that more favourable conditions will prevail on the complete vehicle.

8.2 Upper and Lower Mass Flows

Figs. 40 to 52 present data showing variation with spoiler position of mass flow from upper and lower nozzles separately. These indicate the extent of 'spill' at the extreme spoiler positions and were used to construct curves of differential mass flow.

8.3 Control Force

In certain simple cases it was possible to obtain control force normal to the aircraft by integration of pressures on the 'cheeks' and outer-body. Introduction of guide vanes and mechanical transition rings rendered the method invalid because the pressures on the components were not known. Evaluations were however, made for runs A, B, & J and these are shown on Fig. 53.

8.4 Pressure Distributions

Surface pressure distributions for various configurations are shown in Figs. 54 - 60. These are given at five control settings for runs A, B, D, E, F, G and J. Location of surface pressure taps are shown in Fig. 11.

8.5 Discharge Coefficient

Mass flow, pressure ratio and geometric nozzle area were all known and hence discharge coefficient could be found. Note that calculations were based on pressure ratio obtained from total head probes at inlet to model (upstream of cascades) and on a geometric area which became less when the spoiler moved below the surface of the duct. Discharge coefficient for runs A to J,

8.5 Discharge Coefficient (Continued)

then Q, V, & X may be found in Figs. 61-68. Values did not vary much with spoiler position or configurations; one may consider 0.85 to be an average value for all runs.

8.6 Pressure Loss Coefficient

Total head rakes were located at inlet to model and at the spoiler station, both were located on the centre line of model. Pressure loss between these two stations has been evaluated for runs A, B, E, F, G, H, I and J. The results have been presented as a loss coefficient based on dynamic head at inlet to model and variation is shown with spoiler position.

8.7 Flow Distribution

Measurements were made of total and static pressure distribution across the upper and lower outer nozzles on the centre line of model. These are presented for most of the runs in Figs. 77-93. These graphs were used to determine the upper and lower nozzle mass flow for each test run. Each case may be studied as required; it is interesting to note how that, in general, upon movement of the spoiler the outer nozzles fill from the outside. Similarly, they empty from the inside so that as the change-over takes place, the flow between guide vane and 'cheek' is starved first.

9.0 CONCLUSIONS

Design of the Avrocar wing tip control system was based on tests of small scale models. The twenty degree segment was designed to demonstrate the full scale characteristics of the system and results of the tests may be summarized as follows:

1. Effectiveness of the spoiler type control was demonstrated and small spoiler movements were shown to induce large deflections of the primary jet.

2. Extension of the guide vane in the lower outer nozzle was shown to play a key part in deflection of the jet through a full 180° and causing it to adhere to the underside of the test specimen.

3. Small projections on the outer-body(simulating the mechanical transition ring)were shown to be more effective as a transition control than an alternative design using a secondary jet (simulating the pneumatic transition ring). Presence of the mechanical transition ring caused flow to spill from the upper nozzle, this was eventually reduced to almost negligible proportions by using small projections.

4. Examination of the results suggests that, in the hovering configuration with spoiler fully down, the control jet which issues from the upper nozzle stems from spill characteristics rather than from spoiler action.

5. Lack of ability to measure forces proved to be a serious disadvantage both from the view point of control characteristics and nozzle efficiency.

10.0 LIST OF SYMBOLS

Ae	Effective exhaust area	$in.^2$
C	Orifice plate discharge coefficient	
D	Supply pipe diameter	in.
d	Orifice diameter	in.
E	Velocity of approach factor for incompressible flow $1/(1-m^2)^{\frac{1}{2}}$	
F	Integrated gross thrust for test specimen	lb.
Fi	Ideal gross thrust for test specimen	lb.
f	Total section thrust	lb.
fZ	Normal or control thrust vector	lb.
fR	Radial thrust vector	lb.
h	Orifice plate pressure differential	in. H_2O at 60^oF
m	$(d/D)^2$	
m	Mass flow	slugs/sec.
N	Moisture correction factor	
P	Total pressure	psia.
p	Static pressure	psia.
$\triangle P$	Pressure loss between upstream and spoiler station	psig.
q	Upstream duct dynamic pressure	psig.
QN	Flow function corresponding to p_a/P_t	
R	Gas constant	$ft./^oR$
R	Radial position measured from centre of aircraft	in.
R_e	Reynold's number	
T	Total temperature	^oR
V	Velocity	ft./sec.

LIST OF SYMBOLS (Continued)

W	Mass flow	lbs./sec.
Z	Product of multipliers for R_e, E and D	
$\bar{x}$	Distance from aircraft longitudinal axis	in.
γ	Specific heat ratio	
η	Thrust efficiency	
ρ_1	Density at orifice plate upstream tapping	lb./ft.
τ	Angular position of section thrust vector in relation to the aircraft longitudinal axis	°.

Subscripts

1	Orifice plate upstream tapping
2	Orifice Plate downstream tapping
a	Ambient
L	Lower nozzle plane
R	Radial axis
S	Control spoiler plane
T	Upstream duct plane
U	Upper nozzle plane
Z	Vertical axis

11.0 REFERENCES

1.0 Program Planning Report Avrocar I.
Avro Aircraft Limited May 20, 1958.

2.0 AVRO/SPG/TR 174 - A Brief Technical Description of the Avrocar I - D.C. Whittley and K. Lockwood, May 1958.

3.0 AVRO/SPG/TR 182/1 - Test Specification for the Full Scale 20° Wing Tip Segment of the Avrocar. E.J. Nemeth - July 1958.

4.0 AVRO/SPG/TR 182/2 - Addendum - E.J. Nemeth Dec. 1958.

5.0 Axisymmetric and Two Dimensional Ejector Performance Data - Princeton University Tech. Report No. 2.

6.0 Flow Measurement - British Standard Code B.S. 1042 - 1943 British Standards Institution.

7.0 NACA TR 1235 - Standard Atmosphere - Tables and Data for Altitudes to 65,800 ft. 1955.

12.0 LIST OF ILLUSTRATIONS

Fig. 1 Layout of the Avrocar

Fig. 2 Avrocar Exhaust Nozzle and Control Mechanism

Fig. 3 The Control System Airflow

Fig. 4 Full Scale 20° Segment Test Rig

Fig. 5 General Assembly of the Model

Fig. 6 The Forward Flight Wing Tip

Fig. 7 Mechanical Transition Spoiler Installation

Fig. 8 Details of the Flight Control Spoiler

Fig. 9 Inner Cascade Configurations

Fig. 10 Lower Nozzle Guide Vane Configurations Tested

Fig. 11 General Assembly of the Instrumentation

Fig. 12 View of the Instrumented Model

Fig. 13 Bottom Nozzle Static Rake Assembly

Fig. 14 Top Nozzle Pitot Rake Assembly

Fig. 15 Spoiler Station Pitot Static Rake

Fig. 16 Layout of the Control Room

Fig. 17 Control Room Console

Fig. 18 Schematic of the Electrical System

Fig. 19 Typical Wool Tuft Pattern

Fig. 20 Full Scale 20° Segment Mass Flow VS P_1

Fig. 21 Ejector Mass Flow Calibration

Fig. 22 Control Spoiler Calibration

Fig. 23 Yawmeter Calibration

LIST OF ILLUSTRATIONS (Cont'd)

Fig. 24 External Flow Tuft Pattern - Run W - Full Down Control

Fig. 25 Upper Nozzle Guide Vane Failure

Fig. 26 Lower Nozzle Guide Vane Failure

Fig. 27 Alternate Outerbody for Simplified Transition Control

APPENDIX 'A'

PHOTOGRAPHS AND ILLUSTRATIONS

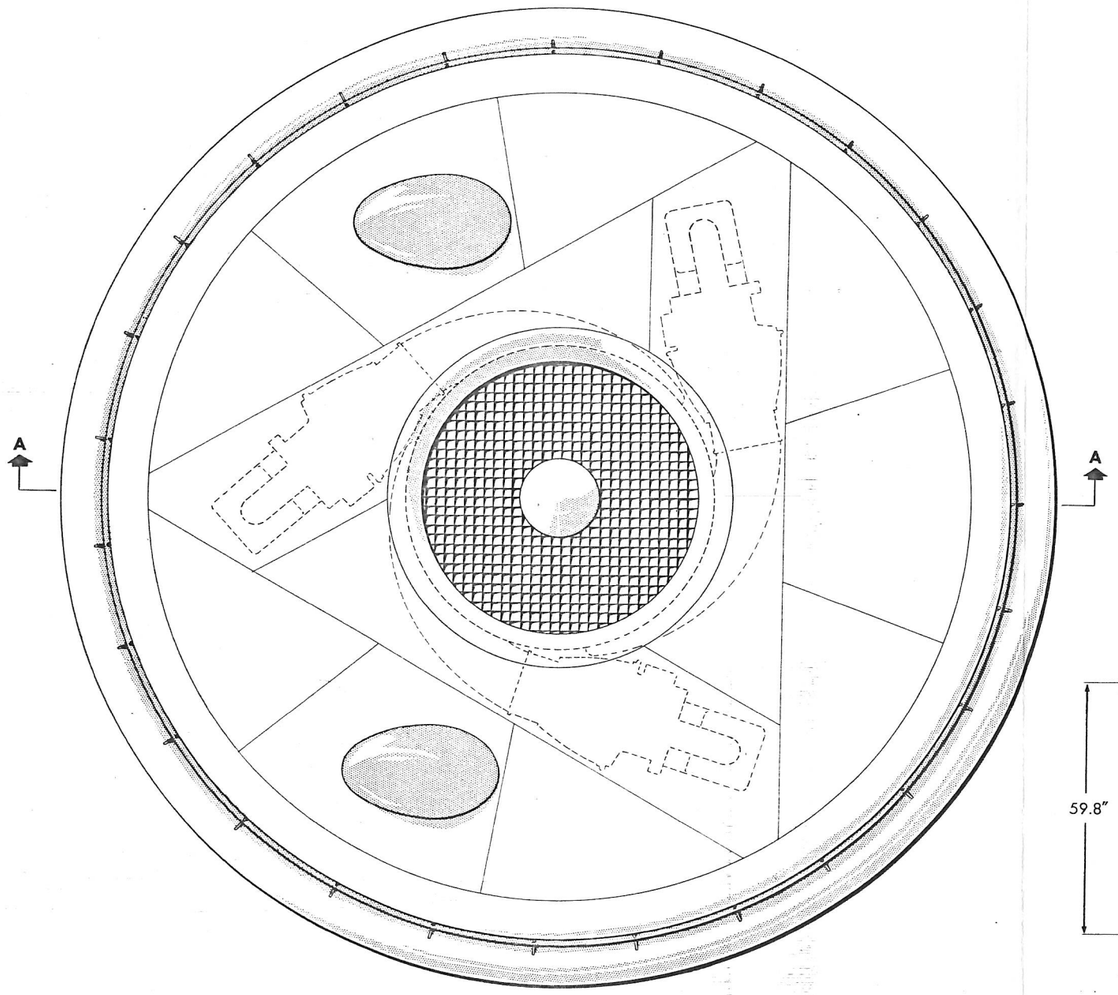

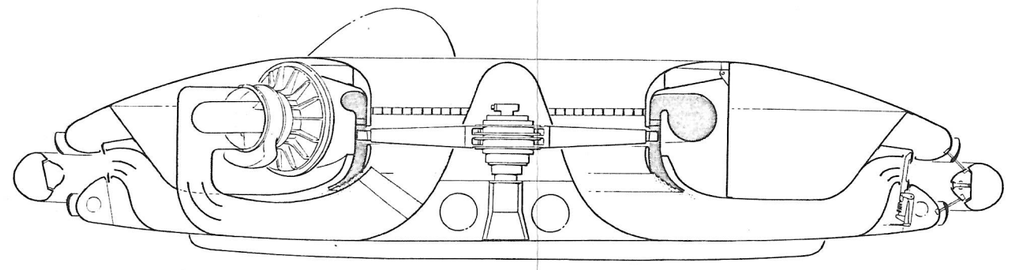

SECTION A-A

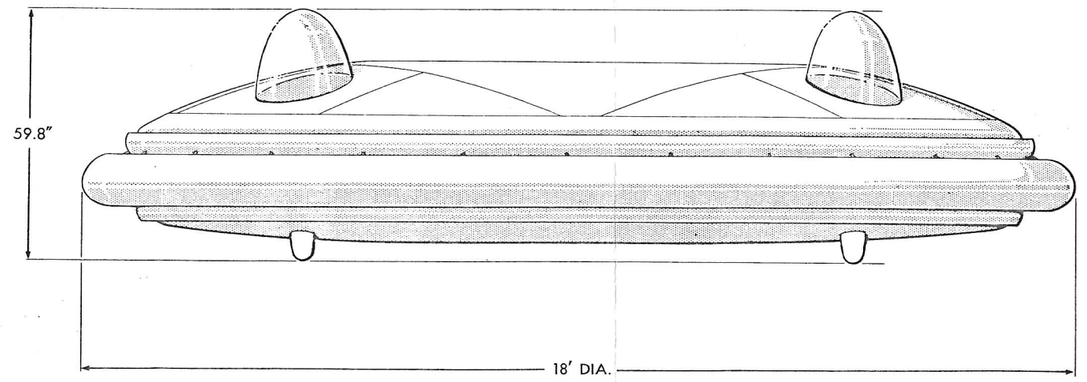

FIG. 1 LAYOUT OF THE AVROCAR

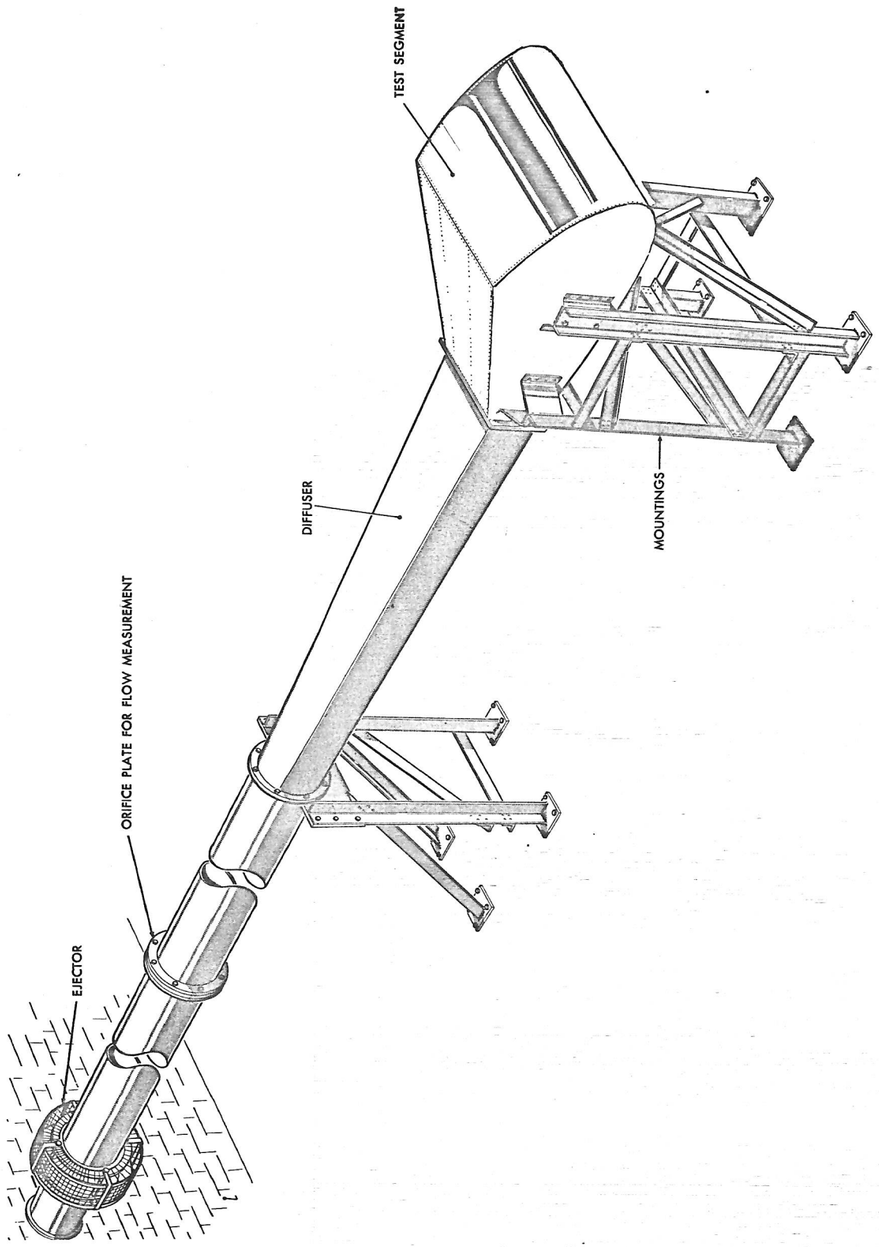

FIG. 4 FULL SCALE 20° SEGMENT TEST RIG

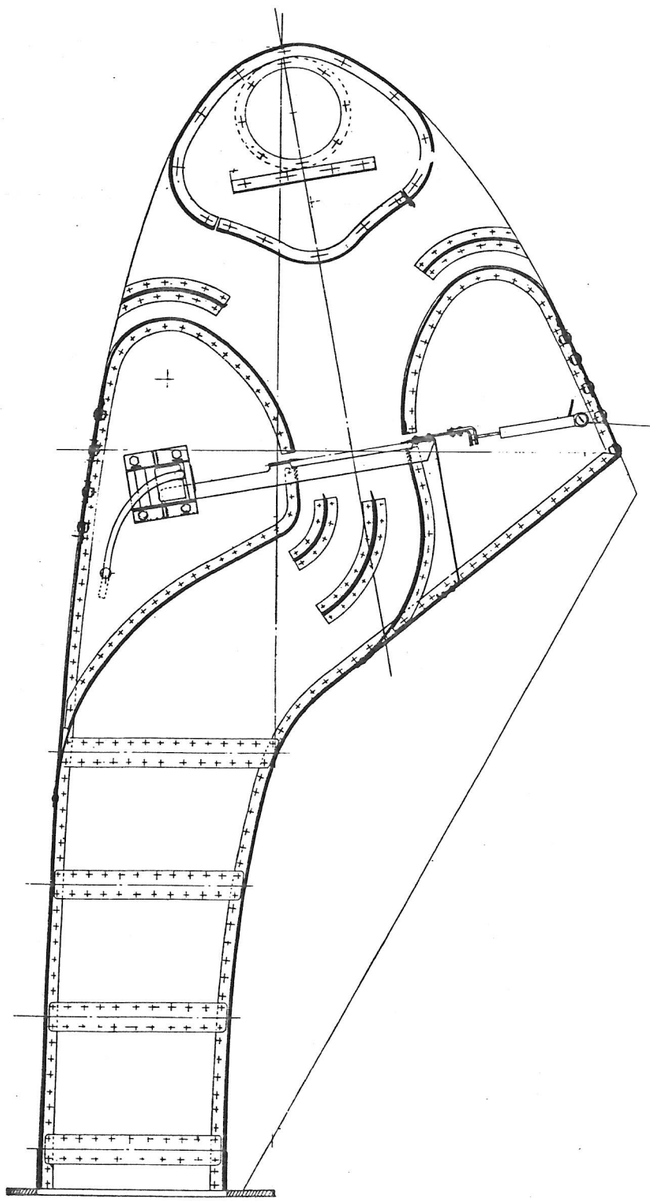

SECTION 'A-A'

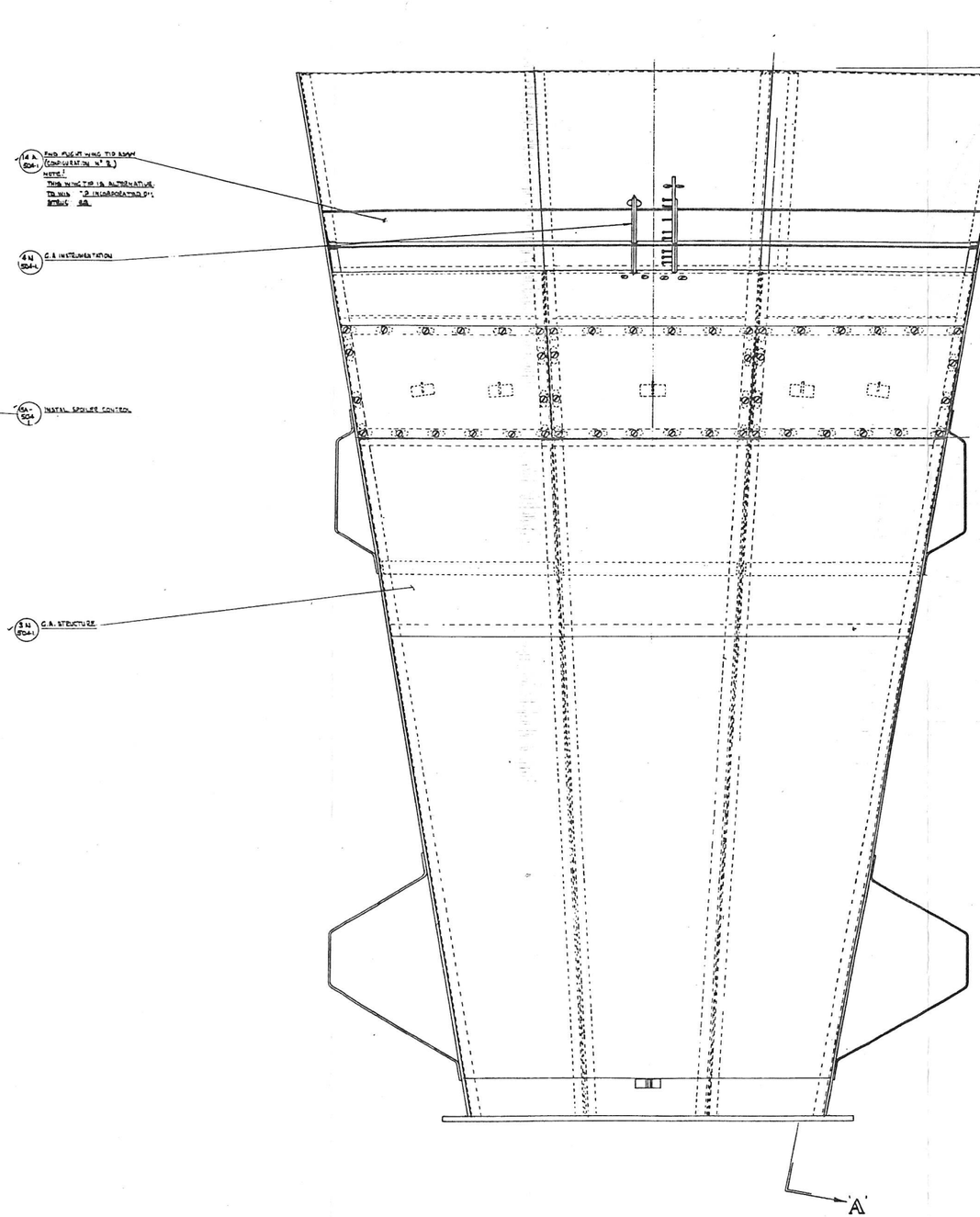

FIG. 5 GENERAL ASSEMBLY OF THE MODEL

3693-503-1

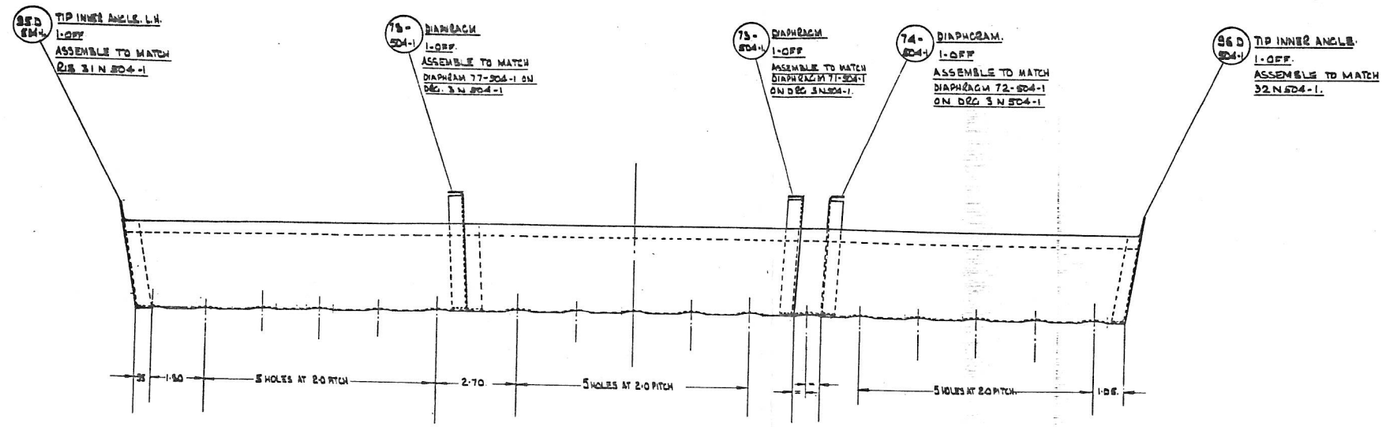

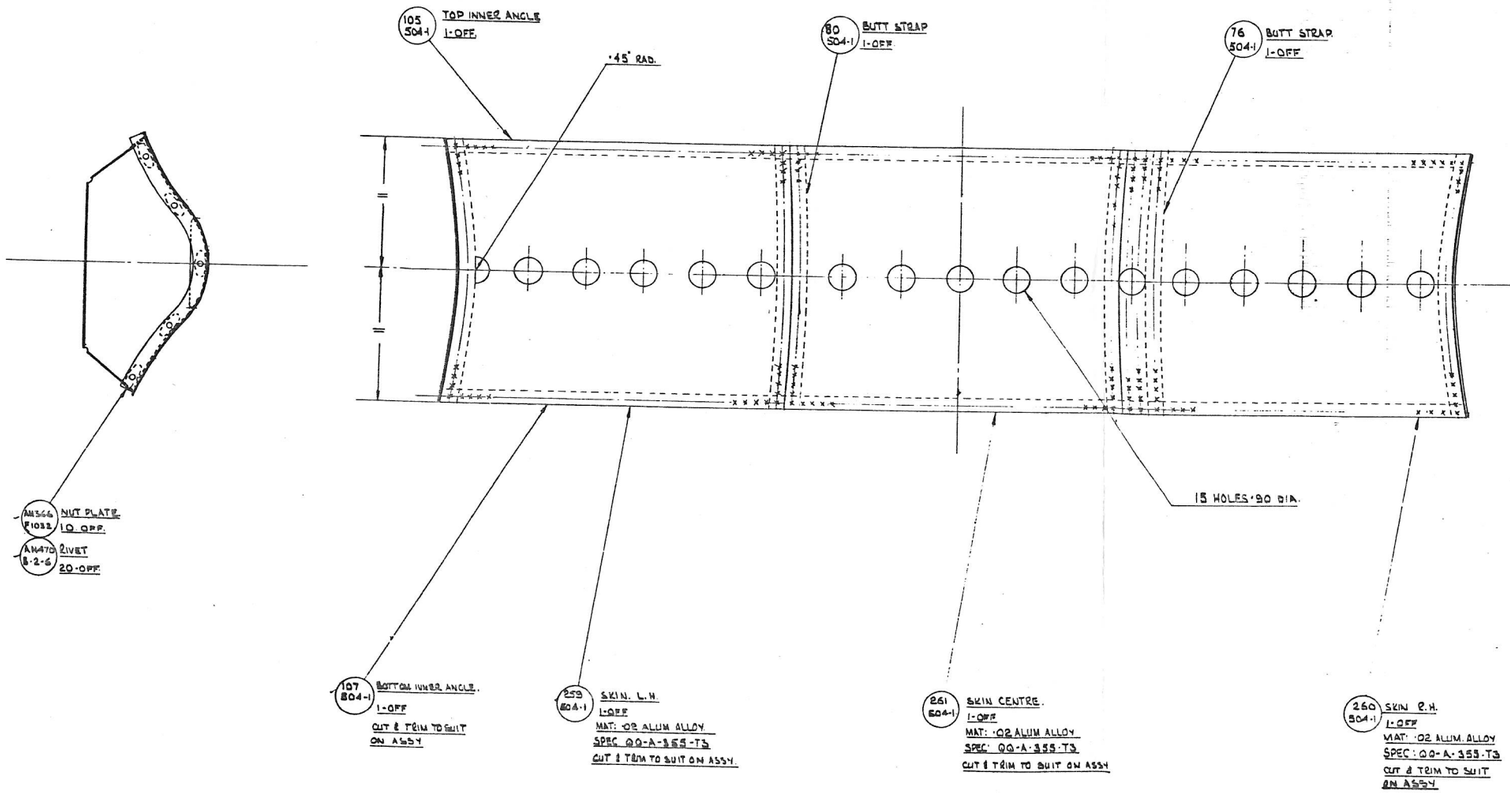

NOTE.

THIS DRG TO BE READ IN CONJUNCTION WITH 3 N 504-1 G.A STRUCTURE.

SPOT WELD WHERE SHOWN THUS x—–x MIN EDGE DISTANCE ·20 MIN PITCH ·31. USE AN 470 B 3-3 RIVETS WHERE SPOT WELDING IS NOT PRACTICABLE.

REMOVE SHARP EDGES TO CS-D-20.

DETAILED ITEMS NOT LISTED ARE CALLED ON DRG. 3 N 504-1.

IDENT MARK TO CS-D-15

FIG. 6 THE FORWARD FLIGHT WING TIP

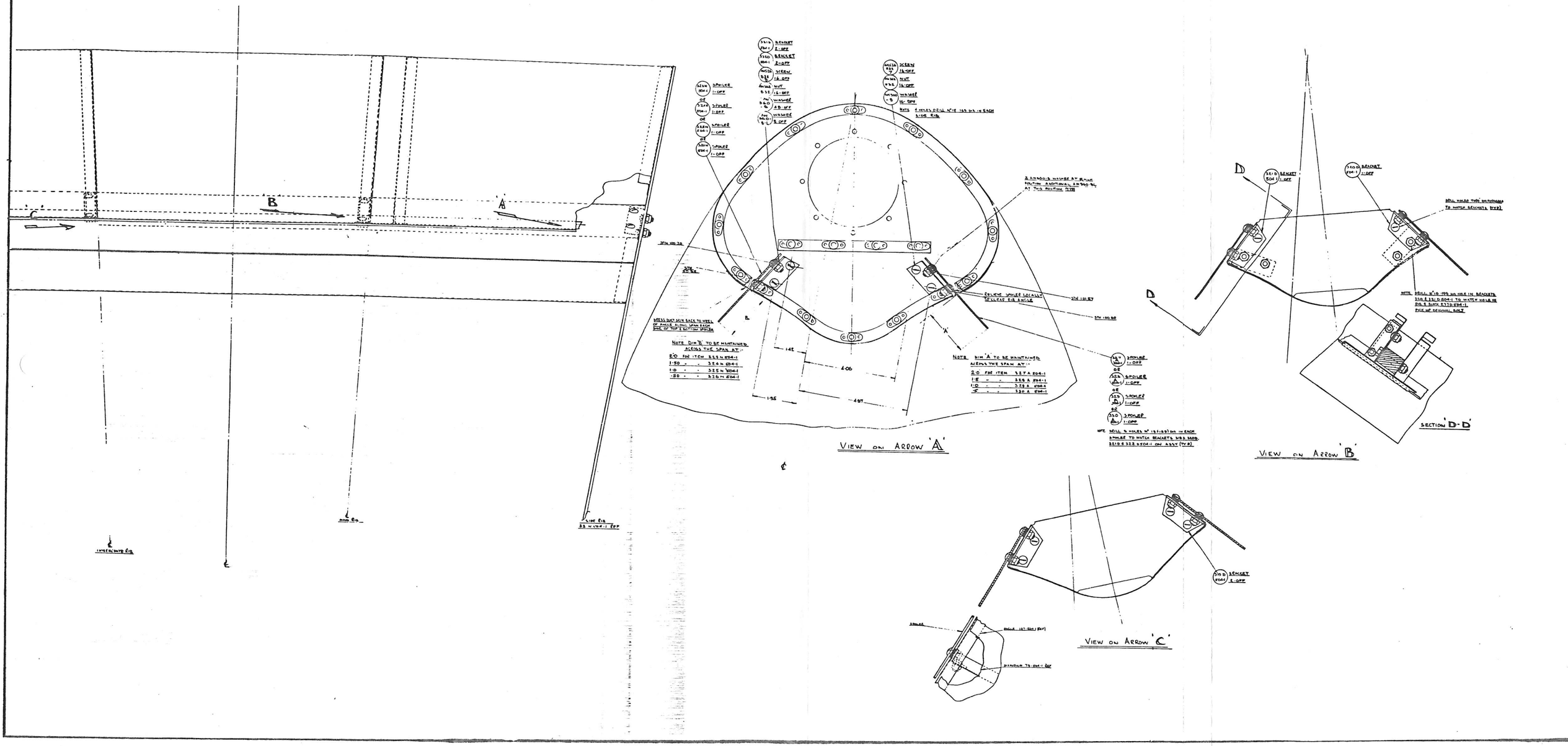

FIG. 7 MECHANICAL TRANSITION SPOILER INSTALLATION

SECRET

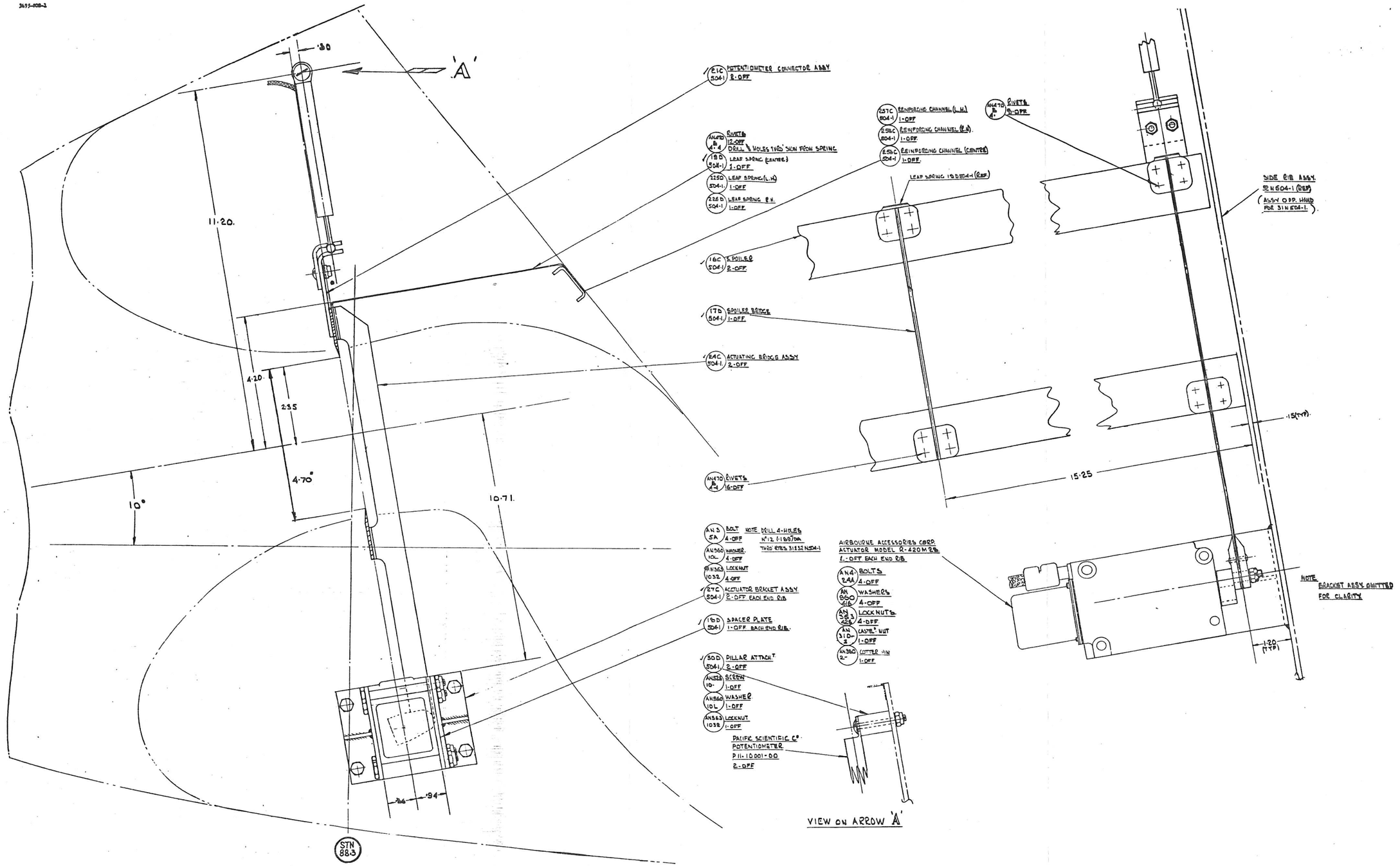

FIG. 8 DETAILS OF THE FLIGHT CONTROL SPOILER

AVRO/SPG/TR267

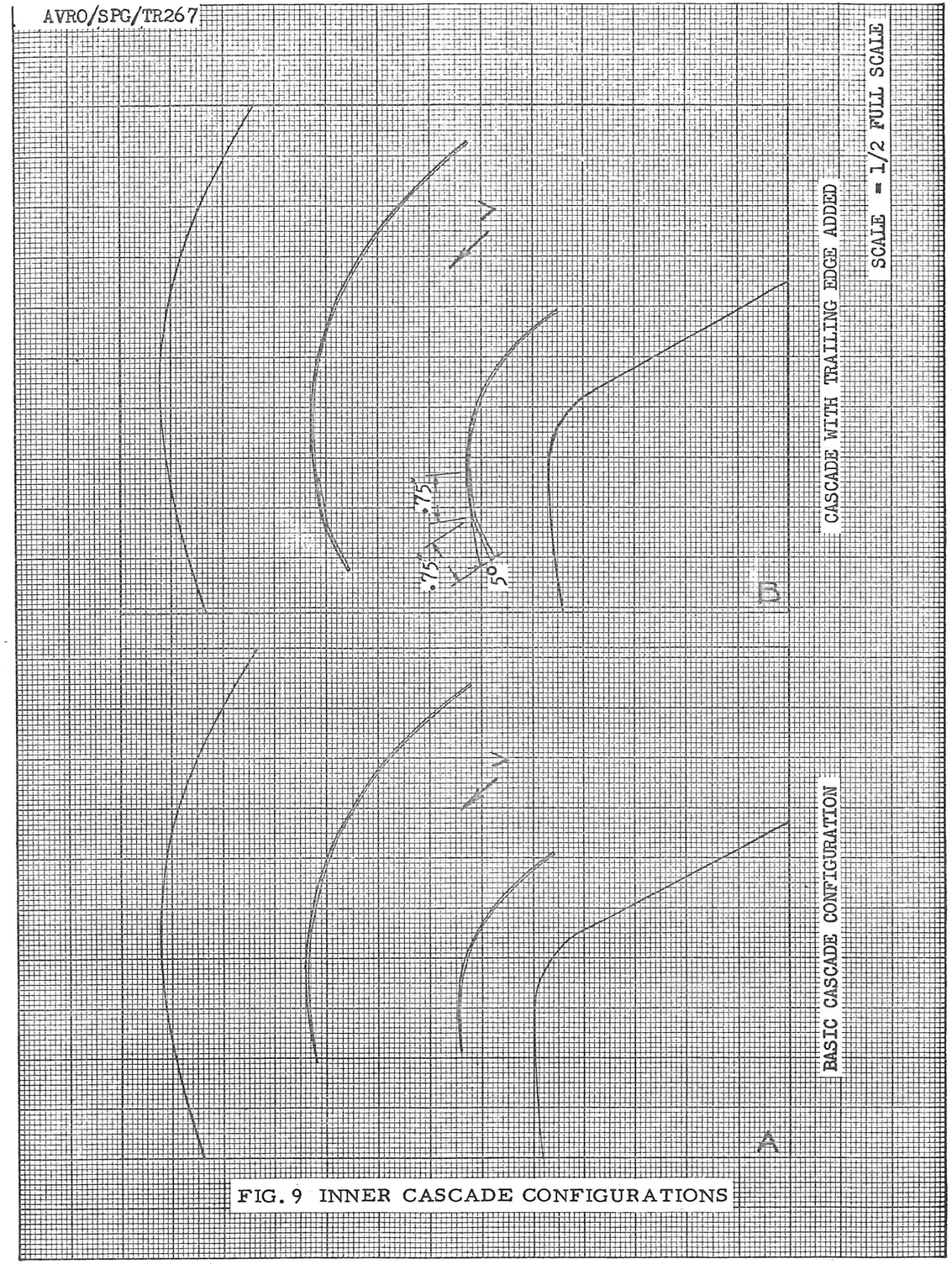

FIG. 9 INNER CASCADE CONFIGURATIONS

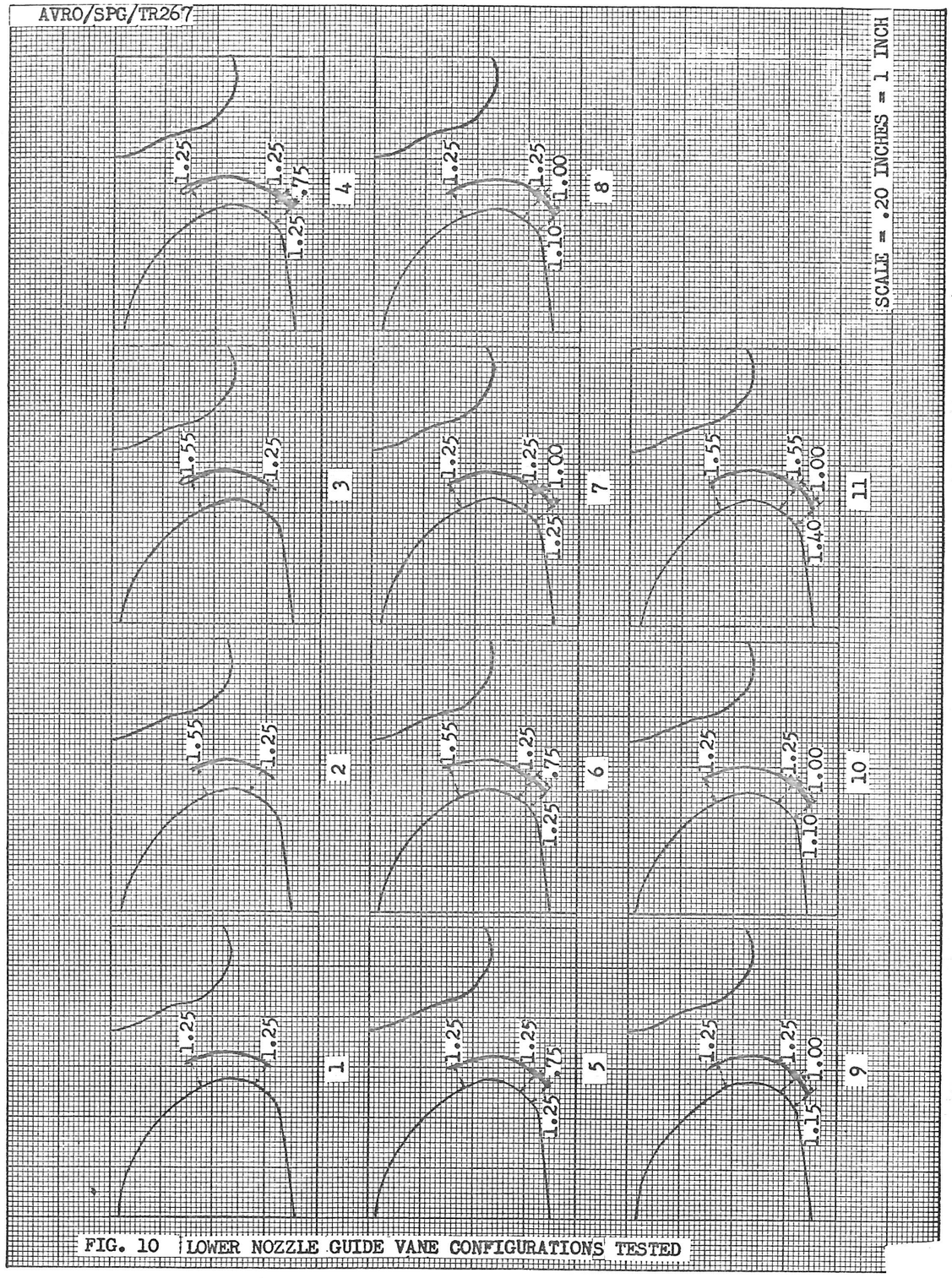

FIG. 10 LOWER NOZZLE GUIDE VANE CONFIGURATIONS TESTED

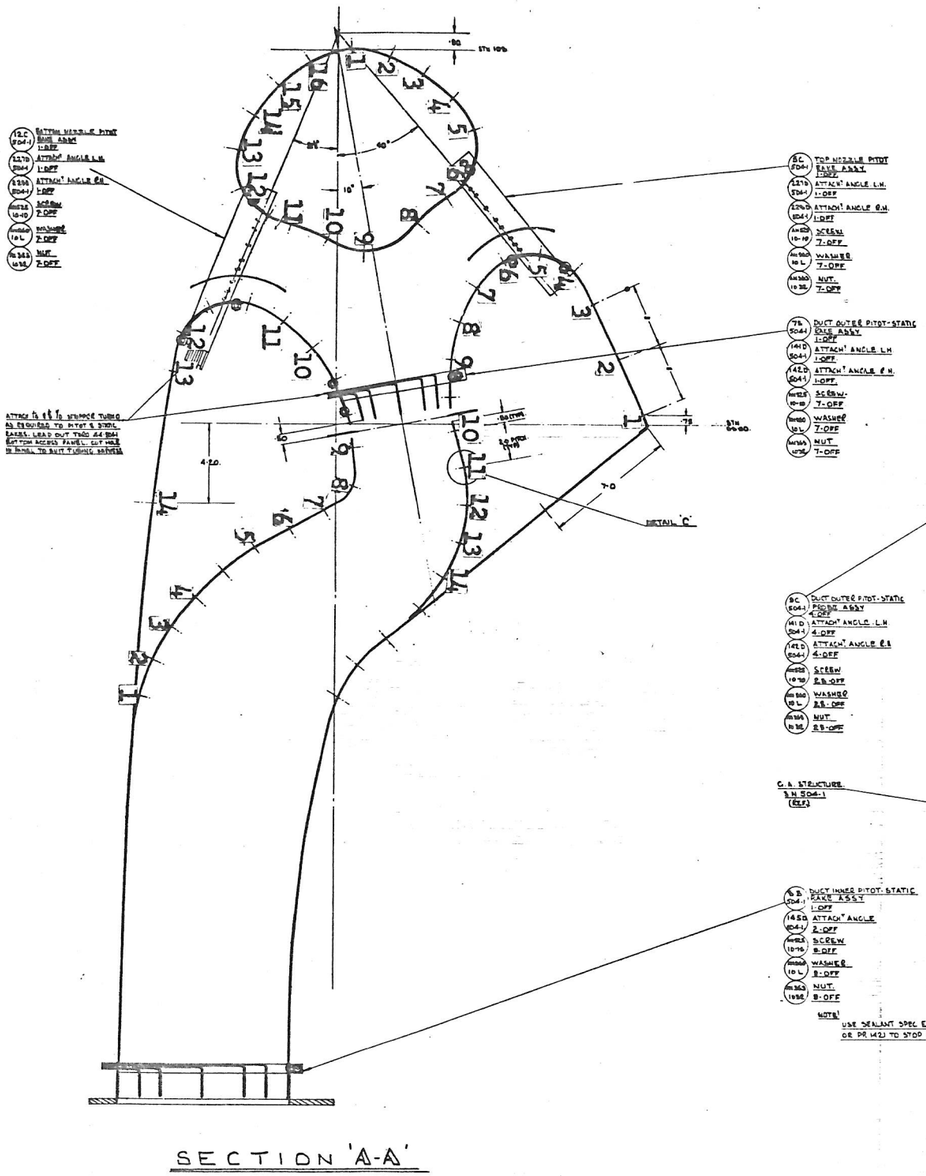

FIG. 11 GENERAL ASSEMBLY OF THE INSTRUMENTATION

SECRET

81819

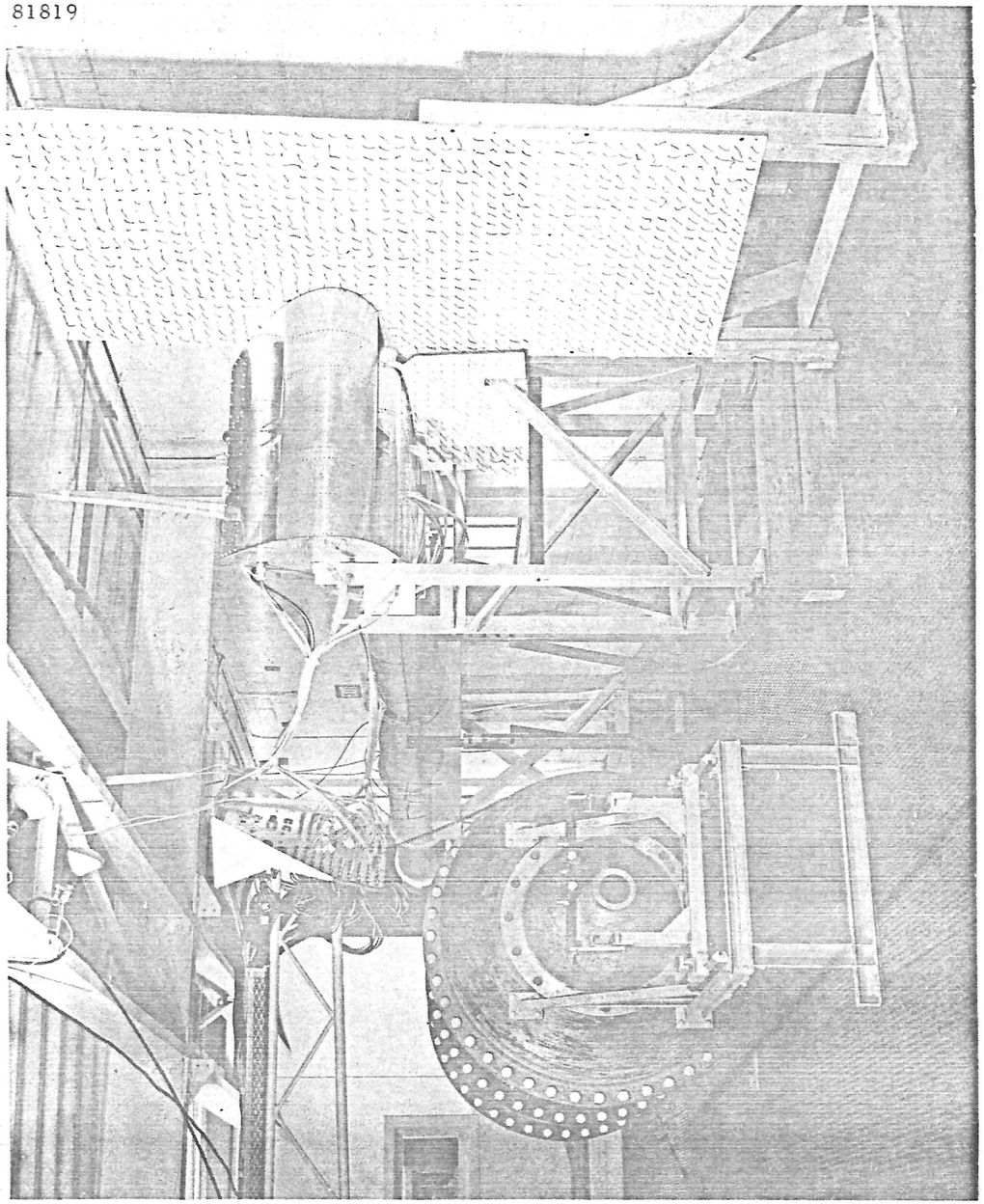

FIG. 12 VIEW OF THE INSTRUMENTED MODEL

3497-802-1

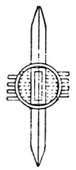

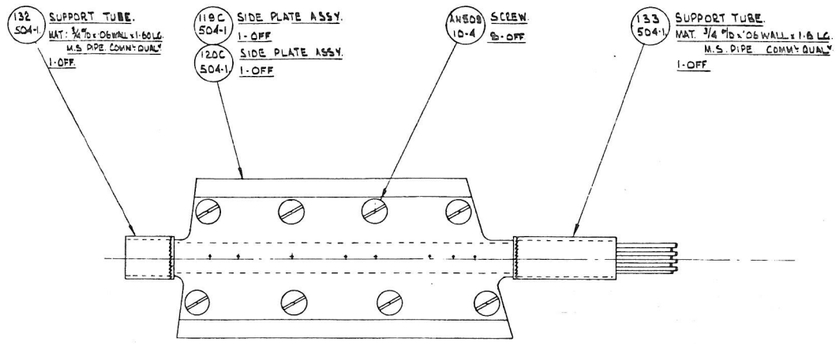

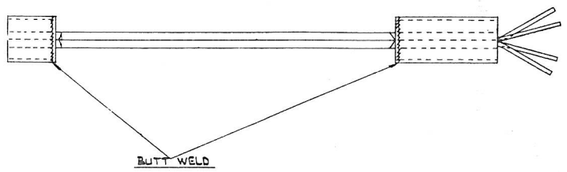

FIG. 13 BOTTOM NOZZLE STATIC RAKE ASSEMBLY

3496-802-1

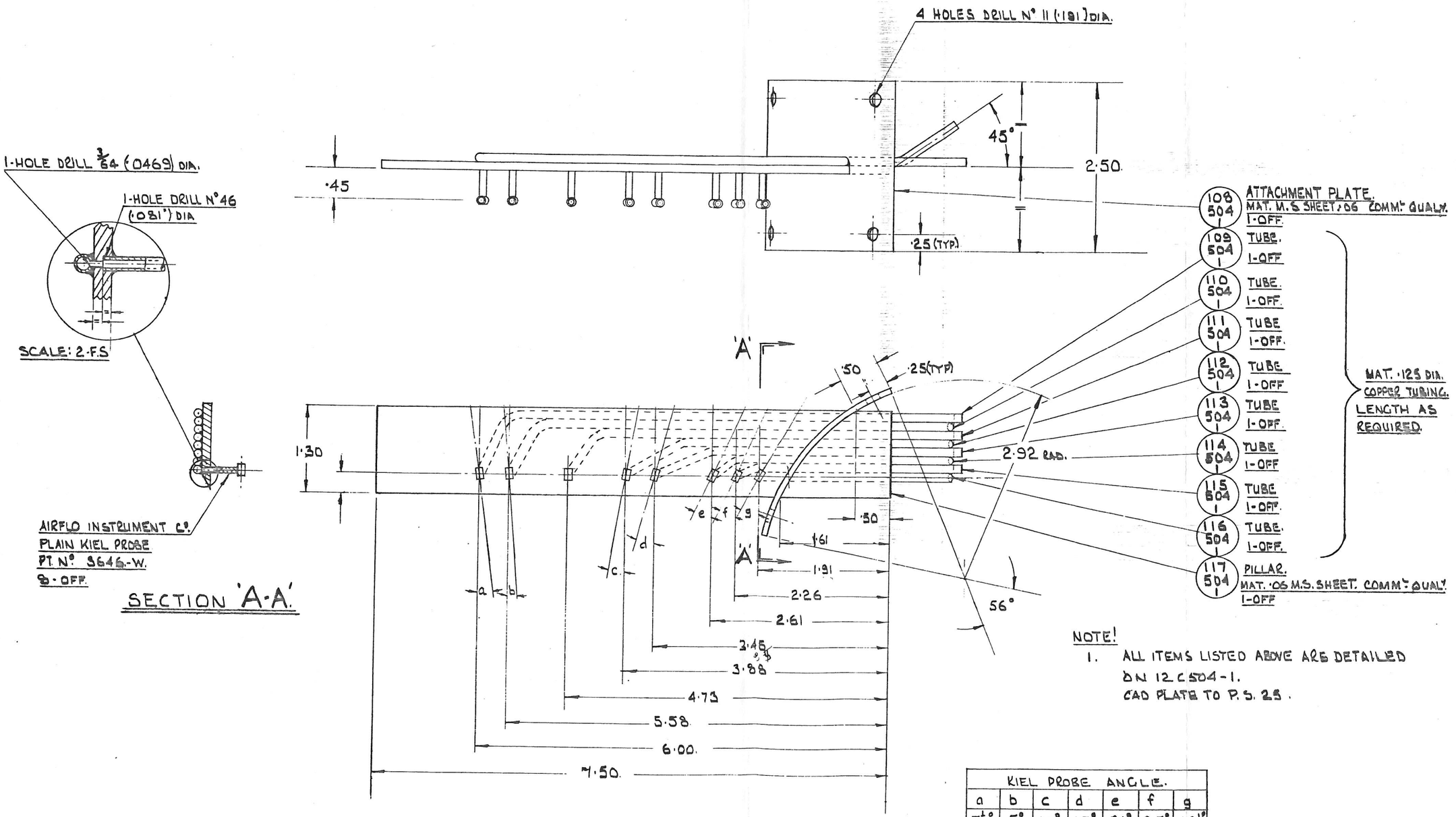

NOTE!

1. ALL ITEMS LISTED ABOVE ARE DETAILED ON 12 C 504-1. CAD PLATE TO P.S. 25.

KIEL PROBE ANGLE.						
a	b	c	d	e	f	g
7½°	5°	10°	15°	21°	25°	29½°

FIG. 14 TOP NOZZLE PITOT RAKE ASSEMBLY

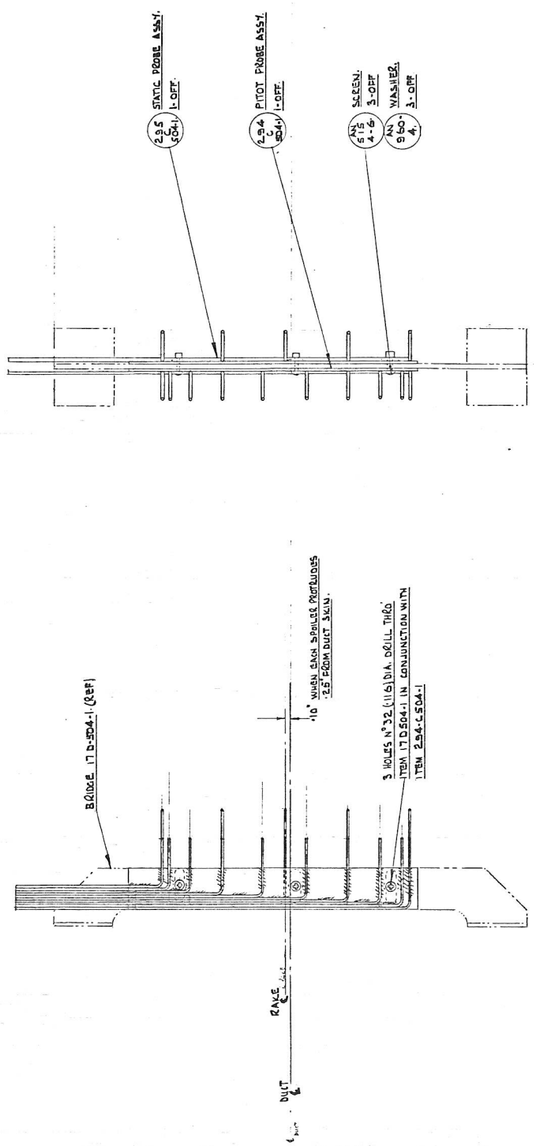

FIG. 15 SPOILER STATION PITOT STATIC RAKE

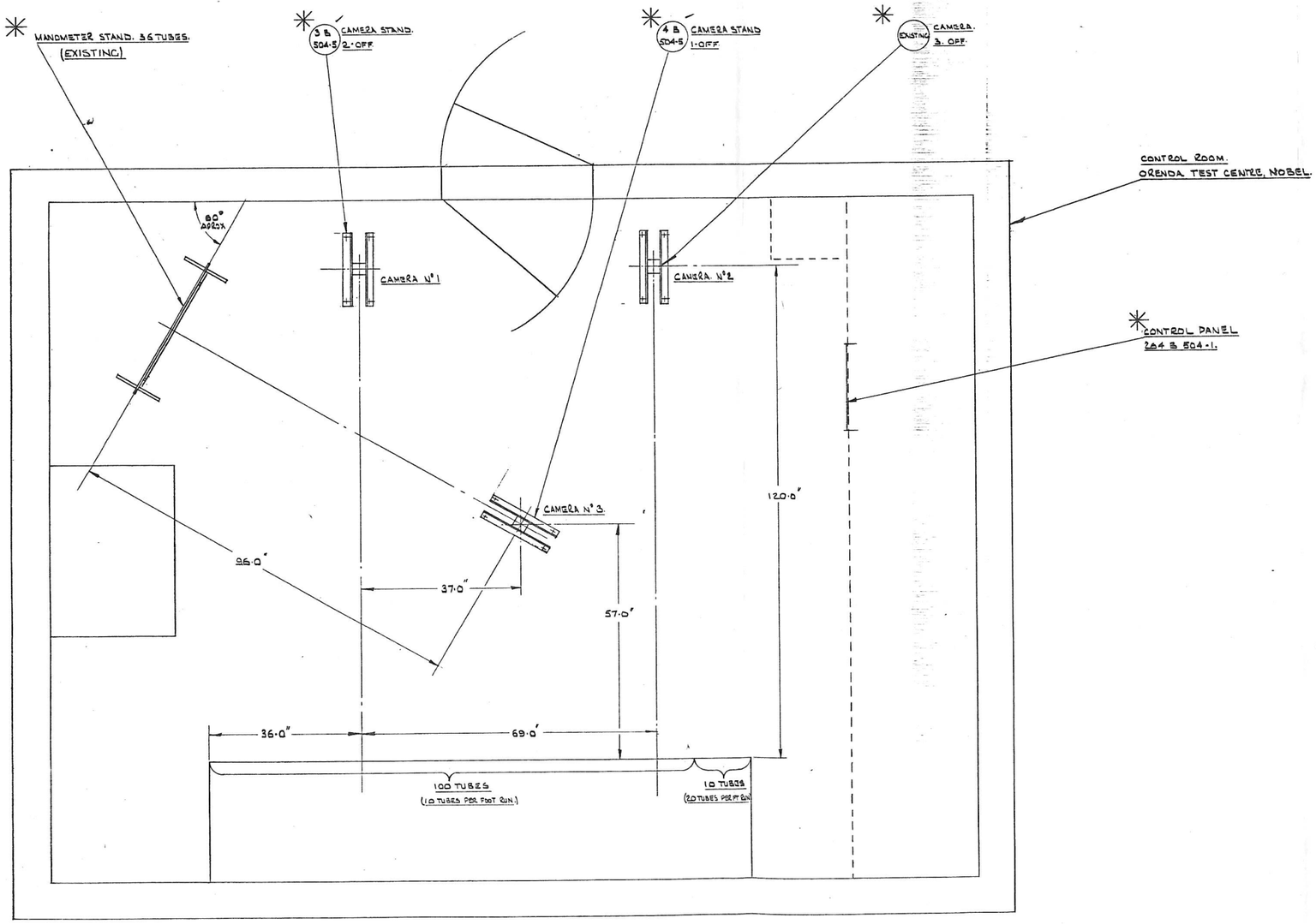

ITEMS MARKED THUS * ARE SUPPLIED BY AVRO AIRCRAFT C°.

FIG. 16 LAYOUT OF THE CONTROL ROOM

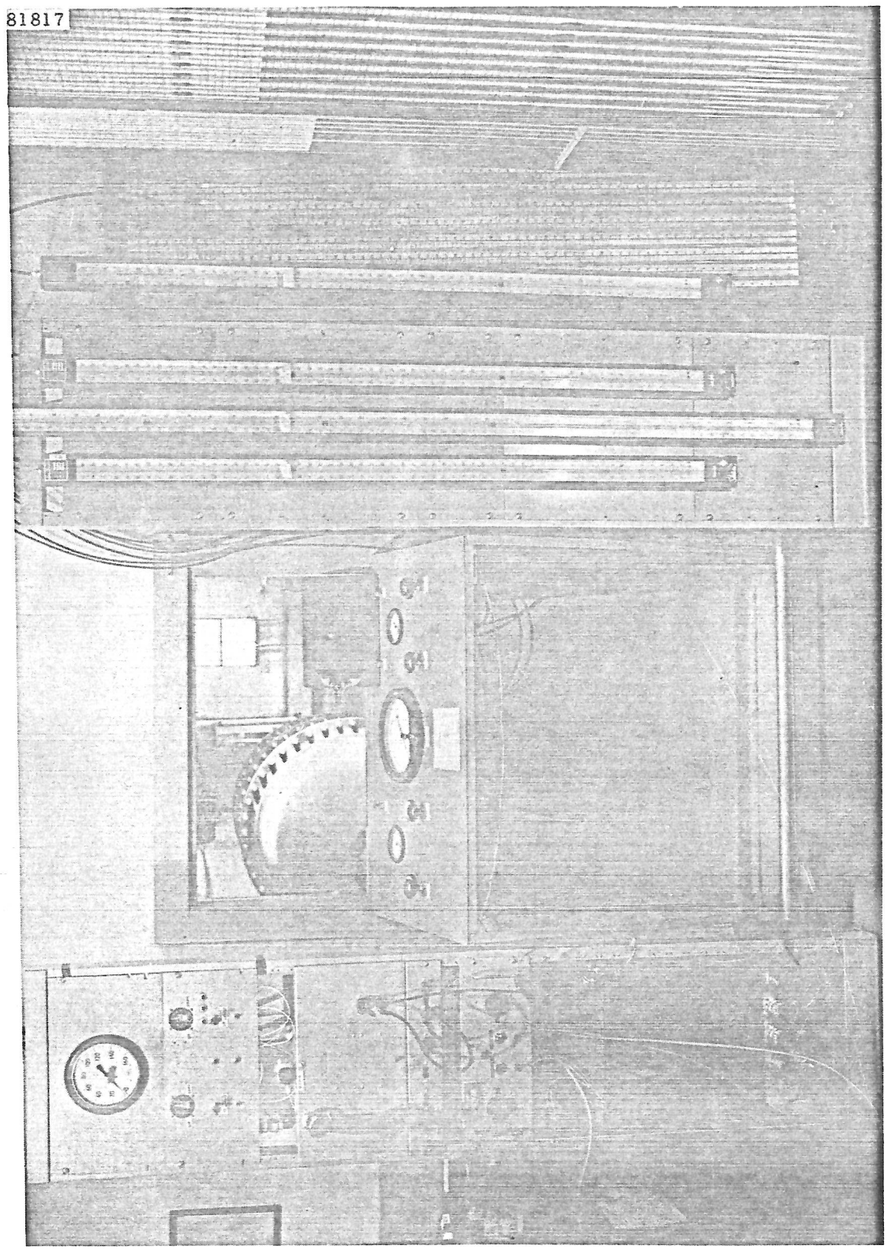

FIG. 17 CONTROL ROOM CONSOLE

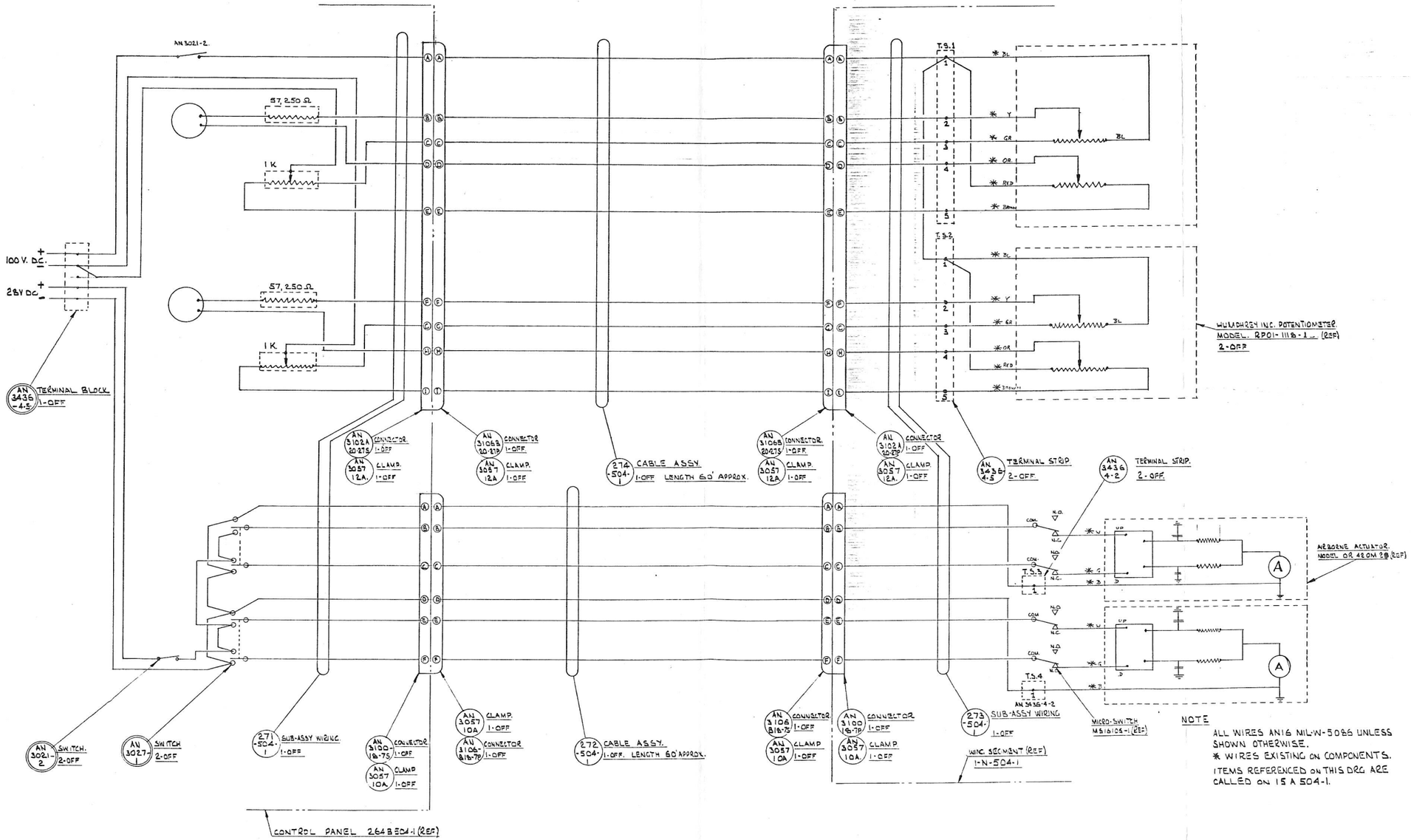

FIG. 18 SCHEMATIC OF THE ELECTRICAL SYSTEM

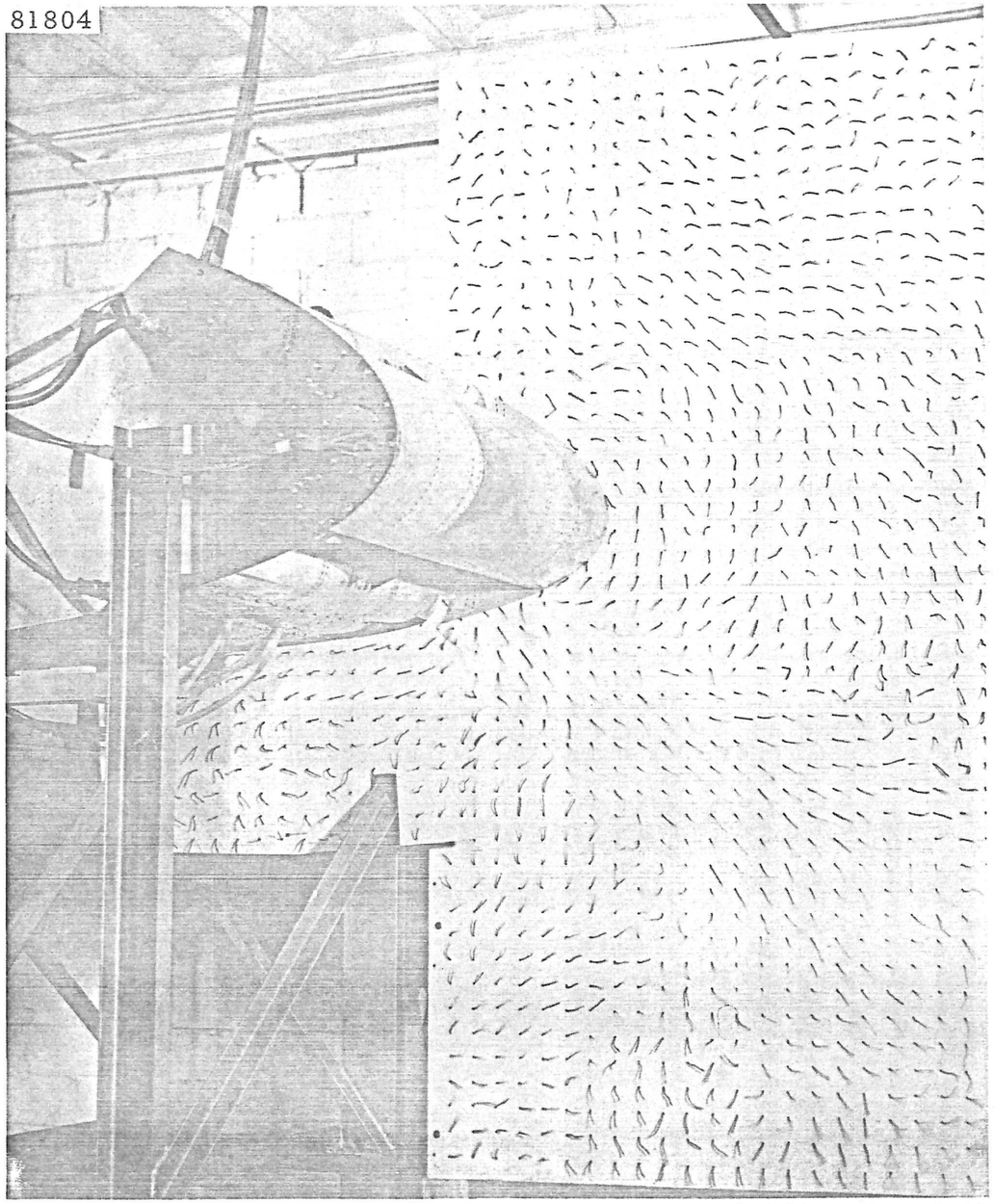

FIG. 19 TYPICAL WOOL TUFT PATTERN

AVRO/SPG/TR 267

FIG. 20 FULL SCALE 20° SEGMENT MASS FLOW VS P_1

SPECIMEN NOT ON

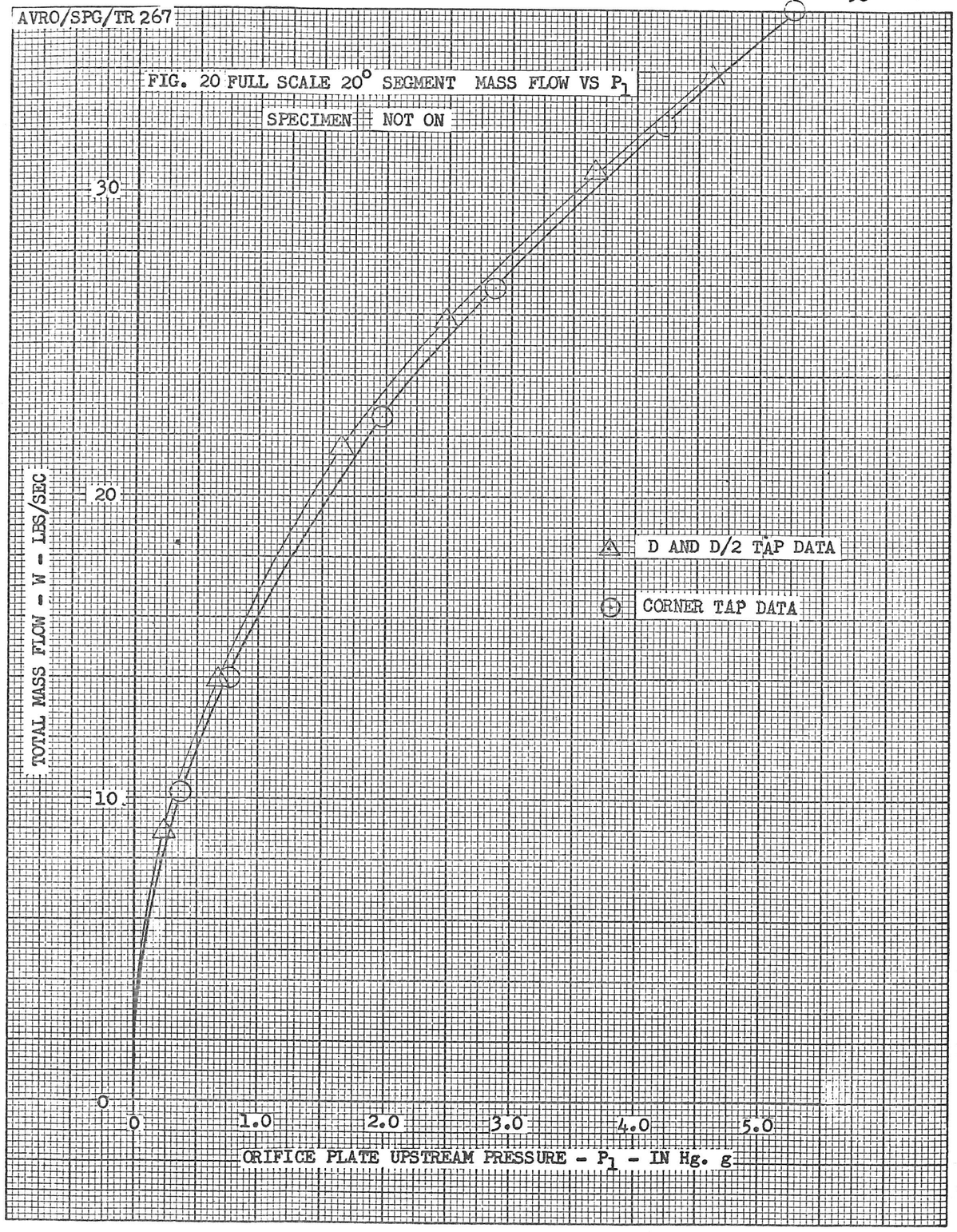

AVRO/SPG/TR 267

FIG. 21 EJECTOR MASS FLOW CALIBRATION

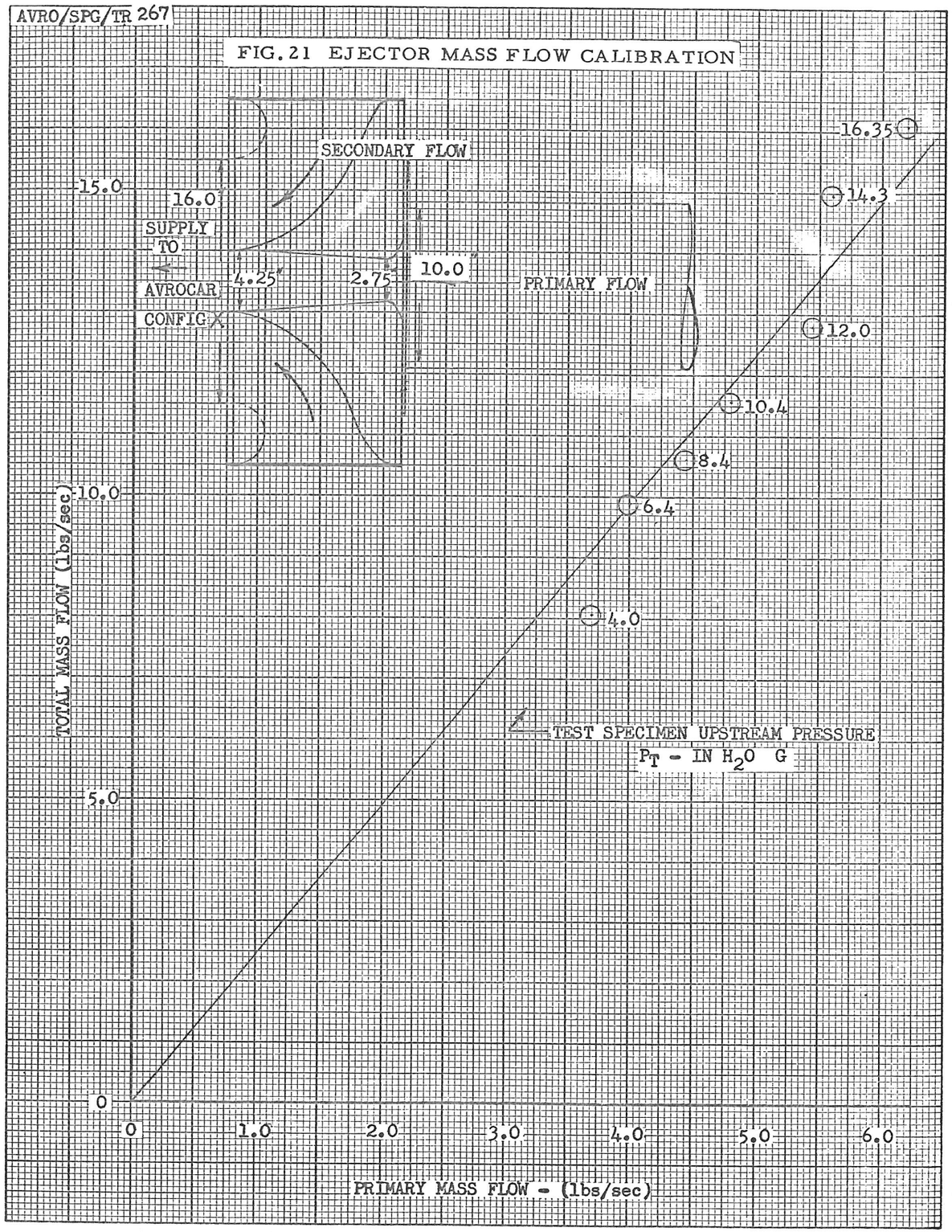

AVRO/SPG/TR 267

FIG. 22 CONTROL SPOILER CALIBRATION

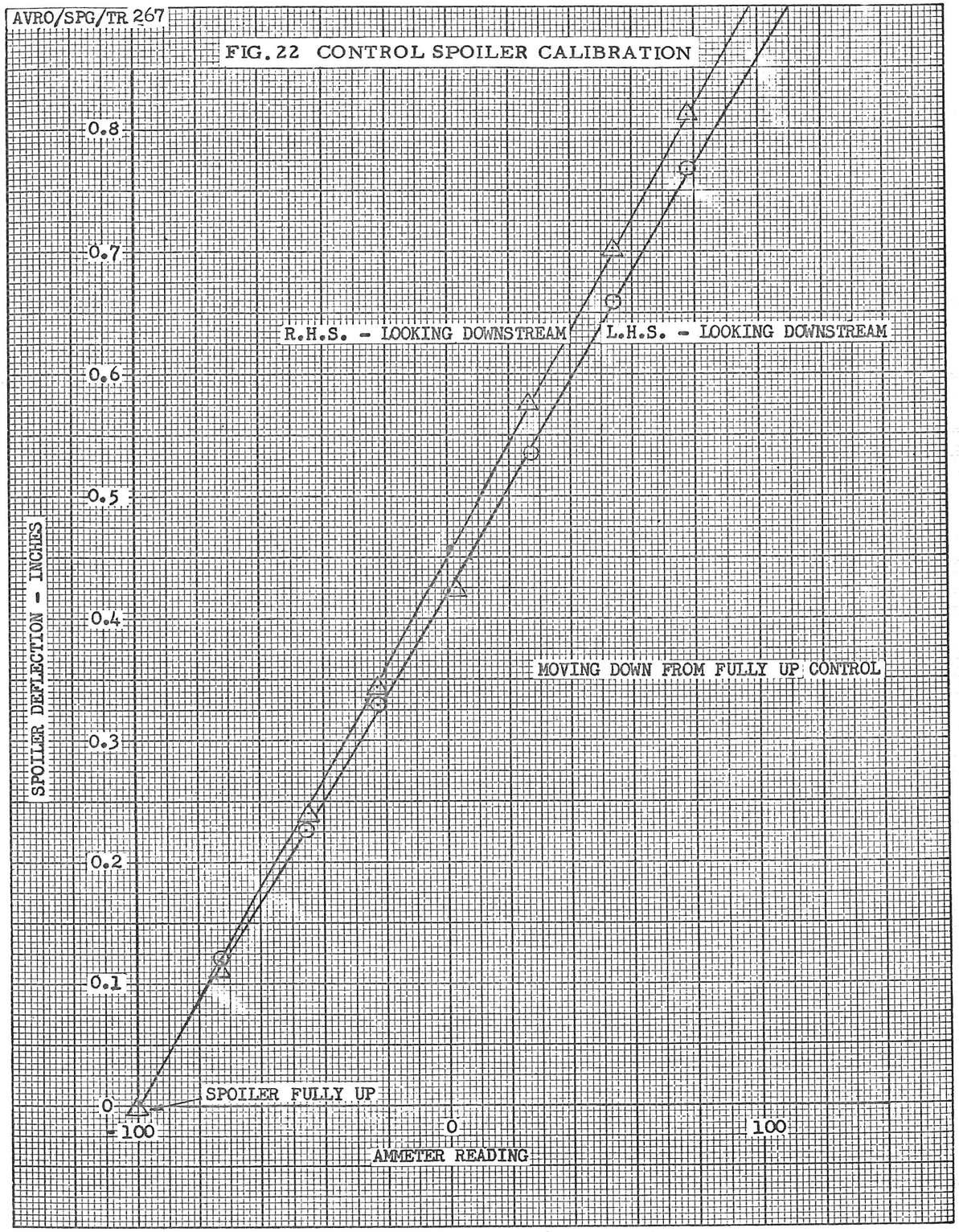

AVRO/SPG/TR 267

FIG.23 YAWMETER CALIBRATION

PROBE NO. 6-B-504-1

SIGN CONVENTION LOOKING UPSTREAM MOVEMENT CLOCKWISE IS A NEGATIVE YAW

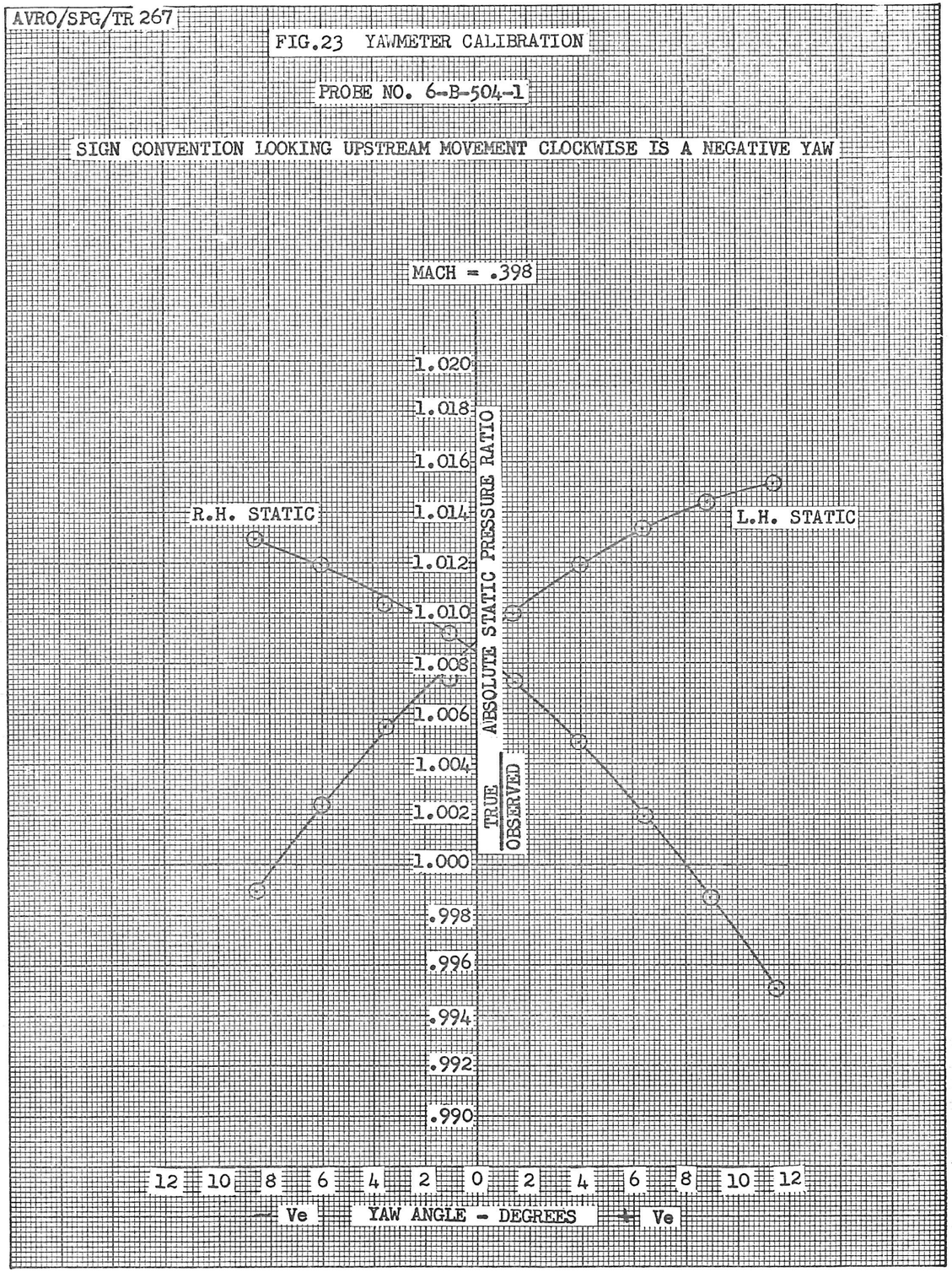

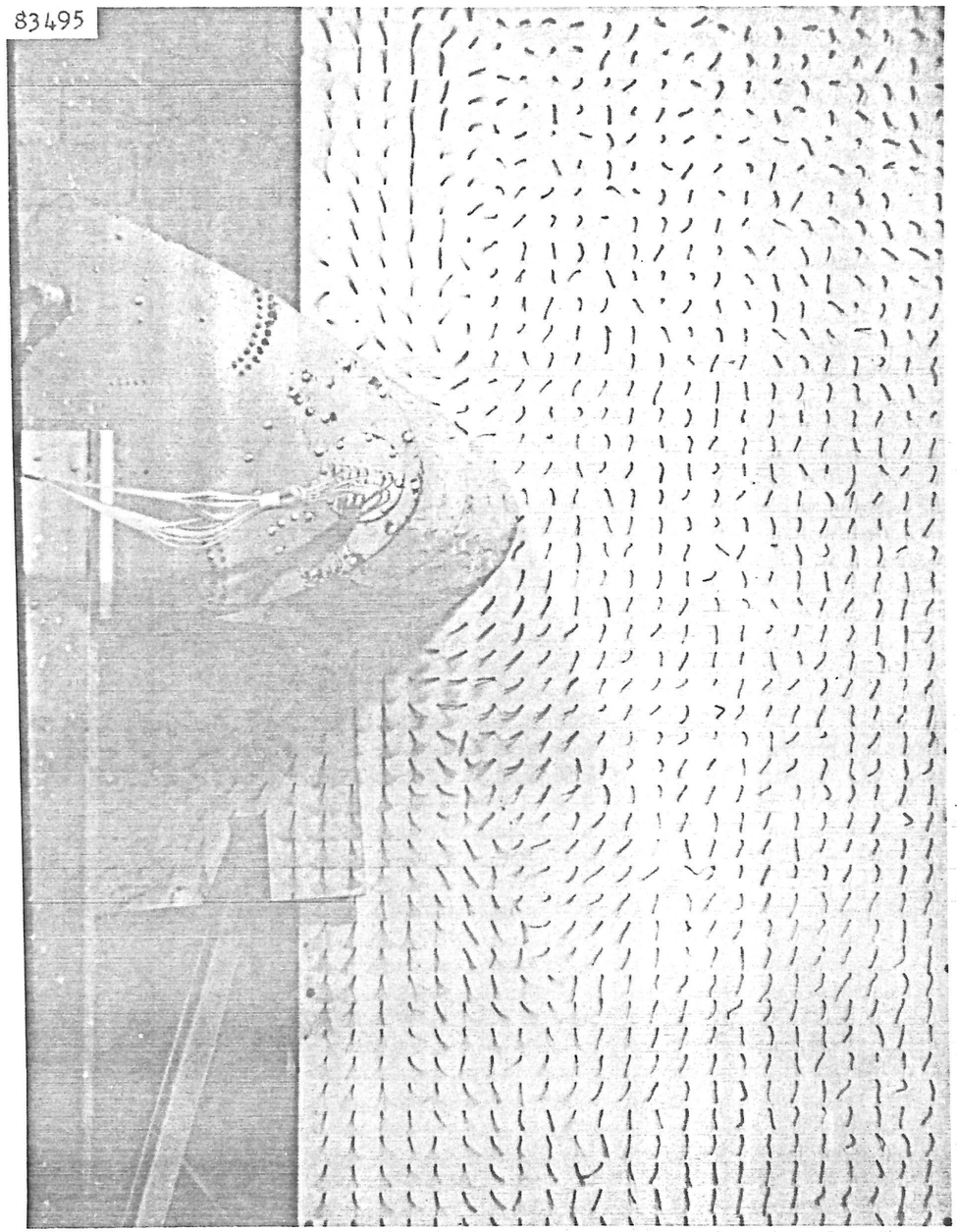

FIG. 24 EXTERNAL FLOW TUFT PATTERN - RUN W - FULL DOWN CONTROL

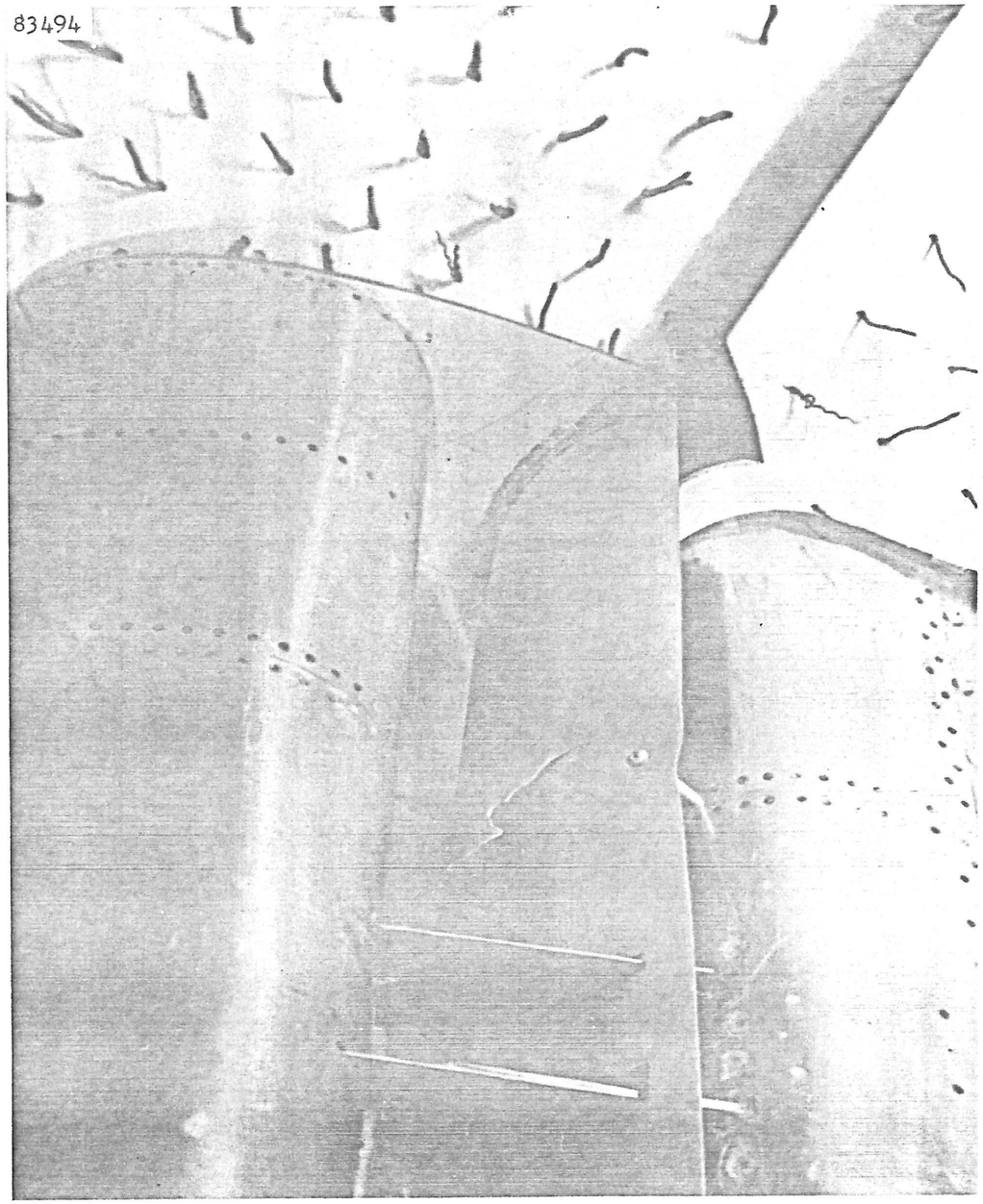

FIG. 25 UPPER NOZZLE GUIDE VANE FAILURE

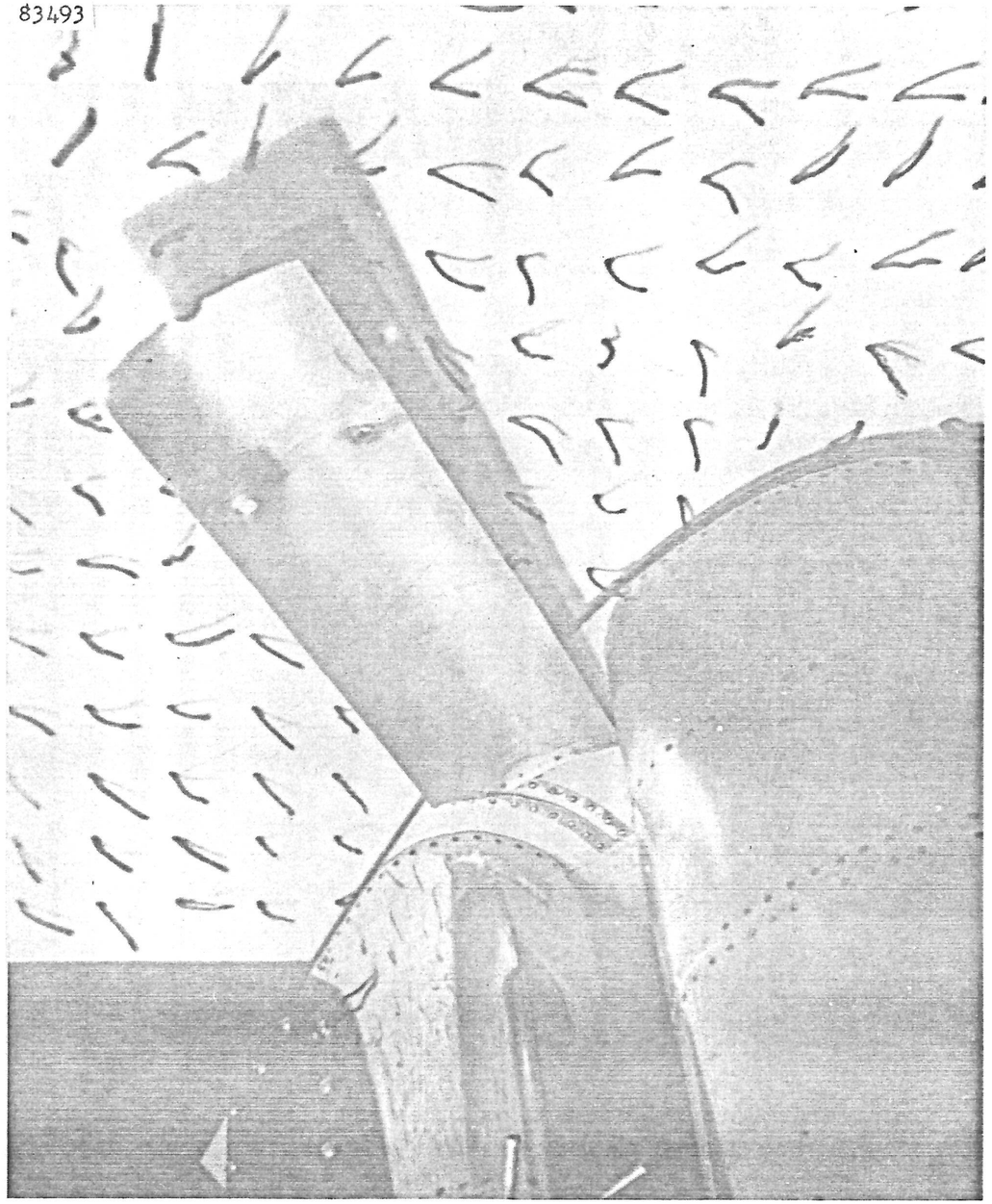

FIG. 26 LOWER NOZZLE GUIDE VANE FAILURE

4298-802-1

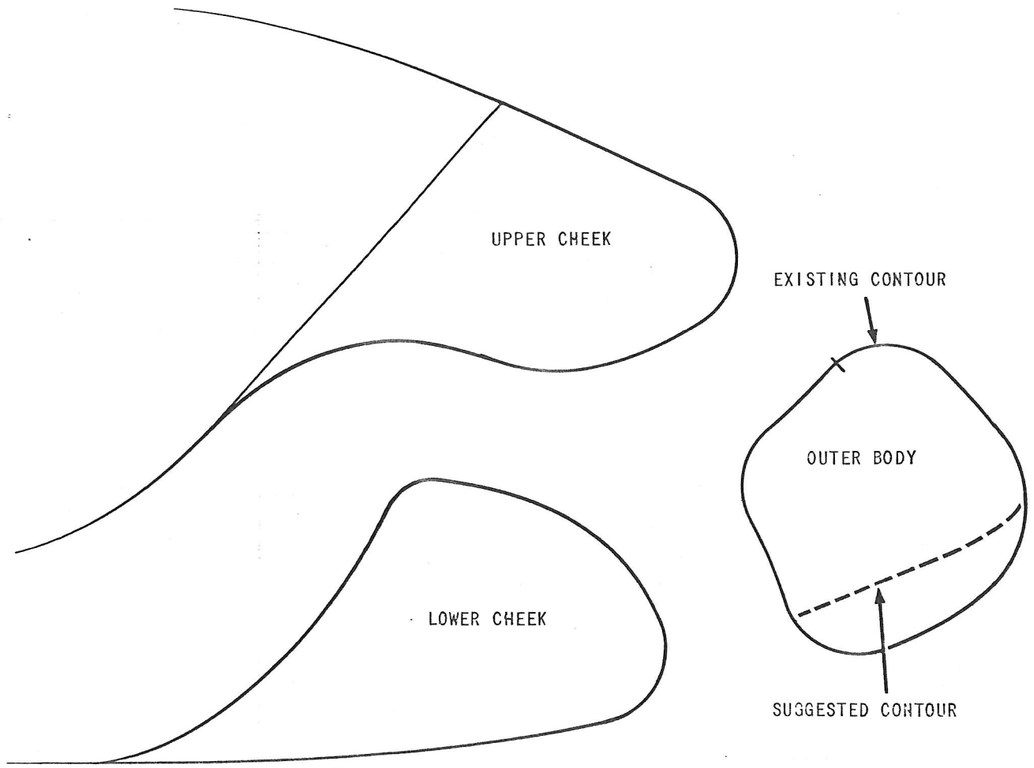

FIG. 27 ALTERNATE OUTERBODY FOR SIMPLIFIED TRANSITION CONTROL

APPENDIX 'B'

TEST DATA

TEST LOG:- FULL SCALE 20° SEGMENT AVROCAR

2.7 Hrs. Logged at 15 inches H20 Gauge

4.8 Hrs. Logged at 25 inches H20 Gauge

AVRO AIRCRAFT LIMITED

TECHNICAL DEPT. (AIRFRAME)

AIRCRAFT - -

WEIGHT - -

C. G. POSITION -

REPORT NO. - AVRO/SPG/TR 267

SHEET - - 67

DATE - -

PREPARED BY -

RUN	1 PHASE	2 3 4 BASIC CONFIGURATION	5 6 7 INNER CASCADE CONFIGURATION	8 9 GUIDE VANE CONFIGURATION	10 PNEUMATIC TRANSITION VENT SETTING	11 12 13 14 MECHANICAL TRANSITION SPOILER PROJECTION (INCHES) LOWER	UPPER	15 TEST DATE	16 TEST TIME START / FINISH	17 PT in H20 g	18 P_a in Hga	19 TEST DESCRIPT.
A	1	Pneumatic Transition Spoiler as in Fig. 3.	Two Inner Turning Vanes as in Fig. 9A	No Exit Guide Vanes	Closed	0	0	Oct. 30/58	1.30 am / 2.50 pm	15	29.44	Complete Data Run
B					"			"	3.25 am / 4.12 am	25	"	"
C					Open			Oct. 31/58	2.00 am / 2.50 am	15	29.31	"
D					"			"	3.25 am / 4.15 am	25	"	"
E	2	Mechanical Transition Spoilers shown in Fig.7	Two Inner Turning Vanes as in Fig. 9A.	No Exit Guide Vanes	Closed	0.5	0.5	Nov. 5/58	1.20 am / 2.05 am	25	29.05	"
F				"		1.0	1.0	"	4.00 am / 4.35 am	25	"	"
G				Exit Guide Vanes in Position A Fig. 10.1		0.5	0.5	Nov. 6/58	12.40 am / 1.30 am	25	28.69	"
H				"		0	0	"	2.55 am / 3.25 am	25	"	"
I				No Exit Guide Vanes		1.5	1.5	Nov. 7/58	12.52 am / 1.38 am	25	29.15	"
J		No Outer Body		"		-	-	"	3.00 am / 3.30 am	15	"	"

TEST LOG:- FULL SCALE 20° SEGMENT AVROCAR

Approximately 8.0 Hrs Logged at 18 in. H20 Gauge.
Approximately 0.5 Hrs Logged at 25 in. H20 Gauge.

AVRO AIRCRAFT LIMITED
TECHNICAL DEPT. (AIRFRAME)

AIRCRAFT - -
WEIGHT - -
C. G. POSITION -

REPORT NO. - AVRO/SPG/TR 267
SHEET - - 69
DATE -
PREPARED BY -

RUN	1 PHASE	2 3 4 BASIC CONFIGURATION	5 6 7 INNER CASCADE CONFIGURATION	8 9 GUIDE VANE CONFIGURATION	10 11 PNEUMATIC TRANSITION VENT SETTING	12 13 14 MECHANICAL TRANSITION SPOILER PROJECTION (INCHES) LOWER	UPPER	15 TEST DATE	16 TEST TIME START FINISH	17 PT in H20 g	18 Pa in Hga	19 TEST DESCRIPT.
Q	4	Mechanical Transition Spoiler as in Fig. 7 End Plates on	3/4" T.E. Extension 5° Droop - Fig. 9B	B with 3/4" T.E. same Radius as Vane(Fig.10-6)	CLOSED	0	0	Jan. 5/59	3.30 pm 4.20 pm	18	29.59	Data Run
R				A with 1" T.E. same Radius as Vane(Fig.10-7)		0.5	0.5	Jan. 5/59		18	29.67	Data Run
-				A with 1" T.E. 1.10" from Cheek (Curled in)		0.5	0.5					Flow Study Only
-				Fig.10-8		0	0					"
S						0.25	0.25			16		Data Run
T		As in Fig.7 with outer part of Wing Tip Removed	T.E. Extension Removed Fig. 9A			0.25	0.25			18		"
-						0	0.25	Jan. 7/59				Flow Study Only
-						0	0					"
-				A with 1" Strt. T.E. 1.15" from Cheek Fig.10-9		0	0					"
U				A with 1" Curled T.E. & 1/8 R.L.E		0	0					Data Run
V		As in Fig. 7		A with 1" Curled T.E. 1.10" from Cheek Fig.10-8		0	0			17		"
W						0.25	0.25			25		"
-		As for Q - End Plates Removed				0.25	0.25			18		"
X		As Fig. 7 with outer Part of Wing Tip Removed End Plates Replaced		C with 1" Curled T.E. 1.40 from Cheek Fig.10-11		0.25	0.25		Jan. 8/59	18	29.59	"
-						0	0.25		"	18	"	Flow Study Only

SECRET

AVRO/SPG/TR 267

FIG. 28 SECTION DIFFERENTIAL MASS FLOW VS CONTROL SETTING

PNEUMATIC TRANSITION SPOILER CONFIGURATION

NO OUTER VANES - VENT CLOSED

RUN A

P_T/Pa

1.04

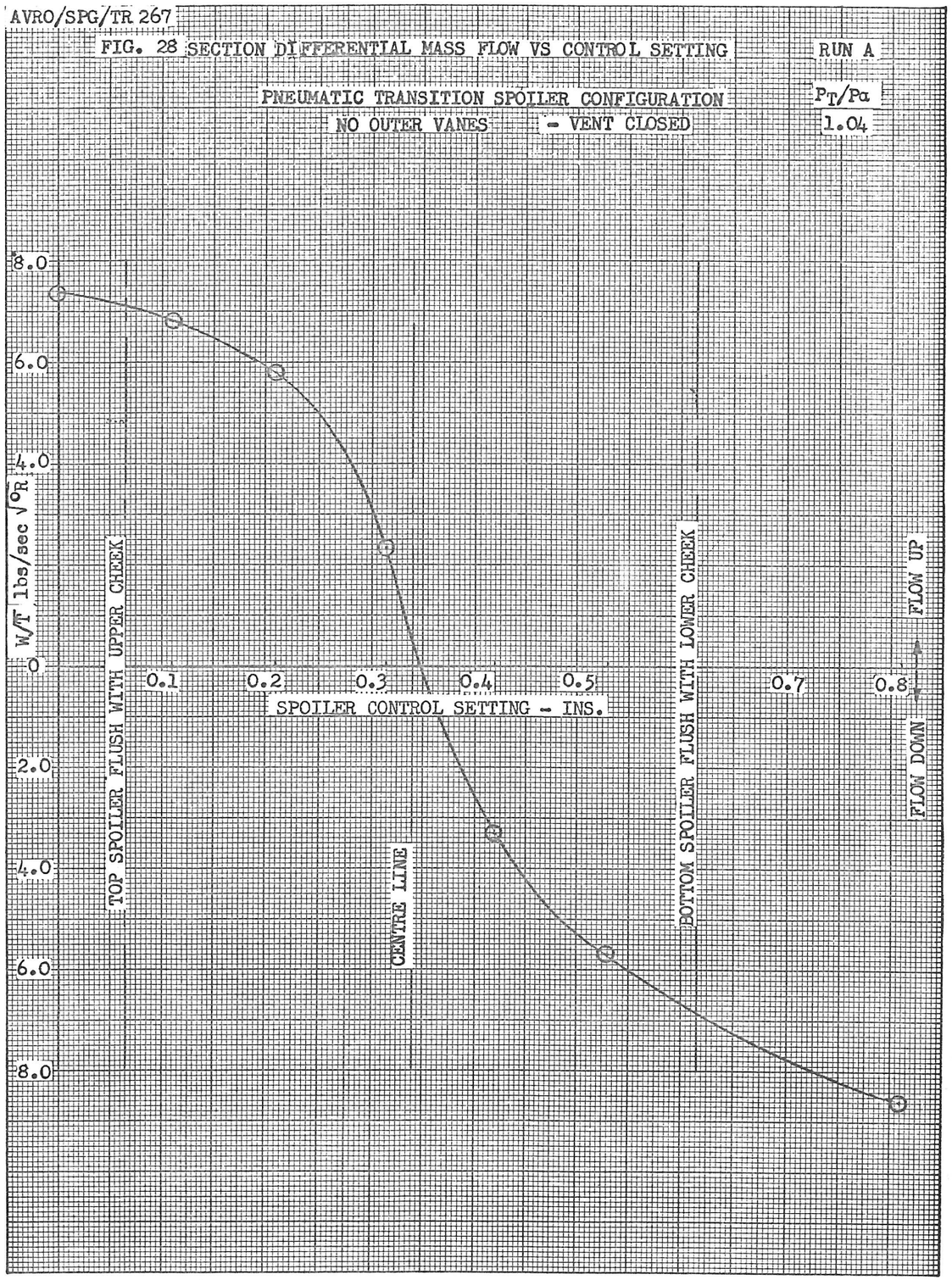

TEST LOG:- FULL SCALE 20° SEGMENT AVROCAR

Approximately 4 hrs. Logged at 15 in. H20 Gauge.

AVRO AIRCRAFT LIMITED

TECHNICAL DEPT. (AIRFRAME)

AIRCRAFT - -

WEIGHT - -

C. G. POSITION -

REPORT NO. - AVRO/SPG/TR 267

SHEET - - 68

DATE - -

PREPARED BY -

RUN	1 PHASE	2 BASIC CONFIGURATION	3	4	5 INNER CASCADE CONFIGURATION	6	7	8 GUIDE VANE CONFIGURATION	9	10 PNEUMATIC TRANSITION VENT SETTING	11	12 MECHANICAL TRANSITION SPOILER PROJECTION INCHES LOWER	13	14 UPPER	15 TEST DATE	16 TEST TIME START FINISH	17 PT in H20 g	18 P_a in Hga	19 TEST DESCRIPT.
K	3	Mechanical Transition Spoiler as in Fig. 7			¾" T.E. Extension 5° Droop - Fig. 9B			Position A Fig. 10-1		Closed		0.5		0.5	Dec. 17/58	11.45 am 12.35 pm	16	29.10	Complete Data Run
L								Position B Fig. 10-2				0.5		0.5	"		15		Flow Study
—		No Outer Body						"							"				"
—		No Outer Body End Plates Added						"							Dec. 18/58				"
—								Position B (Fig. 10-1)							"				"
—								B with Rounded Leading Edge. Fig. 10-3							"				"
M		Mechanical Transition Spoiler as in Fig. 7 End Plates Added						"				0.5		0.5	"		15		"
N								B with Rounded Leading Edge & Trailing Edge (Fig. 10-4)				0.5		0.5	Dec. 19/58	12.20 am 12.35 am	15		"
O								"				-		0	"		16.5		Data Run
—								A with Trailing Edge Fig. 10-5				0.5		0.5	"		"		Flow Study Only
P								B with Trailing Edge Fig. 10-6				0.5		0.5	"	6.45 pm 7.30 pm	13		Data Run

SECRET

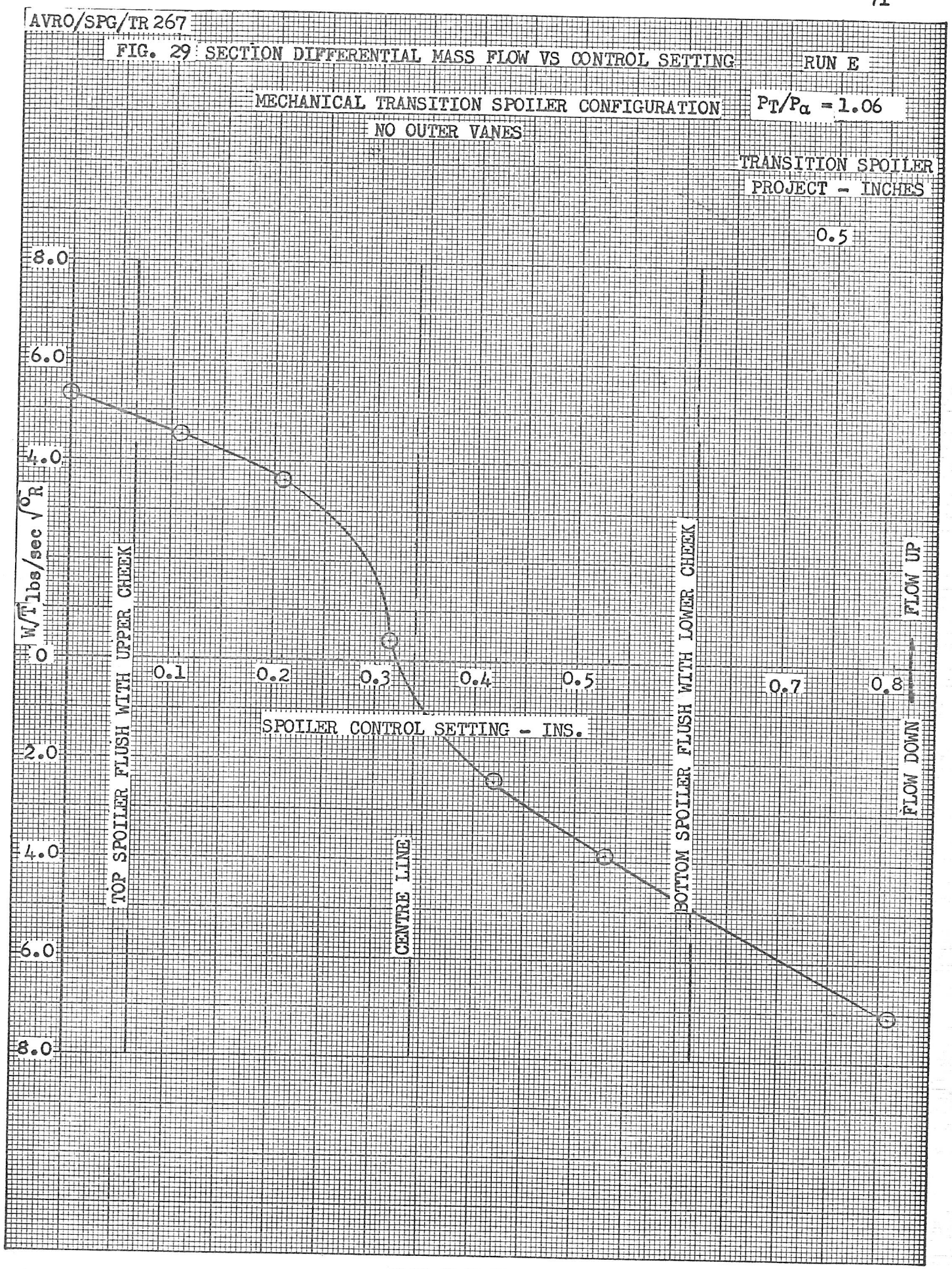
AVRO/SPG/TR 267
FIG. 29 SECTION DIFFERENTIAL MASS FLOW VS CONTROL SETTING
RUN E
MECHANICAL TRANSITION SPOILER CONFIGURATION
NO OUTER VANES
$P_T/P_\alpha = 1.06$
TRANSITION SPOILER PROJECT - INCHES
0.5
8.0
6.0
4.0
2.0
0
4.0
6.0
8.0
$W\sqrt{T}$ lbs/sec $\sqrt{\sigma_R}$
TOP SPOILER FLUSH WITH UPPER CHEEK
CENTRE LINE
BOTTOM SPOILER FLUSH WITH LOWER CHEEK
FLOW UP
FLOW DOWN
0.1
0.2
0.3
0.4
0.5
0.7
0.8
SPOILER CONTROL SETTING - INS.

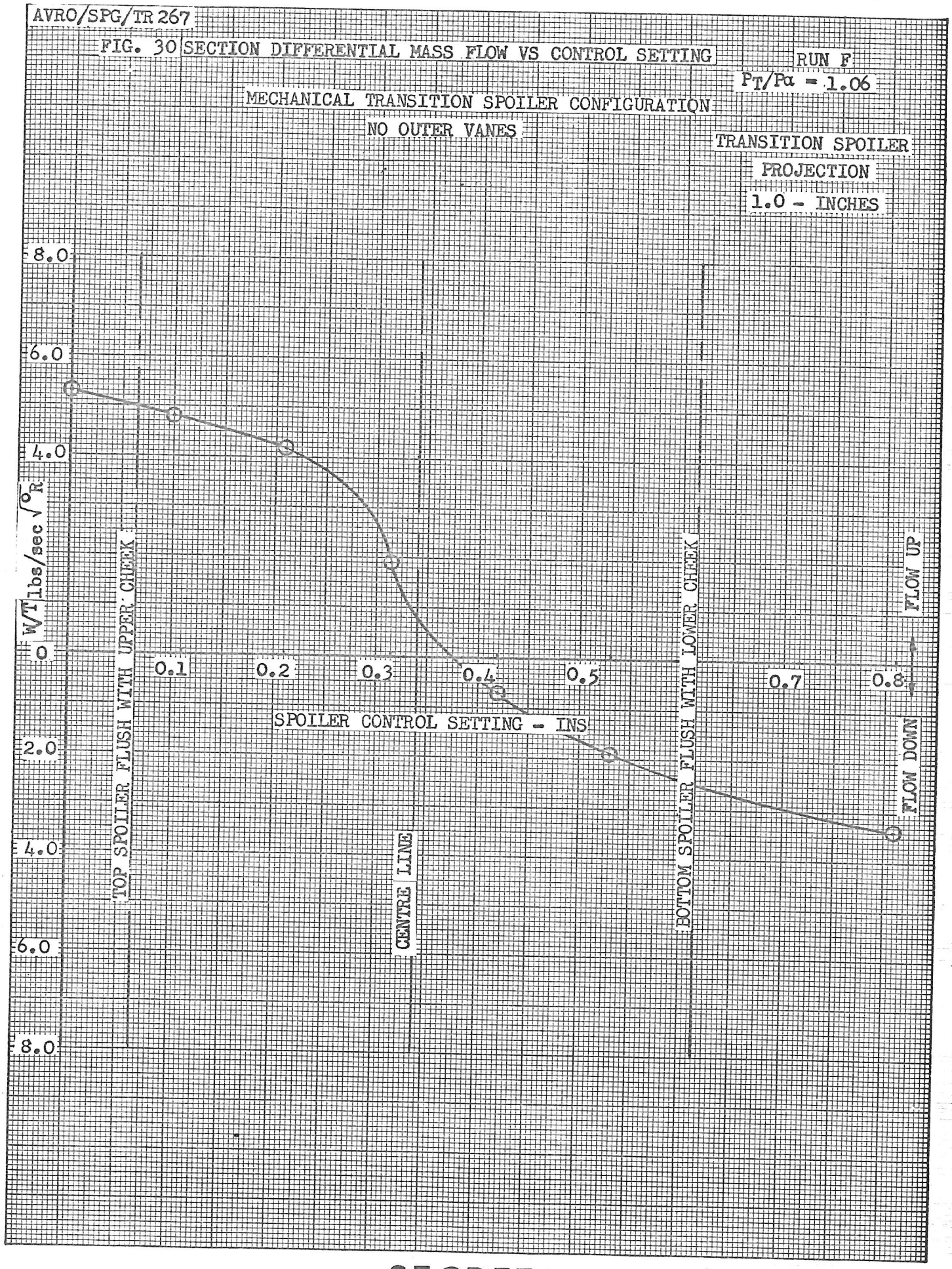
AVRO/SPG/TR 267
FIG. 30 SECTION DIFFERENTIAL MASS FLOW VS CONTROL SETTING
RUN F
P_T/P_α = 1.06
MECHANICAL TRANSITION SPOILER CONFIGURATION
NO OUTER VANES
TRANSITION SPOILER PROJECTION
1.0 - INCHES
8.0
6.0
4.0
$W\sqrt{T}$ lbs/sec $\sqrt{°R}$
0
0.1
0.2
0.3
0.4
0.5
0.7
0.8
FLOW UP
SPOILER CONTROL SETTING - INS
2.0
4.0
6.0
8.0
FLOW DOWN
TOP SPOILER FLUSH WITH UPPER CHEEK
CENTRE LINE
BOTTOM SPOILER FLUSH WITH LOWER CHEEK

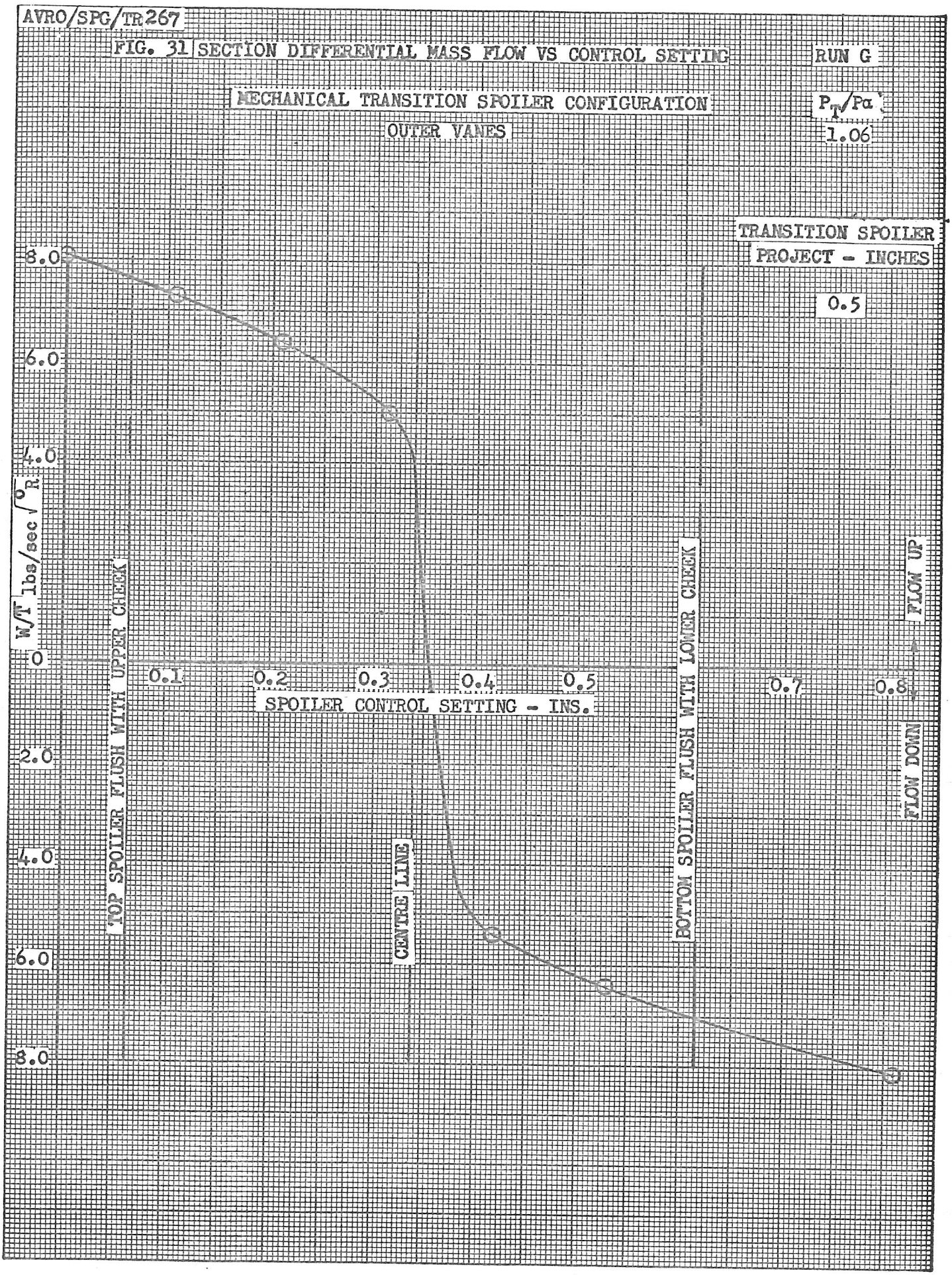
AVRO/SPG/TR267
FIG. 31 SECTION DIFFERENTIAL MASS FLOW VS CONTROL SETTING
RUN G
MECHANICAL TRANSITION SPOILER CONFIGURATION
OUTER VANES
$P_T/P\alpha$
1.06
TRANSITION SPOILER
PROJECT - INCHES
0.5
8.0
6.0
4.0
W/T lbs/sec $\sqrt{\theta_R}$
0
0.1
0.2
0.3
0.4
0.5
0.7
0.8
SPOILER CONTROL SETTING - INS.
FLOW UP
FLOW DOWN
TOP SPOILER FLUSH WITH UPPER CHEEK
CENTRE LINE
BOTTOM SPOILER FLUSH WITH LOWER CHEEK
2.0
4.0
6.0
8.0

AVRO/SPG/TR 267

FIG. 32 SECTION DIFFERENTIAL MASS FLOW VS CONTROL SETTING

RUN I

MECHANICAL TRANSITION SPOILER CONFIGURATION

$P_T/Pa = 1.06$

NO OUTER VANES

TRANSITION SPOILER PROJECT - INCHES

1.5

8.0

6.0

4.0

$W\sqrt{T}$ lbs/sec $\sqrt{°R}$

0

1.0

0.2

0.3

0.4

0.5

0.7

0.8

SPOILER CONTROL SETTING - INS

FLOW UP

FLOW DOWN

TOP SPOILER FLUSH WITH UPPER CHEEK

CENTRE LINE

BOTTOM SPOILER FLUSH WITH LOWER CHEEK

2.0

4.0

6.0

8.0

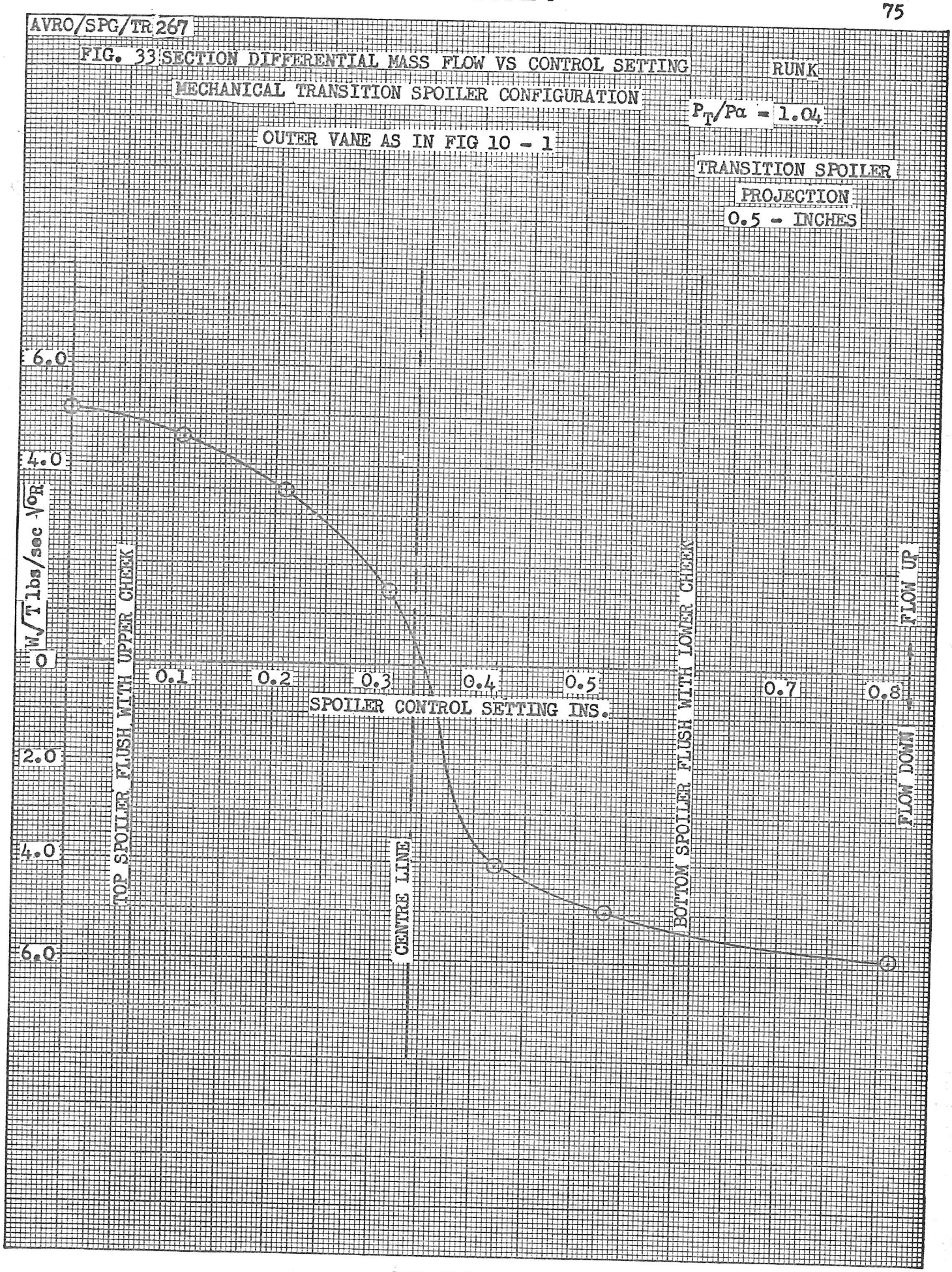
AVRO/SPG/TR 267
FIG. 33 SECTION DIFFERENTIAL MASS FLOW VS CONTROL SETTING
RUNK
MECHANICAL TRANSITION SPOILER CONFIGURATION
$P_T/P\alpha$ = 1.04
OUTER VANE AS IN FIG 10 - 1
TRANSITION SPOILER PROJECTION 0.5 - INCHES
6.0
4.0
$W\sqrt{T}$ lbs/sec $\sqrt{°R}$
0
2.0
4.0
6.0
TOP SPOILER FLUSH WITH UPPER CHEEK
CENTRE LINE
BOTTOM SPOILER FLUSH WITH LOWER CHEEK
FLOW UP
FLOW DOWN
0.1
0.2
0.3
0.4
0.5
0.7
0.8
SPOILER CONTROL SETTING INS.

AVRO/SPG/TR 267

FIG. 34 SECTION DIFFERENTIAL MASS FLOW VS CONTROL SETTING RUN P

MECHANICAL TRANSITION SPOILER CONFIGURATION

OUTER VANES AS IN FIG 10 - 6

PT/pa = 1.04

TRANSITION SPOILER PROJECTION 0.5 - INCHES

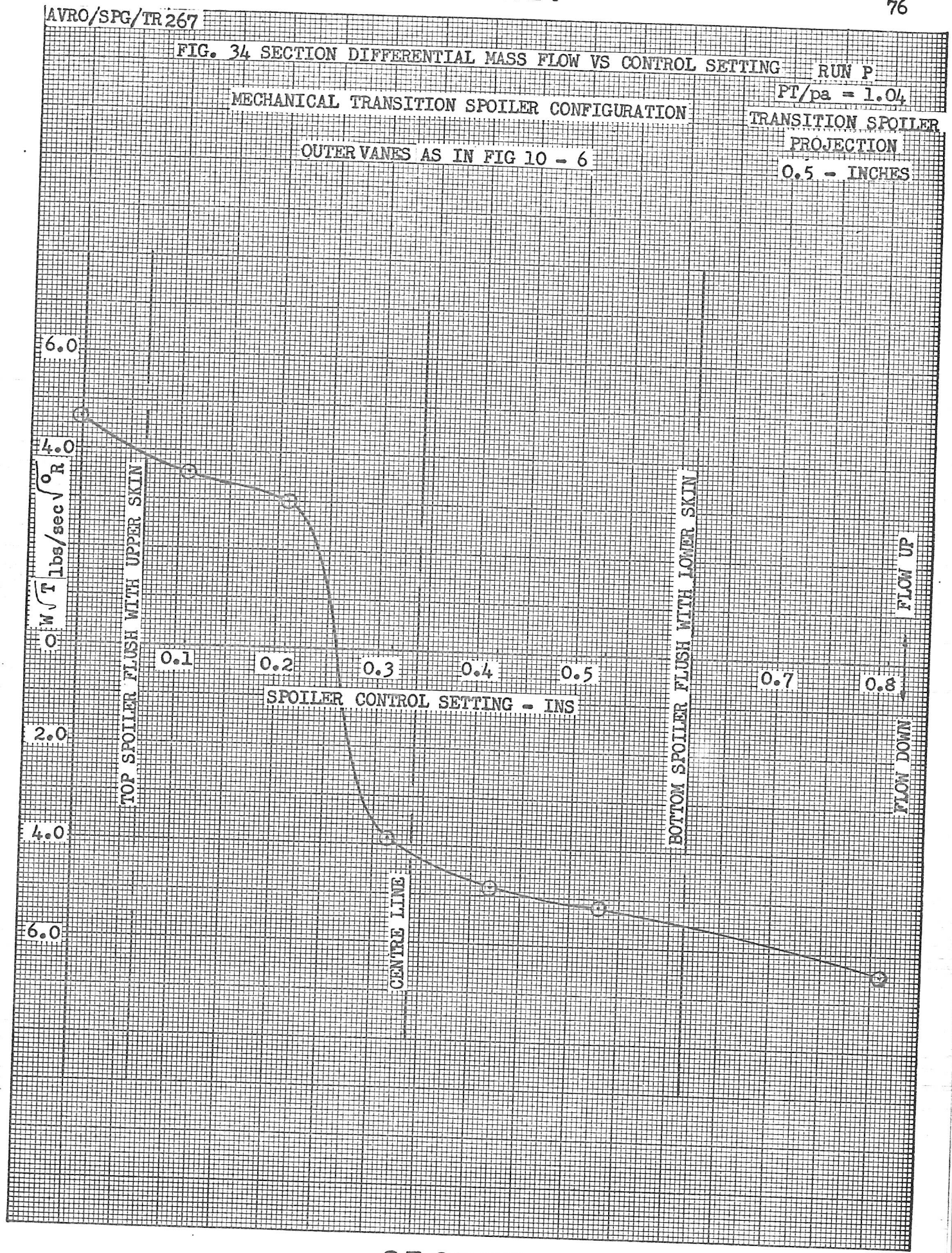

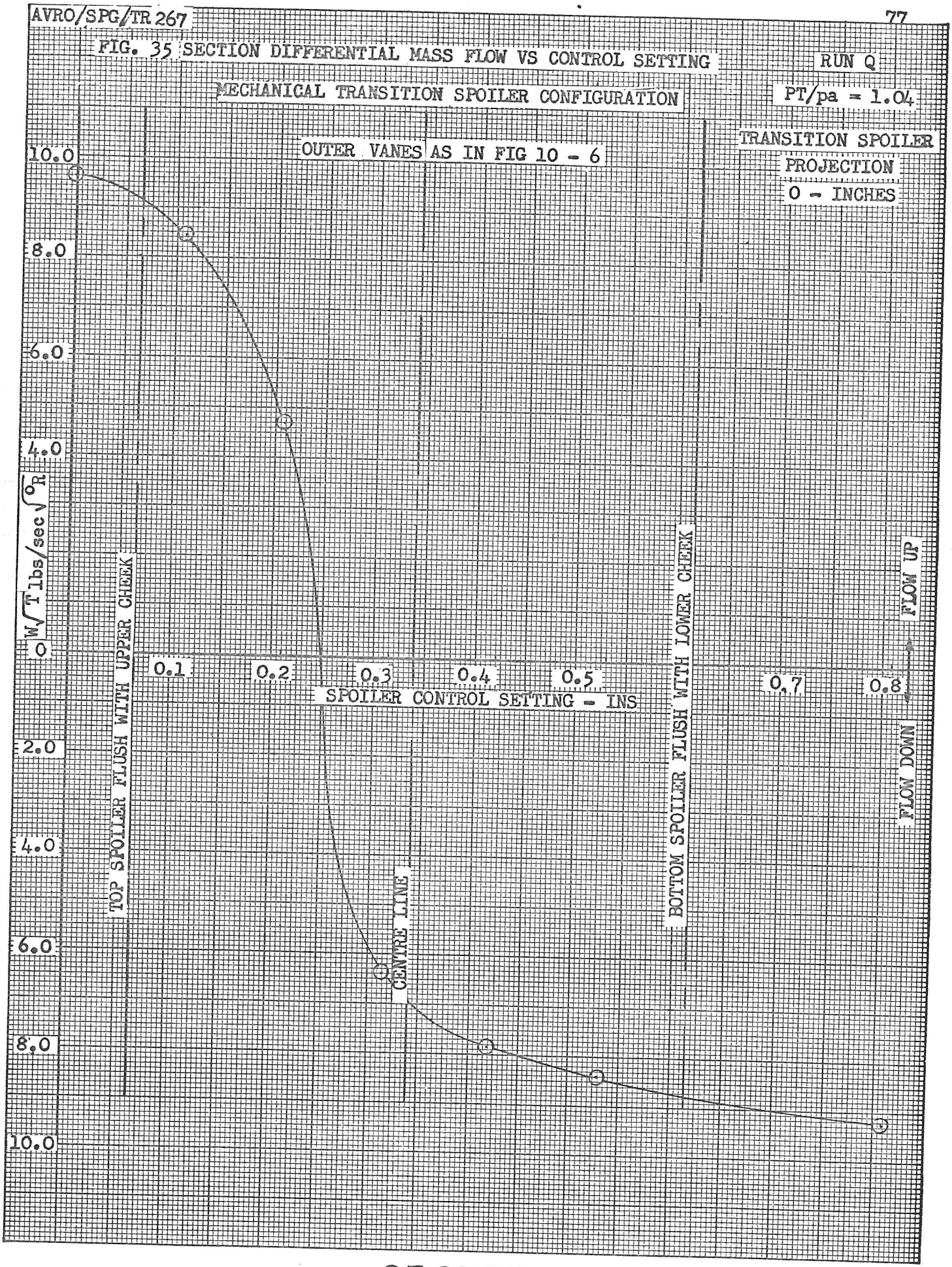
FIG. 35 SECTION DIFFERENTIAL MASS FLOW VS CONTROL SETTING
MECHANICAL TRANSITION SPOILER CONFIGURATION
RUN Q
PT/pa = 1.04
TRANSITION SPOILER PROJECTION 0 - INCHES
OUTER VANES AS IN FIG 10 - 6
10.0
8.0
6.0
4.0
2.0
0
4.0
6.0
8.0
10.0
W√T lbs/sec √°R
TOP SPOILER FLUSH WITH UPPER CHEEK
CENTRE LINE
BOTTOM SPOILER FLUSH WITH LOWER CHEEK
FLOW UP
FLOW DOWN
0.1
0.2
0.3
0.4
0.5
0.7
0.8
SPOILER CONTROL SETTING - INS

FIG. 36 SECTION DIFFERENTIAL MASS FLOW VS CONTROL SETTING

MECHANICAL TRANSITION SPOILER CONFIGURATION

RUN T

PT/pa = 1.04

TRANSITION SPOILER PROJECTION 0.25 - INCHES

OUTER VANES AS IN FIG 10 - 8

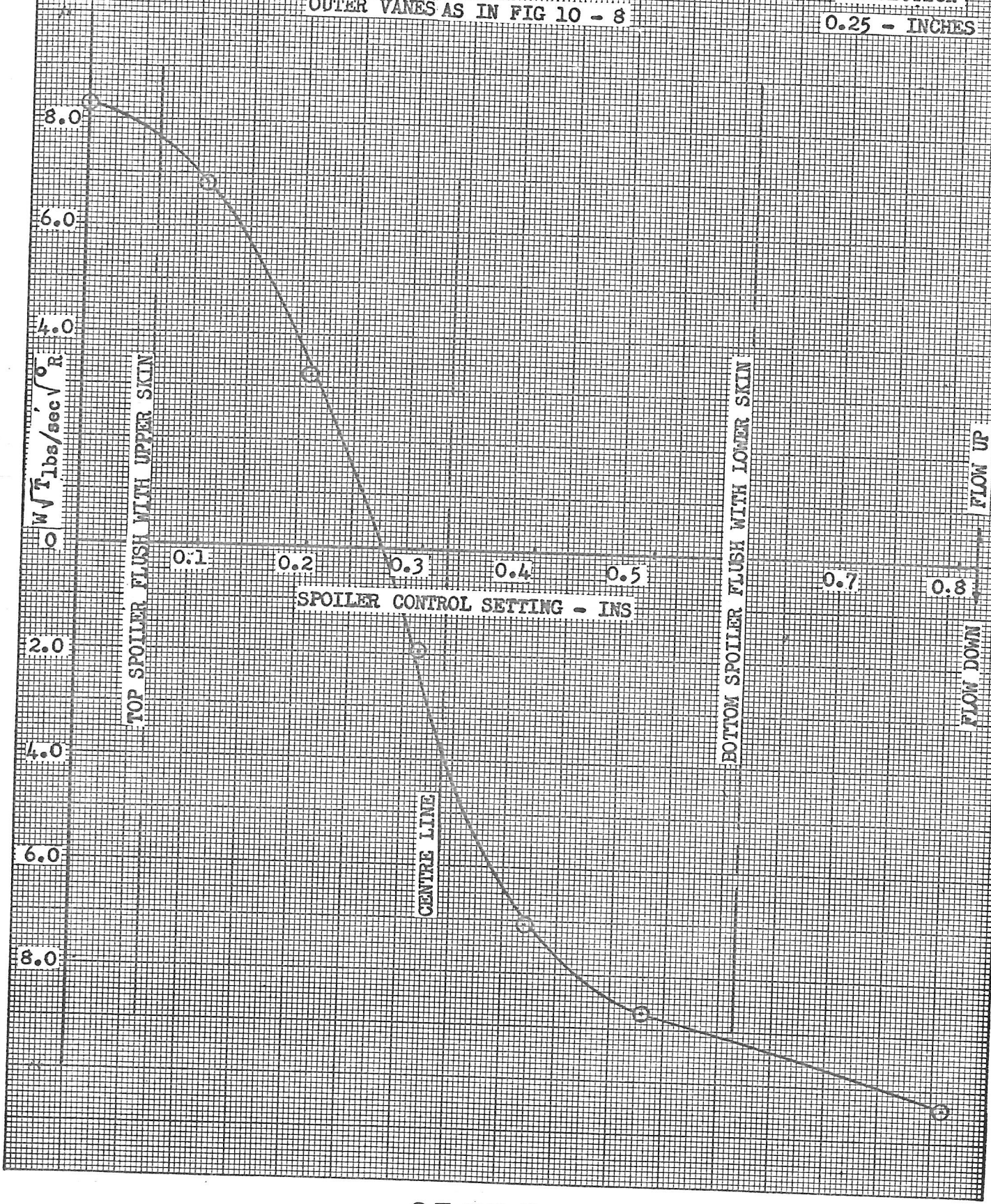

AVRO/SPG/TR267

FIG. 37 SECTION DIFFERENTIAL MASS FLOW VS CONTROL SETTING

MECHANICAL TRANSITION SPOILER CONFIGURATION

OUTER VANES AS IN FIG 10 -8

RUN V

PT/pa = 1.04

TRANSITION SPOILER PROJECTION 0 - INCHES

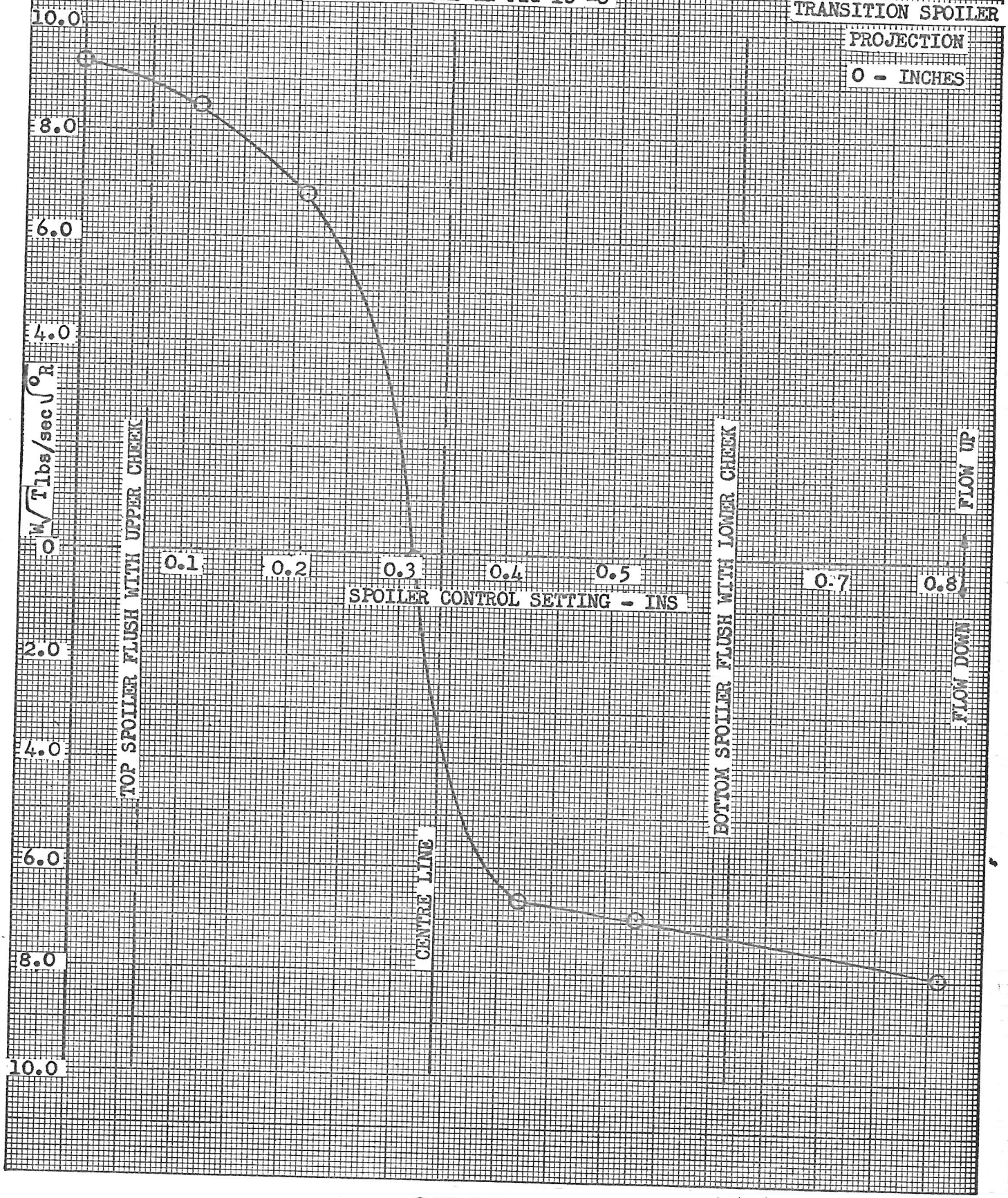

AVRO/SPG/TR267

FIG. 38 SECTION DIFFERENTIAL MASS FLOW VS CONTROL SETTING

RUN W

MECHANICAL TRANSITION SPOILER CONFIGURATION

SAME AS T WITH PT/pa = 1.06

TRANSITION SPOILER PROJECTION 0.25 - INCHES

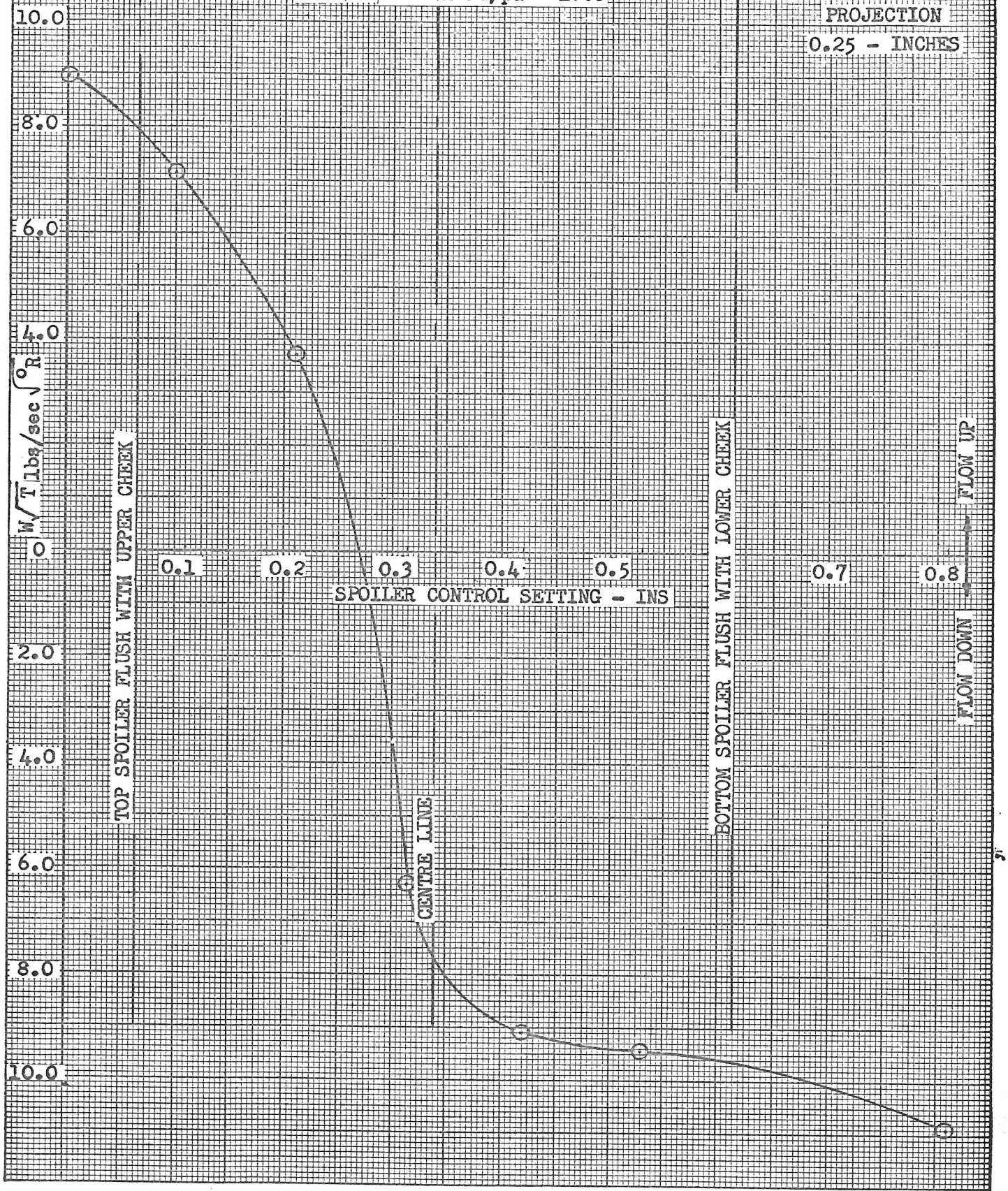

AVRO/SPG/TR 267

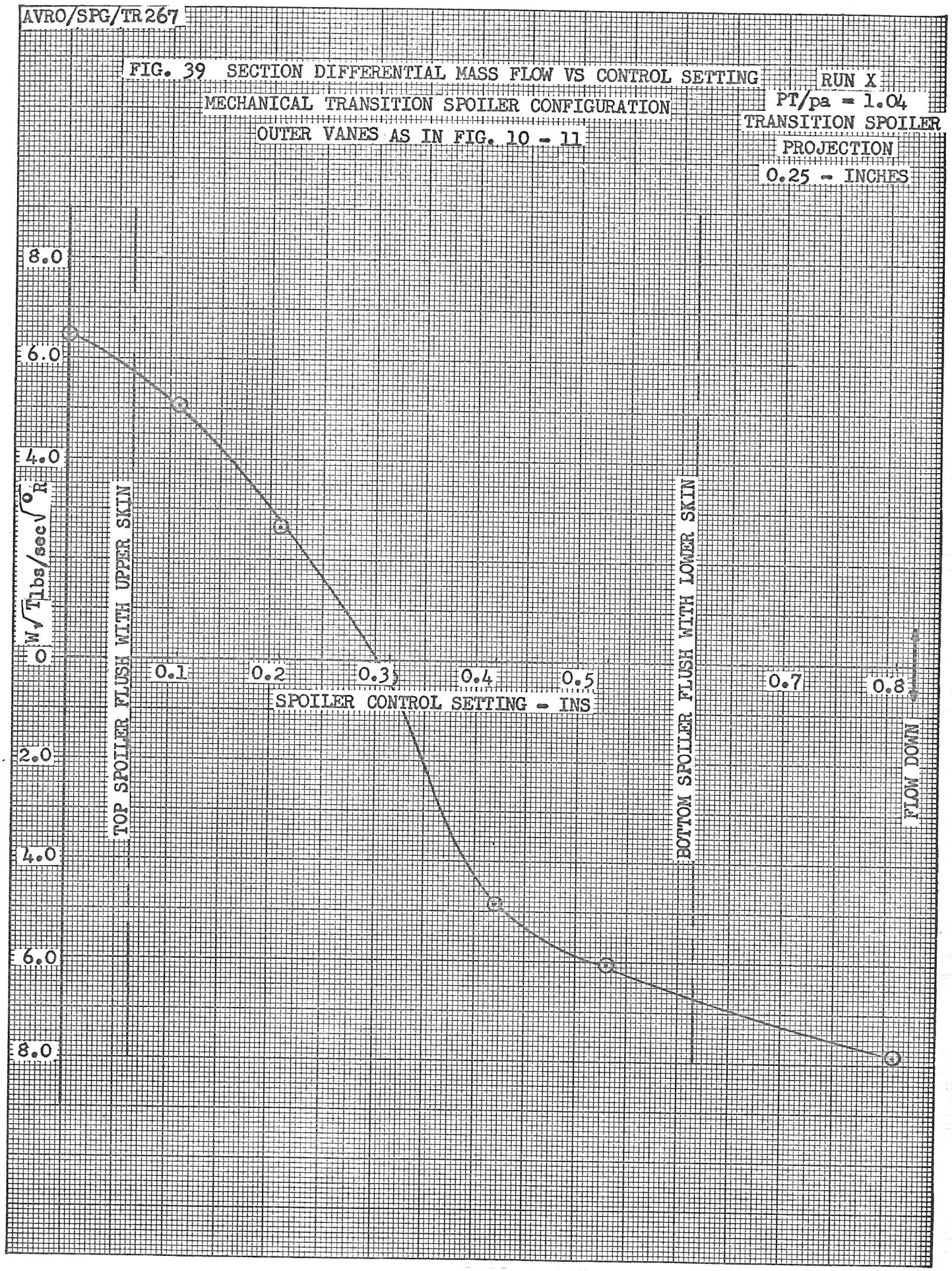

AVRO/SPG/TR 267

FIG. 40 SECTION CONTROL MASS FLOW VS CONTROL SETTING

RUN A

$P_T/P\alpha$ 1.04

PNEUMATIC TRANSITION SPOILER CONFIGURATION

NO OUTER VANES - VENT CLOSED

UPPER NOZZLE RAKE

$W\sqrt{T}$ lbs/sec $\sqrt{\theta_R}$

8.0

6.0

4.0

0

TOP SPOILER FLUSH WITH UPPER CHEEK

CENTRE LINE

BOTTOM SPOILER FLUSH WITH LOWER CHEEK

0 0.1 0.2 0.3 0.4 0.5 0.6 0.7 0.8

SPOILER CONTROL SETTING - INS.

LOWER NOZZLE RAKE

$W\sqrt{T}$ lbs/sec $\sqrt{\theta_R}$

8.0

4.0

2.0

0

TOP SPOILER FLUSH WITH UPPER CHEEK

CENTRE LINE

BOTTOM SPOILER FLUSH WITH LOWER CHEEK

0 0.1 0.2 0.3 0.4 0.5 0.6 0.7 0.8

SPOILER CONTROL SETTING - INS.

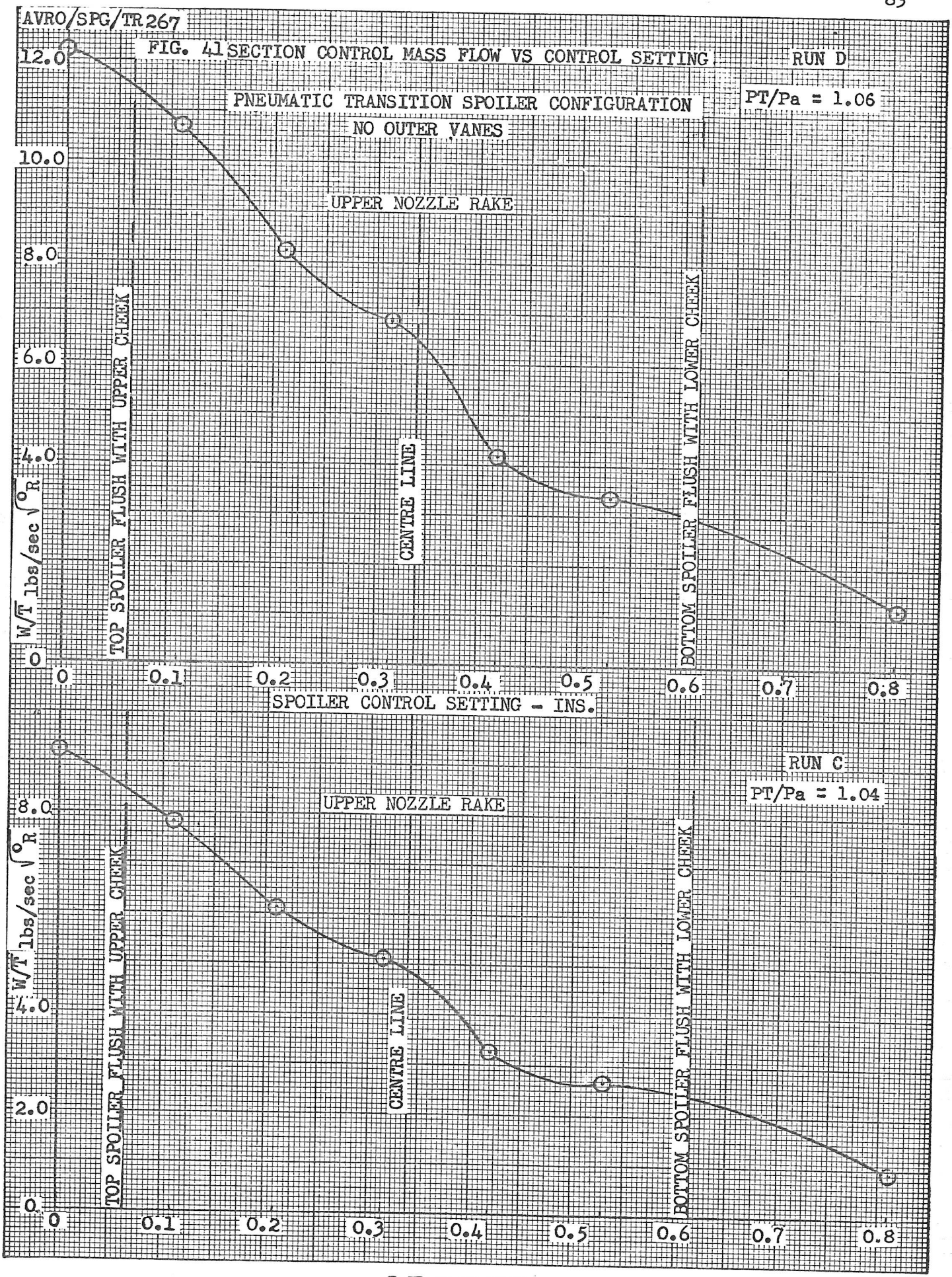
AVRO/SPG/TR 267
FIG. 41 SECTION CONTROL MASS FLOW VS CONTROL SETTING
PNEUMATIC TRANSITION SPOILER CONFIGURATION
NO OUTER VANES
RUN D
PT/Pa = 1.06
UPPER NOZZLE RAKE
CENTRE LINE
TOP SPOILER FLUSH WITH UPPER CHEEK
BOTTOM SPOILER FLUSH WITH LOWER CHEEK
W√T lbs/sec √°R
SPOILER CONTROL SETTING - INS.
RUN C
PT/Pa = 1.04
UPPER NOZZLE RAKE
CENTRE LINE
TOP SPOILER FLUSH WITH UPPER CHEEK
BOTTOM SPOILER FLUSH WITH LOWER CHEEK
W√T lbs/sec √°R

AVRO/SPG/TR267

FIG. 42 SECTION CONTROL MASS FLOW VS CONTROL SETTING

MECHANICAL TRANSITION SPOILER CONFIGURATION

NO OUTER VANES

RUN E

$P_T/P\alpha = 1.06$

TRANSITION SPOILER PROJECT - INCHES 0.5

UPPER NOZZLE RAKE

$\frac{W\sqrt{T}}{\sigma_R}$ lbs/sec

TOP SPOILER FLUSH WITH UPPER CHEEK

CENTRE LINE

BOTTOM SPOILER FLUSH WITH LOWER CHEEK

10.0
8.0
6.0
4.0
0

0 0.1 0.2 0.3 0.4 0.5 0.6 0.7 0.8

SPOILER CONTROL SETTING - INS

LOWER NOZZLE RAKE

$\frac{W\sqrt{T}}{\sigma_R}$ lbs/sec

TOP SPOILER FLUSH WITH UPPER CHEEK

CENTRE LINE

BOTTOM SPOILER FLUSH WITH LOWER CHEEK

10.0
8.0
4.0
2.0
0

0 0.1 0.2 0.3 0.4 0.5 0.6 0.7 0.8

SPOILER CONTROL SETTING - INS.

AVRO/SPG/TR267

FIG. 43 SECTION CONTROL MASS FLOW VS CONTROL SETTING

RUN F

MECHANICAL TRANSITION SPOILER CONFIGURATION

NO OUTER VANES

P_T/P_a = 1.06

TRANSITION SPOILER PROJECTION 1.0 - INCHES

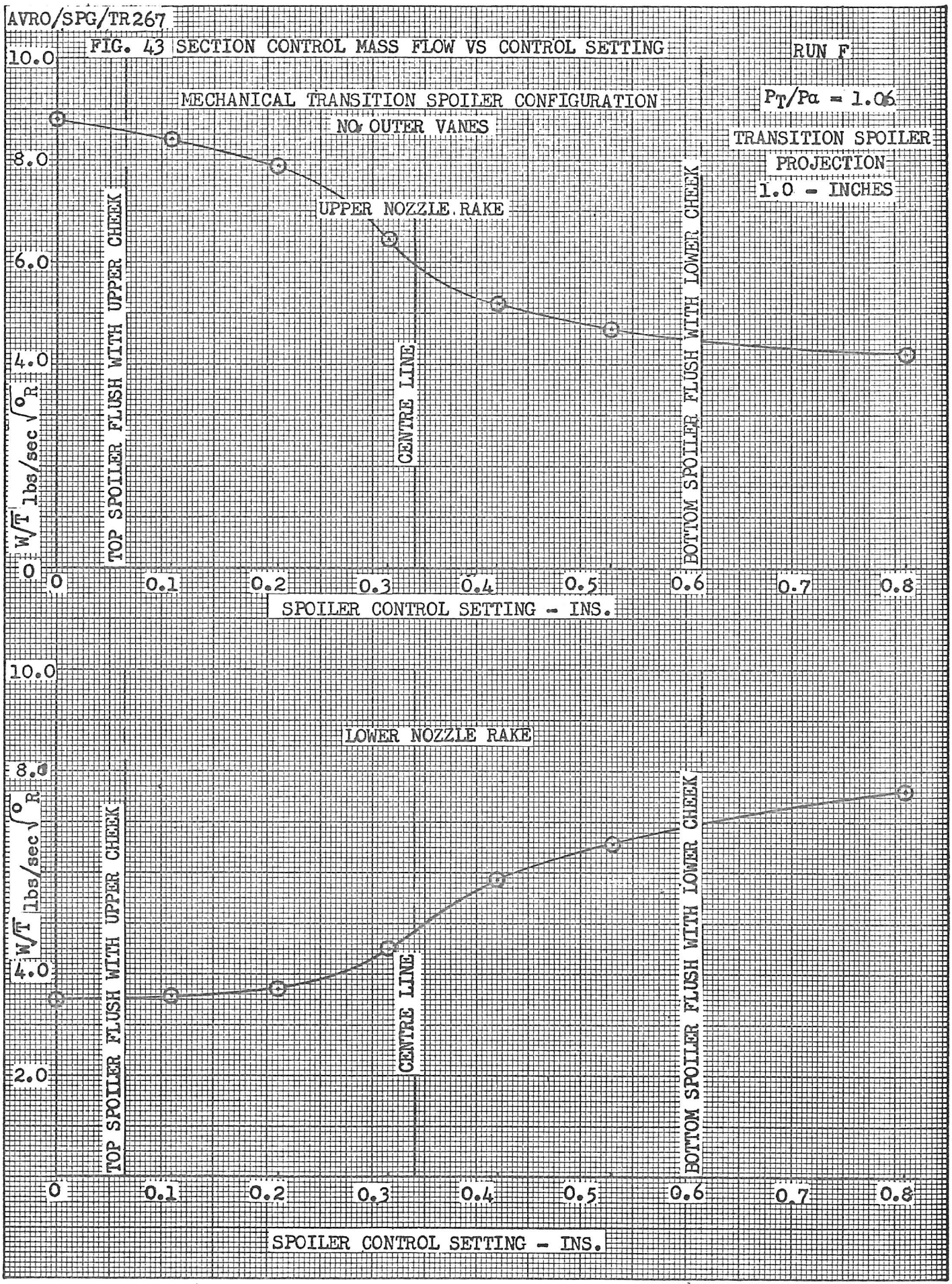

AVRO/SPG/TR267

FIG. 44 SECTION CONTROL MASS FLOW VS CONTROL SETTING

RUN G

MECHANICAL TRANSITION SPOILER CONFIGURATION

$P_T/P\alpha = 1.06$

TRANSITION SPOILER PROJECT - INCHES

0.5

OUTER VANES

UPPER NOZZLE RAKE

CENTRE LINE

TOP SPOILER FLUSH WITH UPPER CHEEK

BOTTOM SPOILER FLUSH WITH LOWER CHEEK

W/T lbs/sec $\sqrt{°R}$

10.0
8.0
6.0
4.0
0

0 0.1 0.2 0.3 0.4 0.5 0.7 0.8

SPOILER CONTROL SETTING - INS.

LOWER NOZZLE RAKE

CENTRE LINE

TOP SPOILER FLUSH WITH UPPER CHECK

BOTTOM SPOILER FLUSH WITH LOWER CHEEK

W/T lbs/sec $\sqrt{°R}$

10.0
8.0
4.0
2.0
0

0 0.1 0.2 0.3 0.4 0.5 0.6 0.7 0.8

SPOILER CONTROL SETTING - INS.

AVRO/SPG/TR267

FIG. 45 SECTION CONTROL MASS FLOW VS CONTROL SETTING

RUN I

MECHANICAL TRANSITION SPOILER CONFIGURATION

NO OUTER VANES

P_T/P_α = 1.06

TRANSITION SPOILER PROJECT - INCHES

1.5

UPPER NOZZLE RAKE

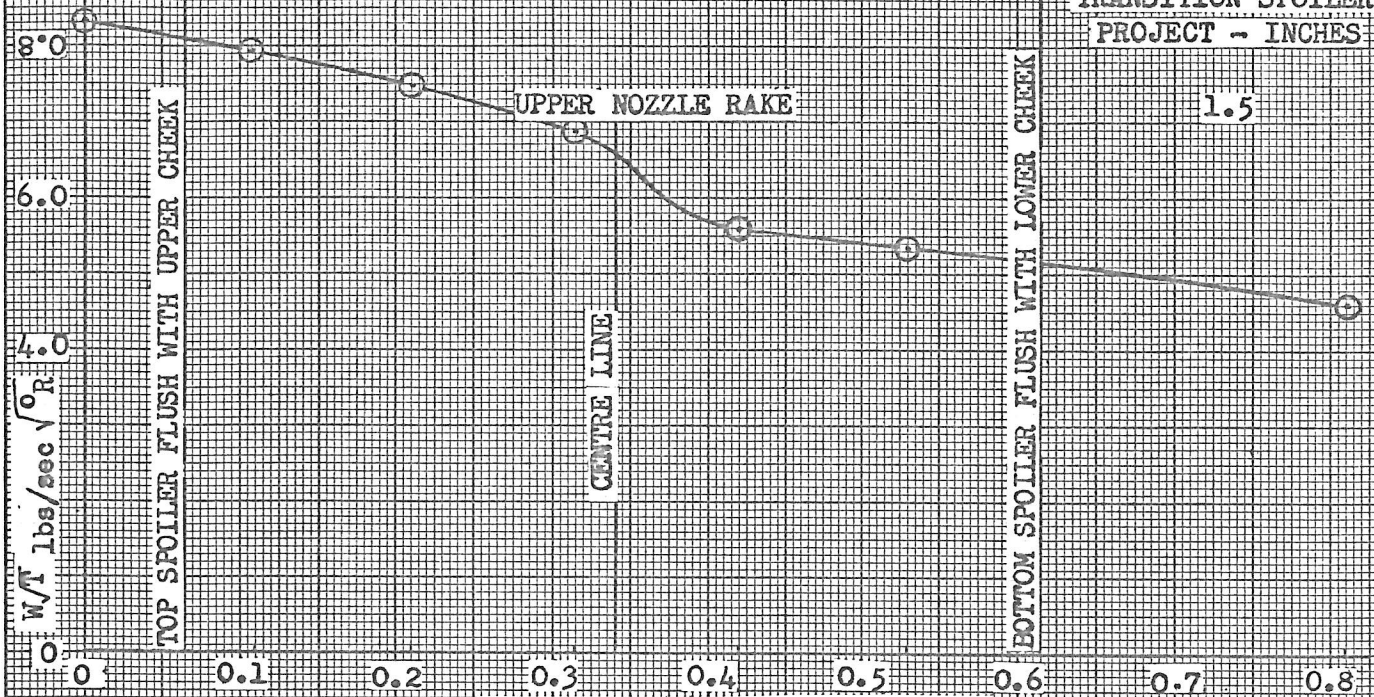

LOWER NOZZLE RAKE

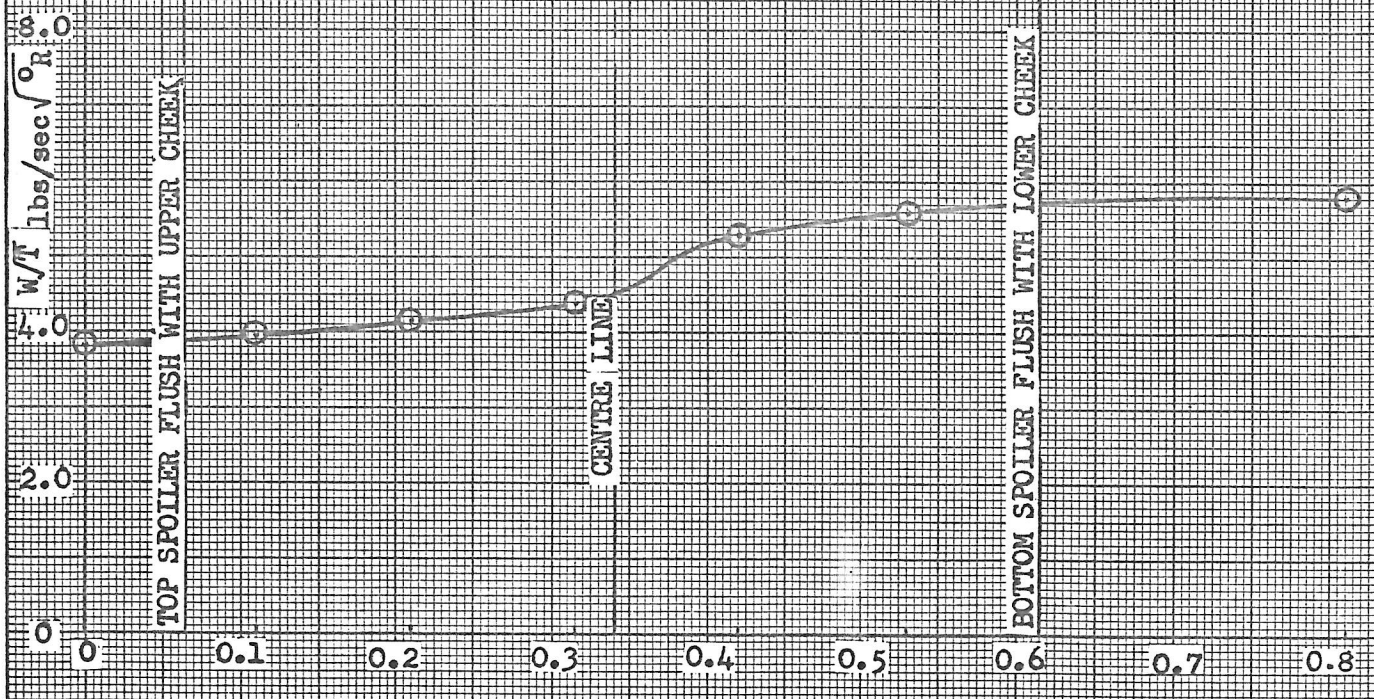

AVRO/SPG/TR267

FIG. 46 SECTION CONTROL MASS FLOW VS CONTROL SETTING

MECHANICAL TRANSITION SPOILER CONFIGURATION

RUN K

$P_T/P\alpha$ = 1.04

OUTER VANES AS IN FIG. 10 - 1

TRANSITION SPOILER PROJECTION 0.5 - INCHES

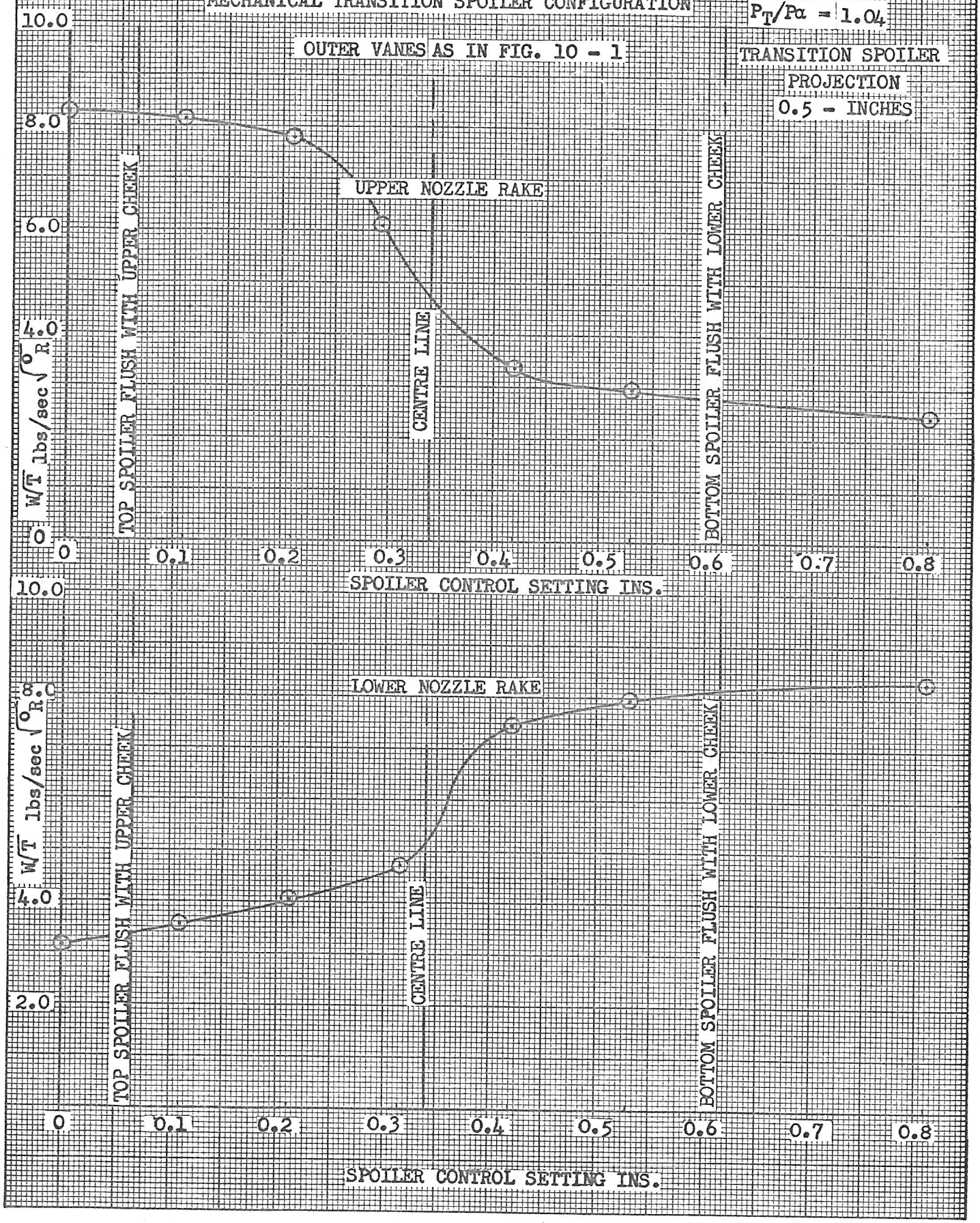

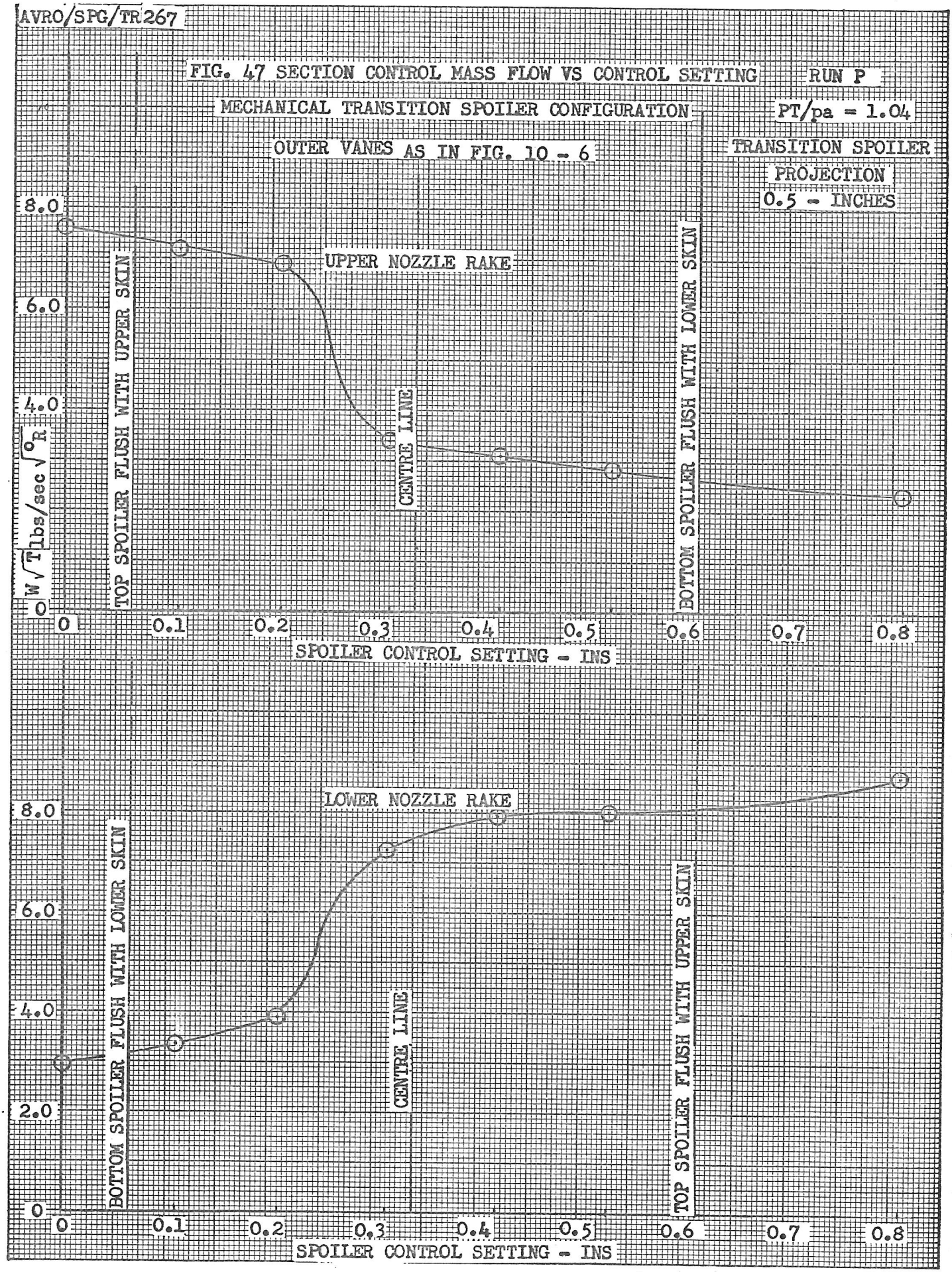
AVRO/SPG/TR267
FIG. 47 SECTION CONTROL MASS FLOW VS CONTROL SETTING
RUN P
MECHANICAL TRANSITION SPOILER CONFIGURATION
PT/pa = 1.04
OUTER VANES AS IN FIG. 10 - 6
TRANSITION SPOILER PROJECTION 0.5 - INCHES
UPPER NOZZLE RAKE
CENTRE LINE
TOP SPOILER FLUSH WITH UPPER SKIN
BOTTOM SPOILER FLUSH WITH LOWER SKIN
$W\sqrt{T}$ lbs/sec $\sqrt{°R}$
8.0
6.0
4.0
0
0
0.1
0.2
0.3
0.4
0.5
0.6
0.7
0.8
SPOILER CONTROL SETTING - INS
LOWER NOZZLE RAKE
CENTRE LINE
BOTTOM SPOILER FLUSH WITH LOWER SKIN
TOP SPOILER FLUSH WITH UPPER SKIN
8.0
6.0
4.0
2.0
0
0
0.1
0.2
0.3
0.4
0.5
0.6
0.7
0.8
SPOILER CONTROL SETTING - INS

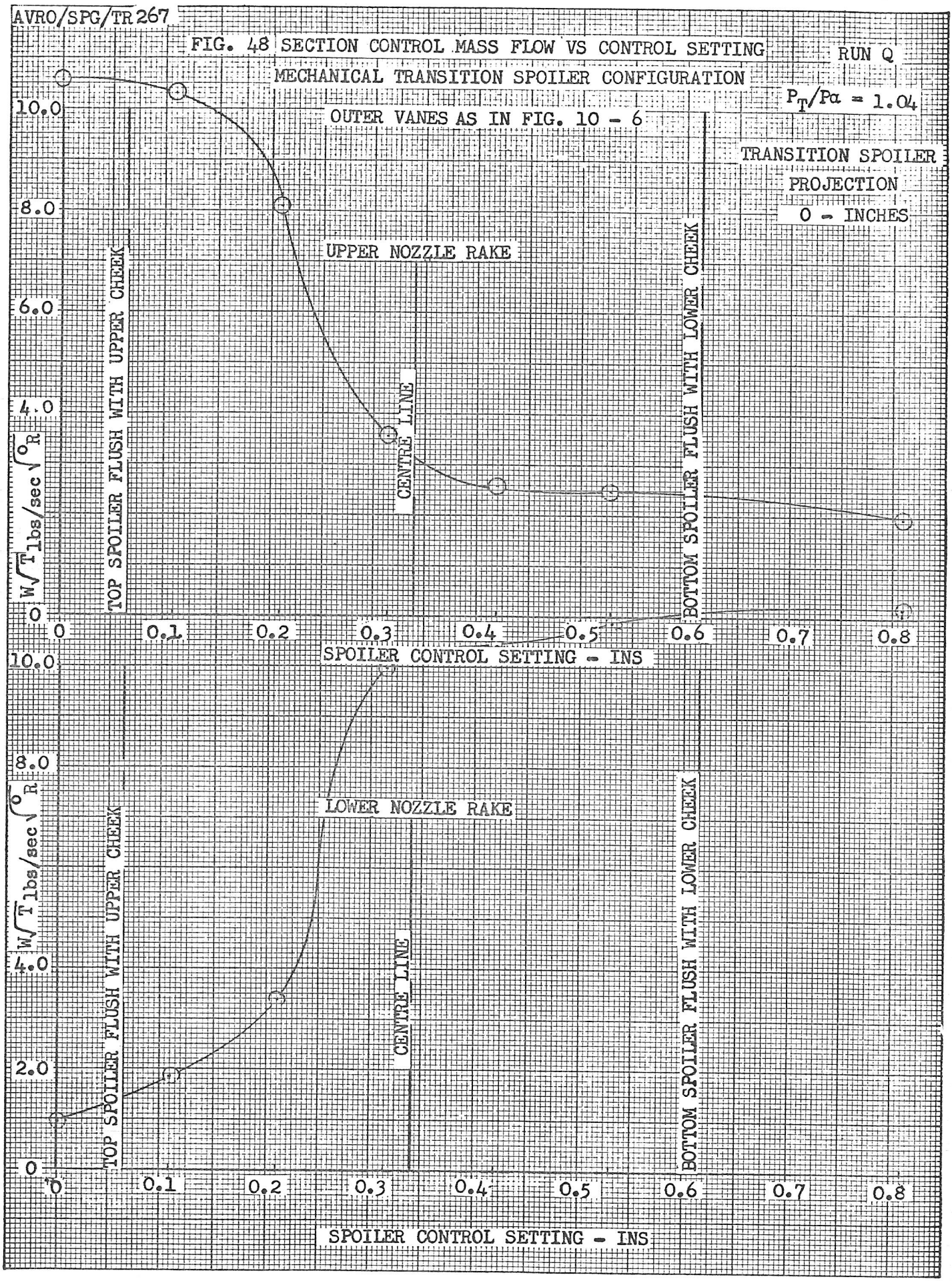
AVRO/SPG/TR 267
FIG. 48 SECTION CONTROL MASS FLOW VS CONTROL SETTING
RUN Q
MECHANICAL TRANSITION SPOILER CONFIGURATION
$P_T/Pa = 1.04$
OUTER VANES AS IN FIG. 10 - 6
TRANSITION SPOILER PROJECTION 0 - INCHES
UPPER NOZZLE RAKE
CENTRE LINE
TOP SPOILER FLUSH WITH UPPER CHEEK
BOTTOM SPOILER FLUSH WITH LOWER CHEEK
$W\sqrt{T}$ lbs/sec $\sqrt{°R}$
SPOILER CONTROL SETTING - INS
LOWER NOZZLE RAKE
CENTRE LINE
TOP SPOILER FLUSH WITH UPPER CHEEK
BOTTOM SPOILER FLUSH WITH LOWER CHEEK
$W\sqrt{T}$ lbs/sec $\sqrt{°R}$
SPOILER CONTROL SETTING - INS

AVRO/SPG/TR267

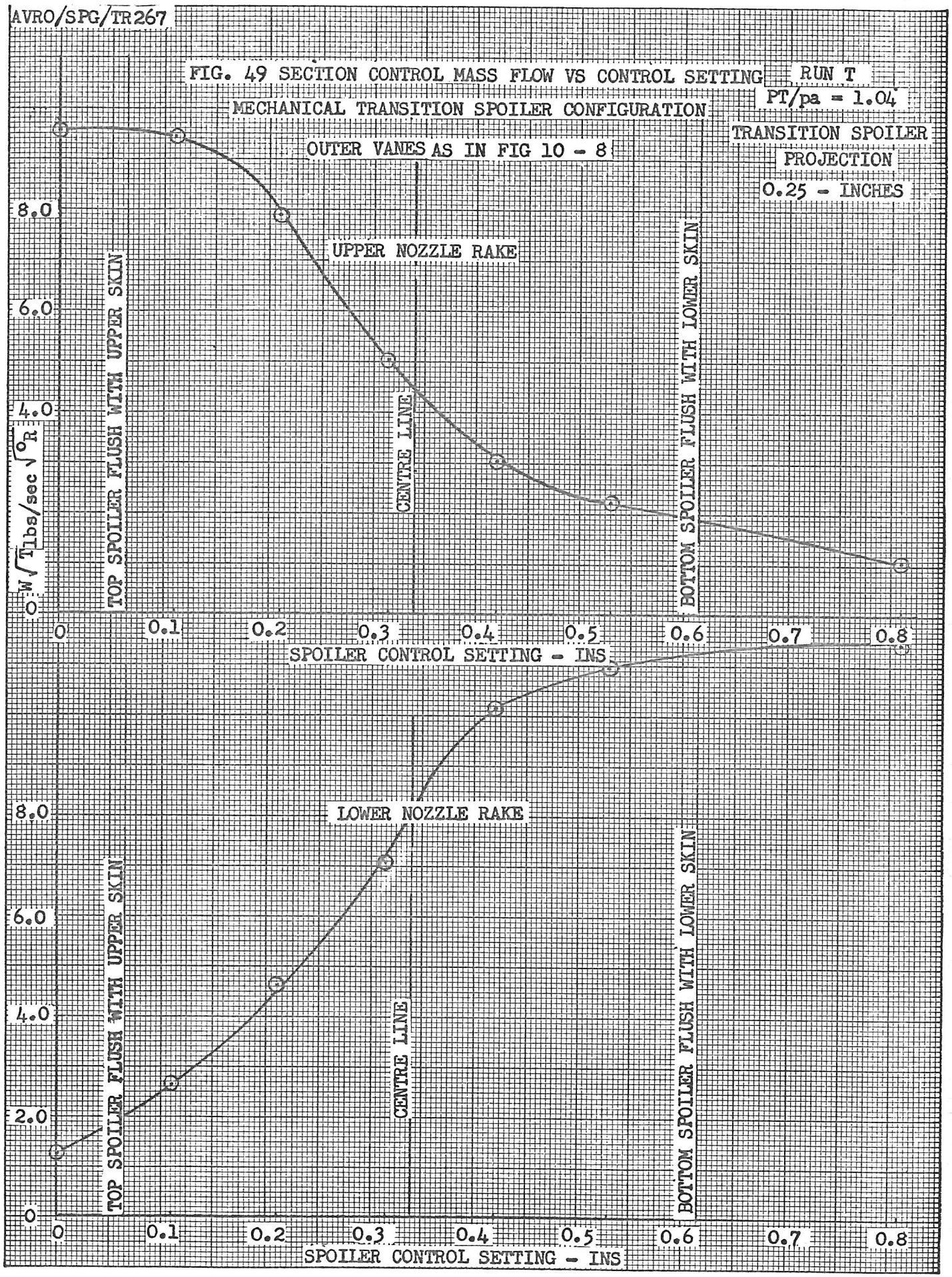

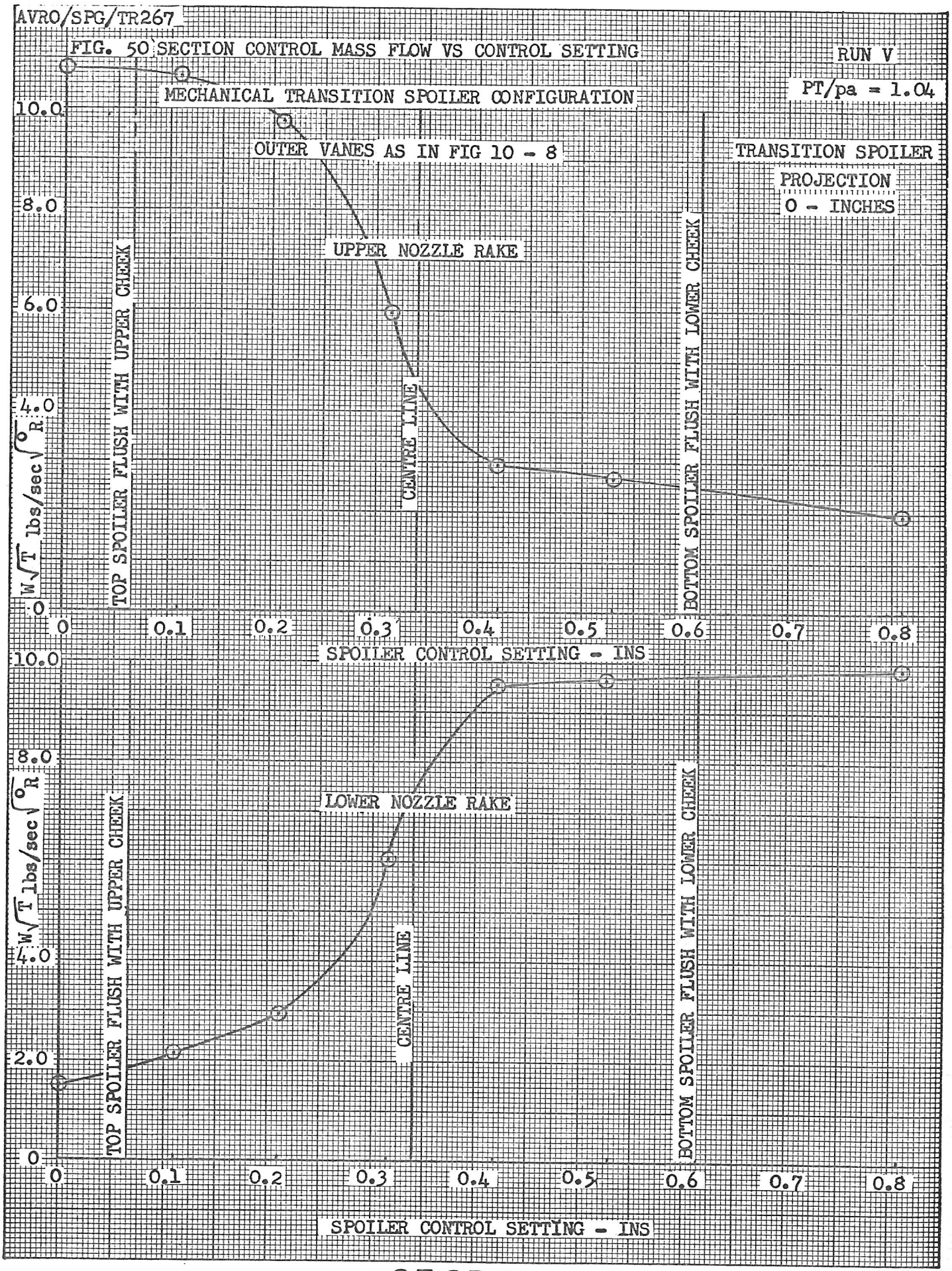
AVRO/SPG/TR267
FIG. 50 SECTION CONTROL MASS FLOW VS CONTROL SETTING
MECHANICAL TRANSITION SPOILER CONFIGURATION
RUN V
PT/pa = 1.04
TRANSITION SPOILER PROJECTION 0 - INCHES
OUTER VANES AS IN FIG 10 - 8
UPPER NOZZLE RAKE
CENTRE LINE
TOP SPOILER FLUSH WITH UPPER CHEEK
BOTTOM SPOILER FLUSH WITH LOWER CHEEK
W√T lbs/sec √°R
10.0
8.0
6.0
4.0
0
0.1
0.2
0.3
0.4
0.5
0.6
0.7
0.8
SPOILER CONTROL SETTING - INS
LOWER NOZZLE RAKE
CENTRE LINE
TOP SPOILER FLUSH WITH UPPER CHEEK
BOTTOM SPOILER FLUSH WITH LOWER CHEEK
W√T lbs/sec √°R
10.0
8.0
4.0
2.0
0
0.1
0.2
0.3
0.4
0.5
0.6
0.7
0.8
SPOILER CONTROL SETTING - INS

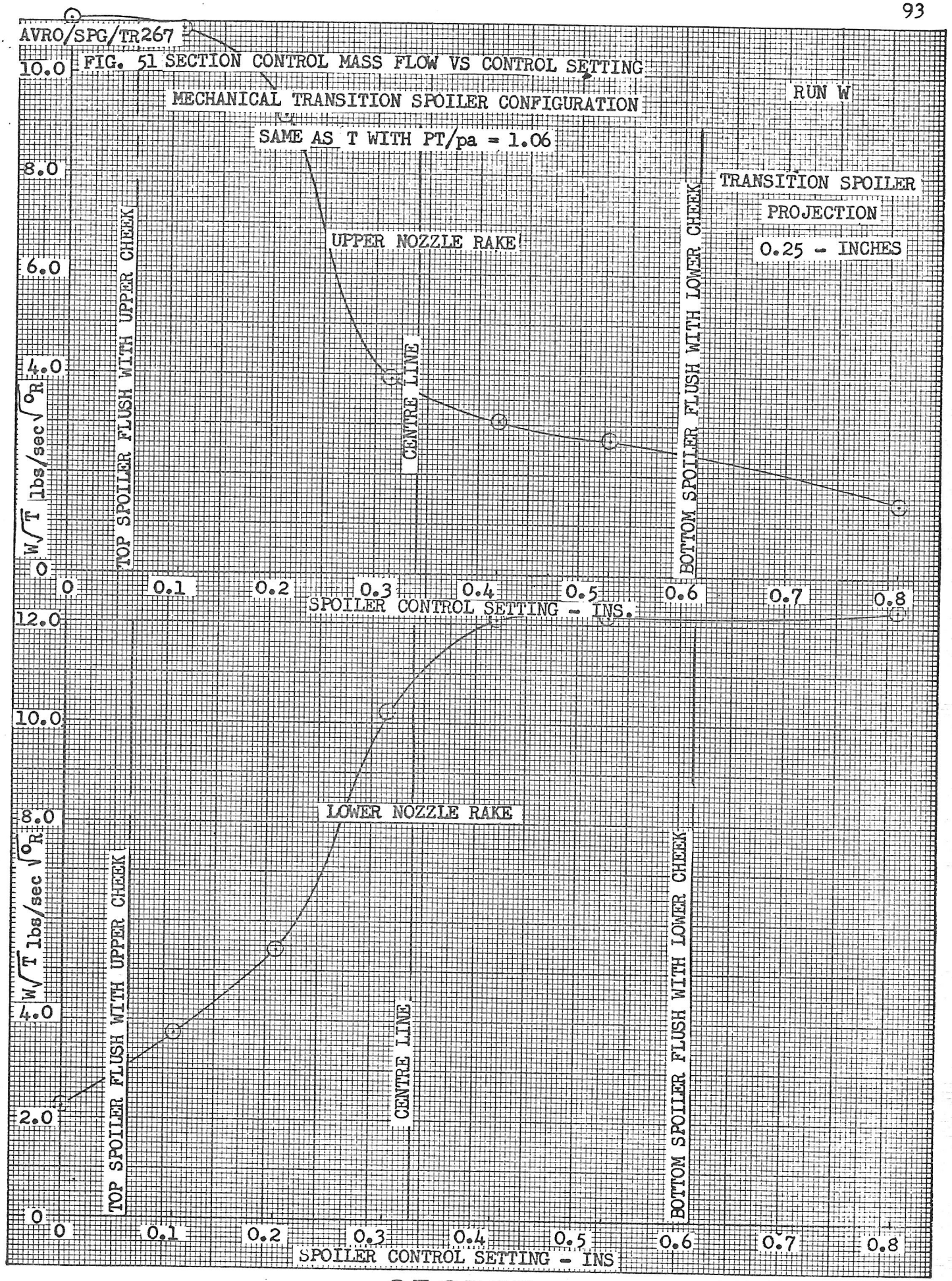
AVRO/SPG/TR267
FIG. 51 SECTION CONTROL MASS FLOW VS CONTROL SETTING
MECHANICAL TRANSITION SPOILER CONFIGURATION
RUN W
SAME AS T WITH PT/pa = 1.06
TRANSITION SPOILER PROJECTION 0.25 - INCHES
UPPER NOZZLE RAKE
CENTRE LINE
TOP SPOILER FLUSH WITH UPPER CHEEK
BOTTOM SPOILER FLUSH WITH LOWER CHEEK
W√T / θR lbs/sec √°R
SPOILER CONTROL SETTING - INS.
LOWER NOZZLE RAKE
CENTRE LINE
TOP SPOILER FLUSH WITH UPPER CHEEK
BOTTOM SPOILER FLUSH WITH LOWER CHEEK
W√T / θR lbs/sec √°R
SPOILER CONTROL SETTING - INS

AVRO/SPG/TR267

FIG. 52 SECTION CONTROL MASS FLOW VS CONTROL SETTING RUN X

MECHANICAL TRANSITION SPOILER CONFIGURATION

OUTER VANES AS IN FIG 10 - 11

TRANSITION SPOILER PROJECTION 0.25 - INCHES

UPPER NOZZLE RAKE

$W\sqrt{T}$ lbs/sec $\sqrt{°R}$

8.0
6.0
4.0
0

TOP SPOILER FLUSH WITH UPPER SKIN

CENTRE LINE

BOTTOM SPOILER FLUSH WITH LOWER SKIN

0 0.1 0.2 0.3 0.4 0.5 0.6 0.7 0.8

SPOILER CONTROL SETTING - INS

LOWER NOZZLE RAKE

8.0
6.0
4.0
2.0
0

TOP SPOILER FLUSH WITH UPPER SKIN

CENTRE LINE

BOTTOM SPOILER FLUSH WITH LOWER SKIN

0 0.1 0.2 0.3 0.4 0.5 0.6 0.7 0.8

SPOILER CONTROL SETTING - INS

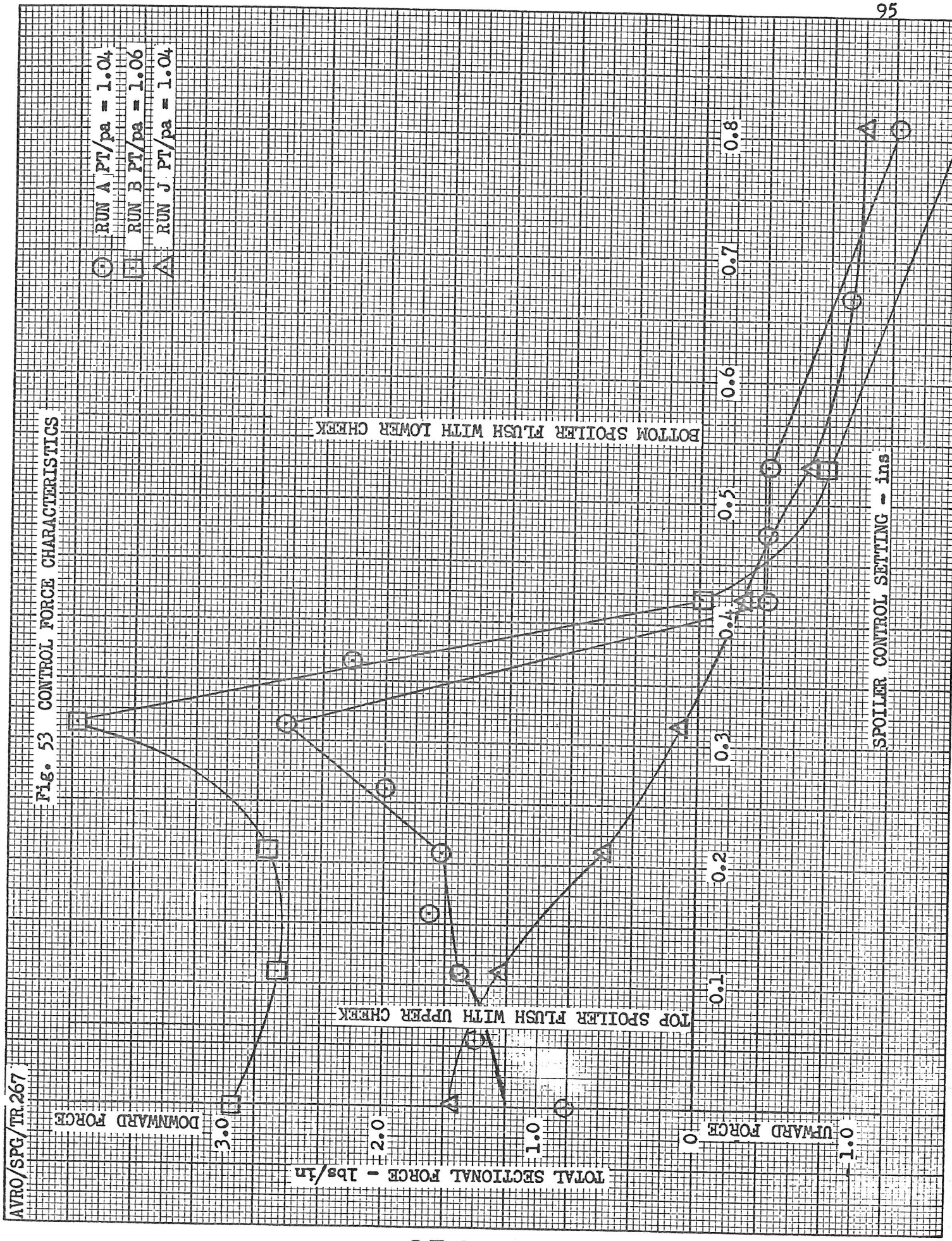

Fig. 53 CONTROL FORCE CHARACTERISTICS

AVRO/SPG/TR.267

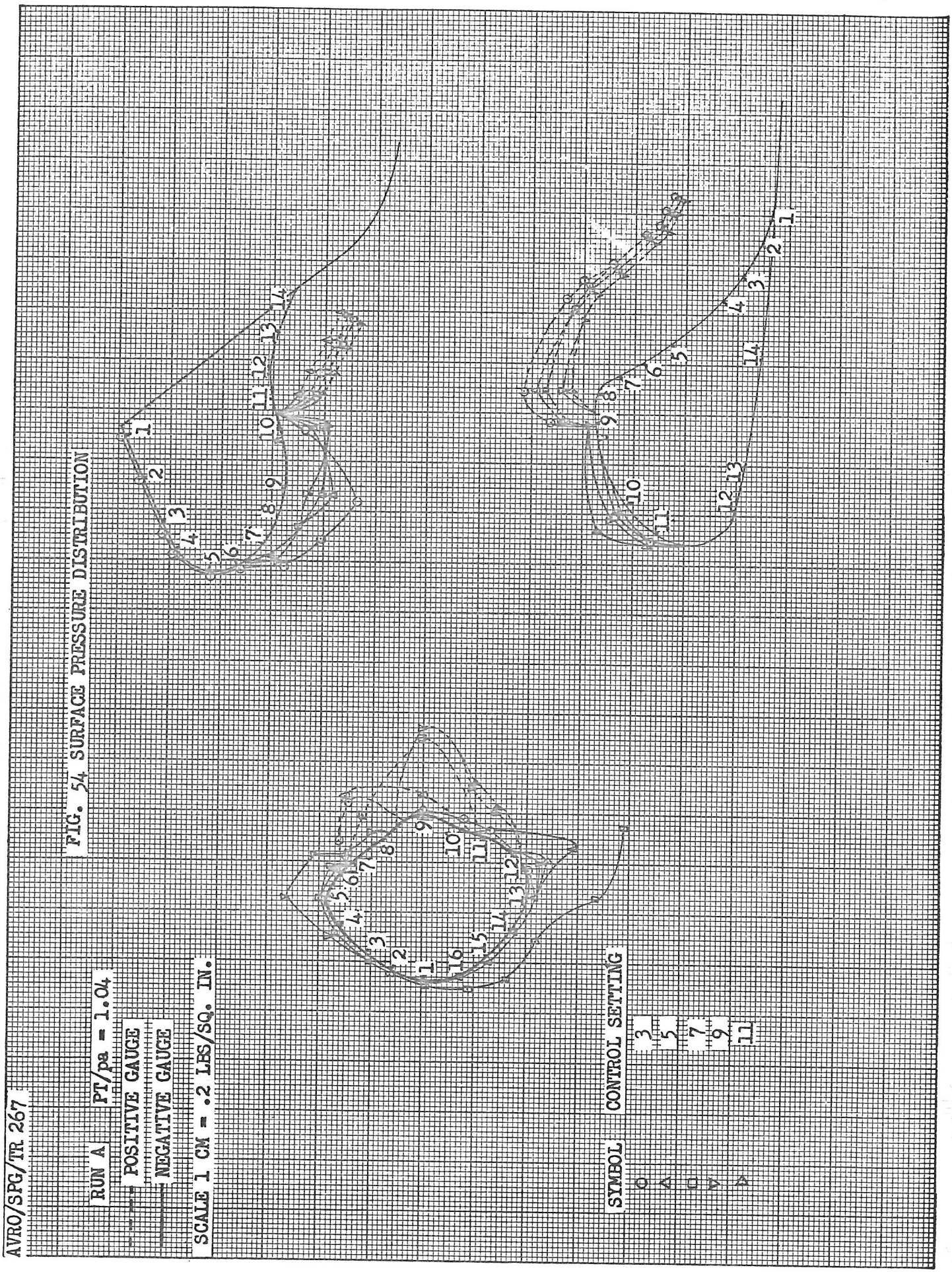
AVRO/SPG/TR 267
FIG. 54 SURFACE PRESSURE DISTRIBUTION
RUN A
PT/ps = 1.04
POSITIVE GAUGE
NEGATIVE GAUGE
SCALE 1 CM = .2 LBS/SQ. IN.
SYMBOL
CONTROL SETTING
3
5
7
9
11

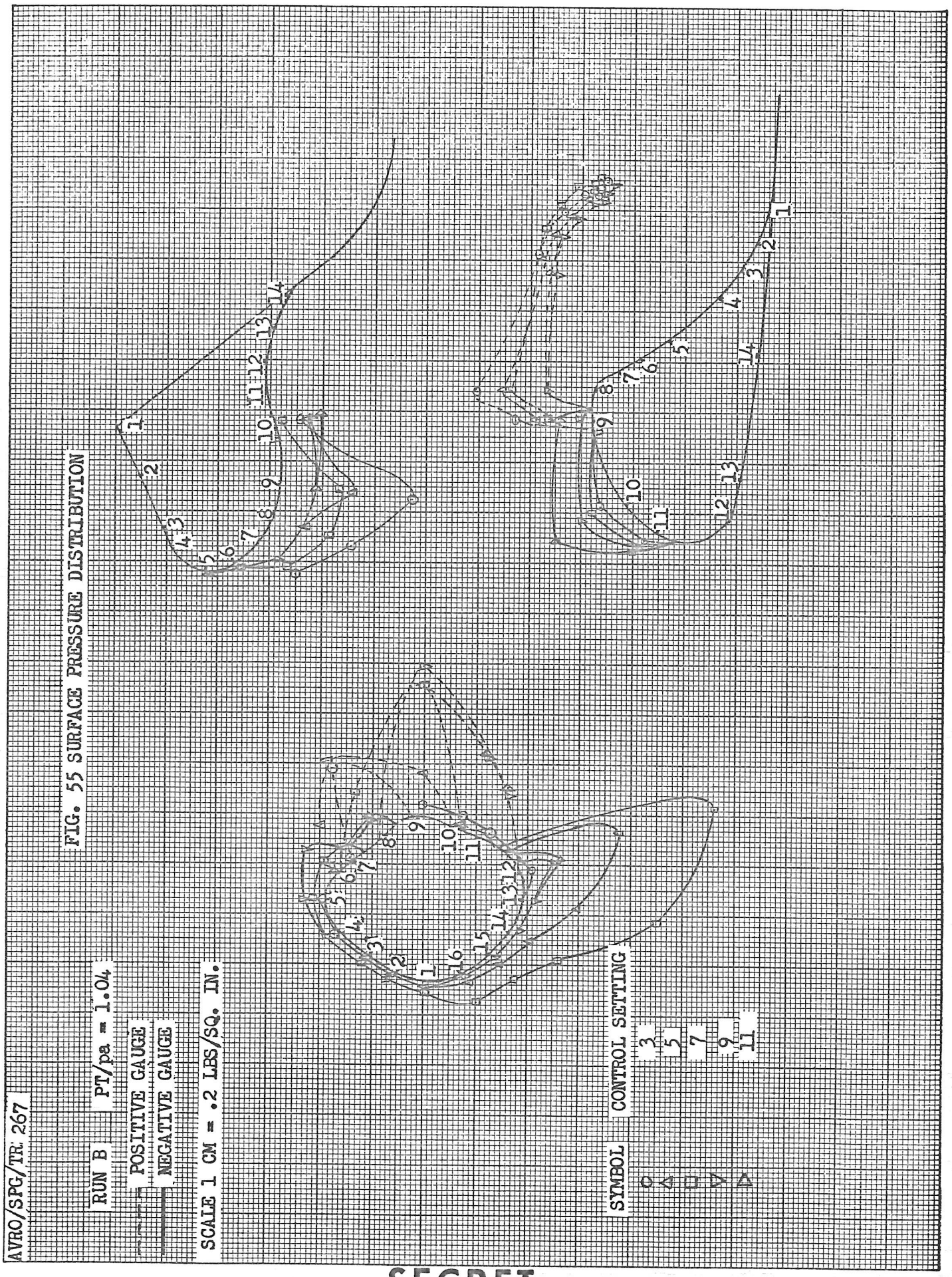

FIG. 55 SURFACE PRESSURE DISTRIBUTION

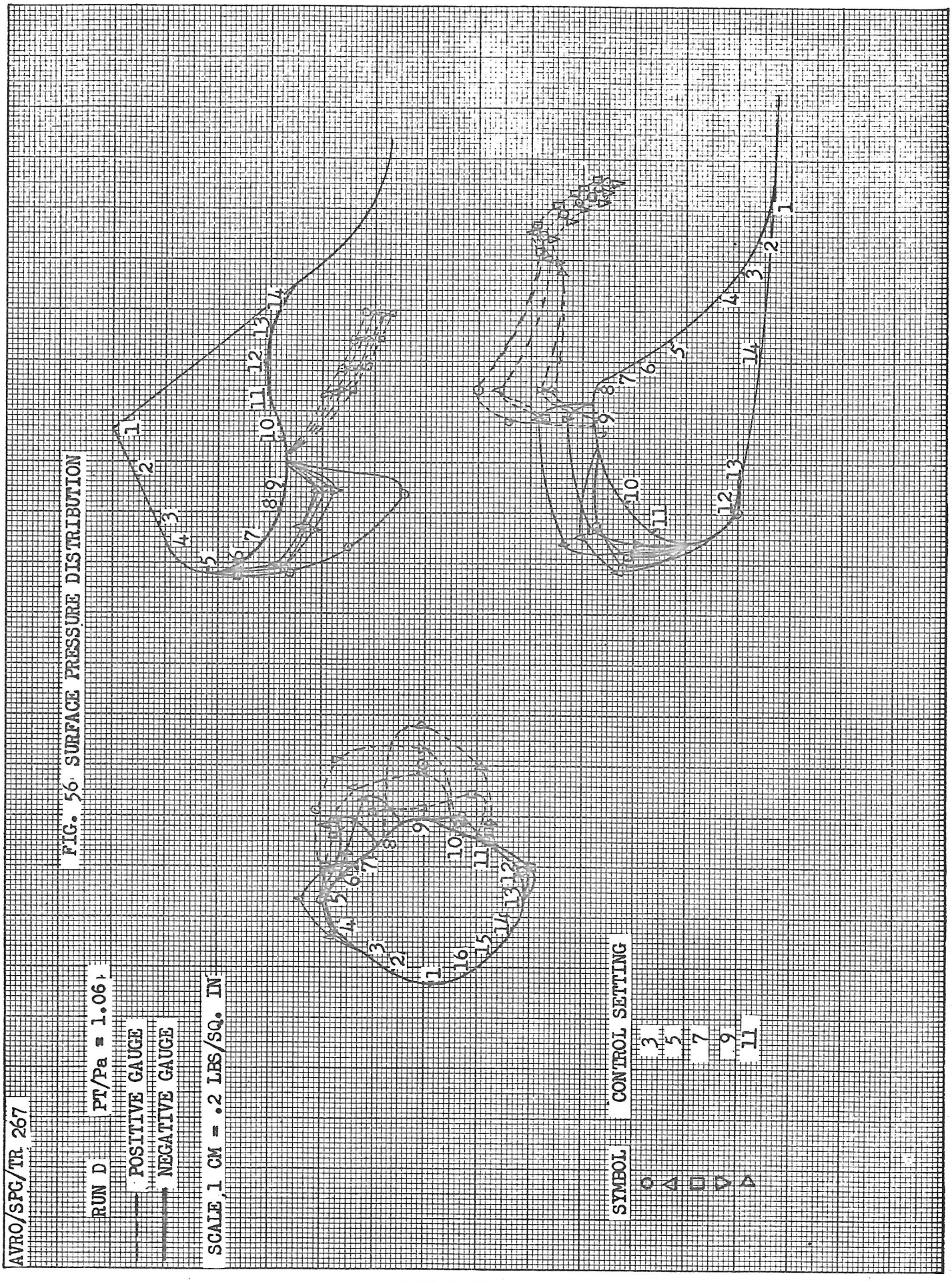
AVRO/SPG/TR 267
FIG. 56 SURFACE PRESSURE DISTRIBUTION
RUN D
PT/Pa = 1.06
POSITIVE GAUGE
NEGATIVE GAUGE
SCALE, 1 CM = .2 LBS/SQ. IN
SYMBOL
CONTROL SETTING
3
5
7
9
11

AVRO/SPG/TR 267
FIG. 57 SURFACE PRESSURE DISTRIBUTION
RUN E
PT/Pa = 1.06
POSITIVE GAUGE
NEGATIVE GAUGE
SCALE 1 CM = .2 LBS/SQ. IN.
SYMBOL
CONTROL SETTING
3
5
7
9
11

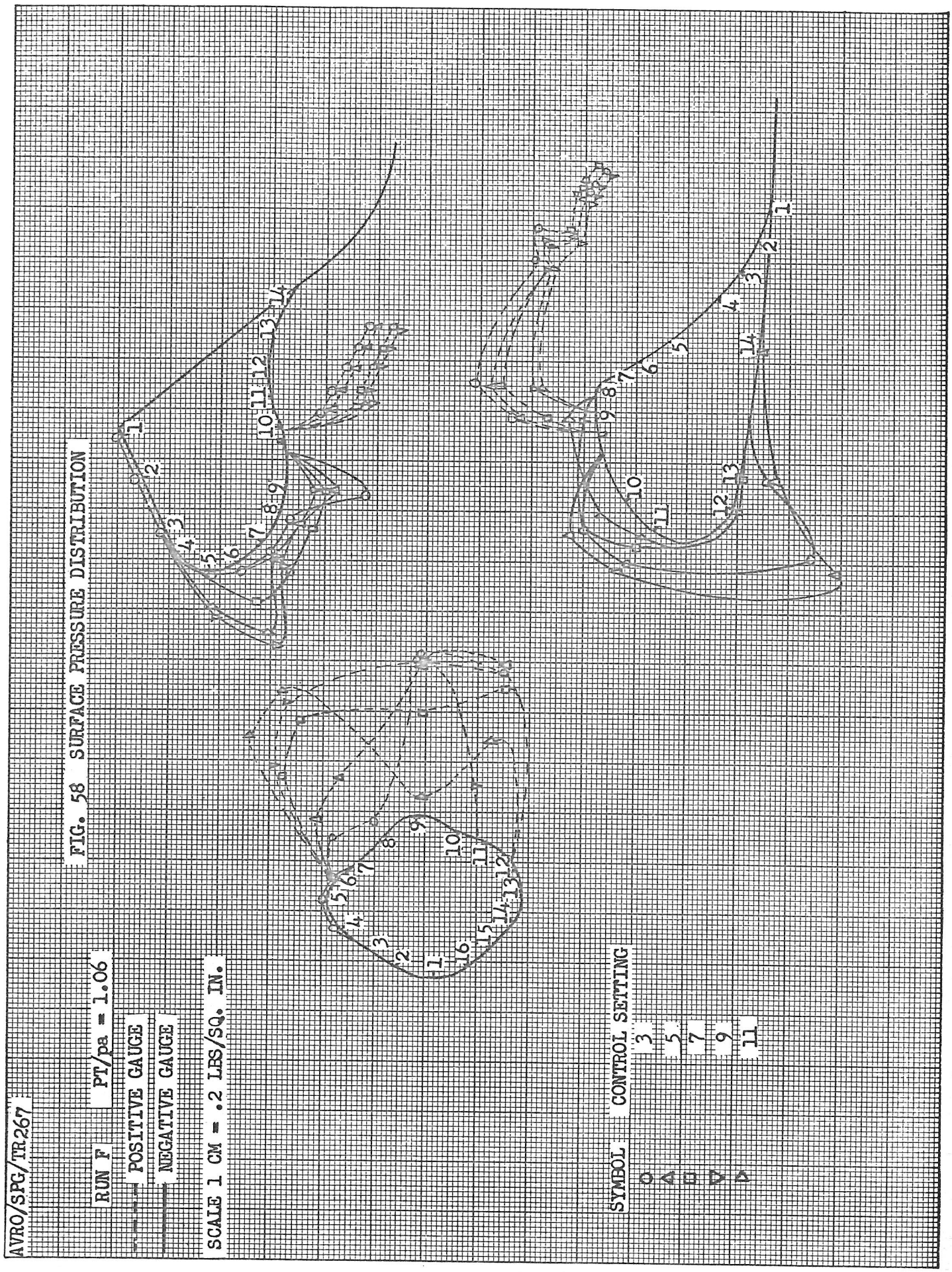
AVRO/SPG/TR267
FIG. 58 SURFACE PRESSURE DISTRIBUTION
RUN F
PT/pa = 1.06
POSITIVE GAUGE
NEGATIVE GAUGE
SCALE 1 CM = .2 LBS/SQ. IN.
SYMBOL CONTROL SETTING
3
5
7
9
11

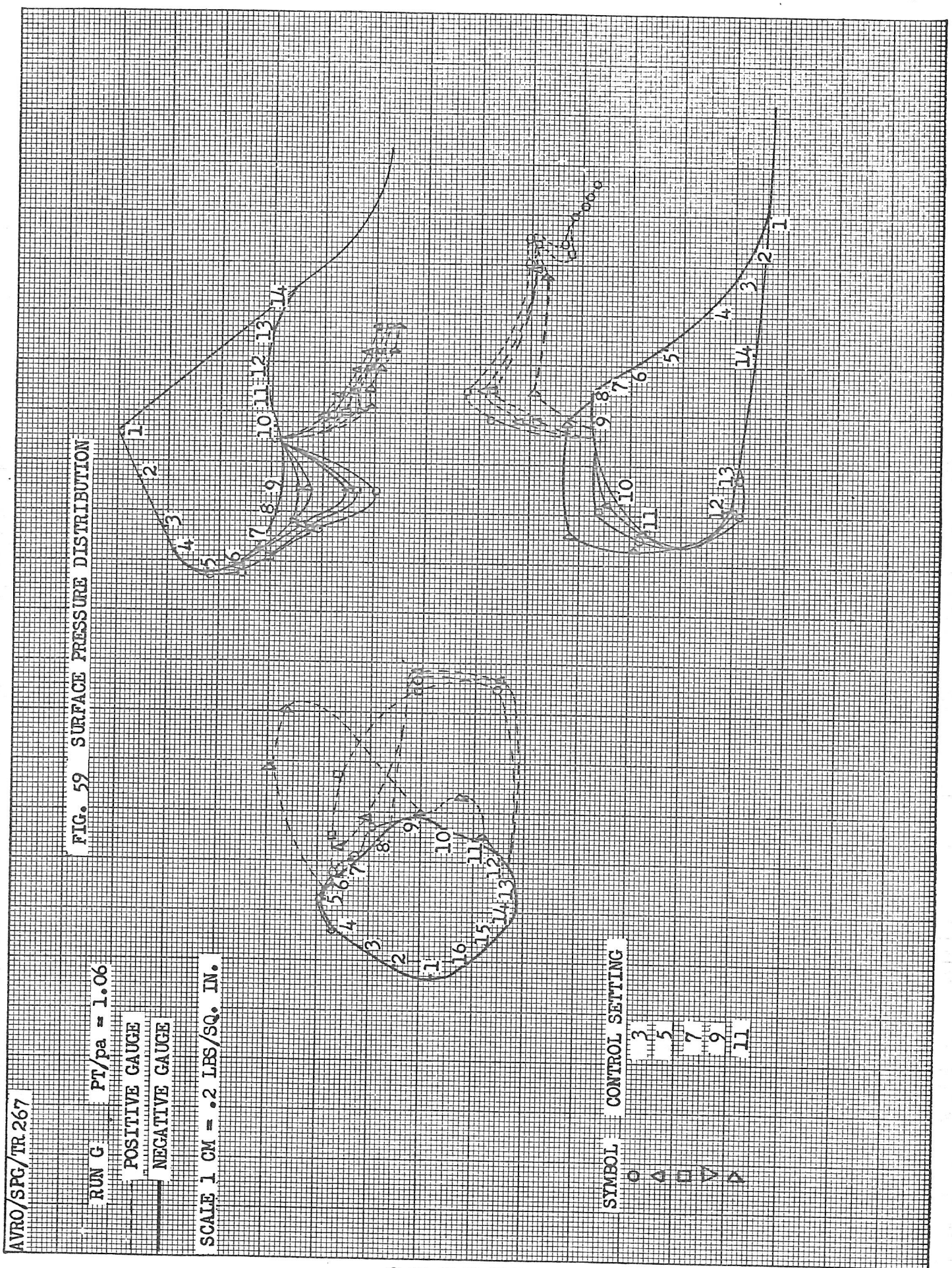

FIG. 59 SURFACE PRESSURE DISTRIBUTION

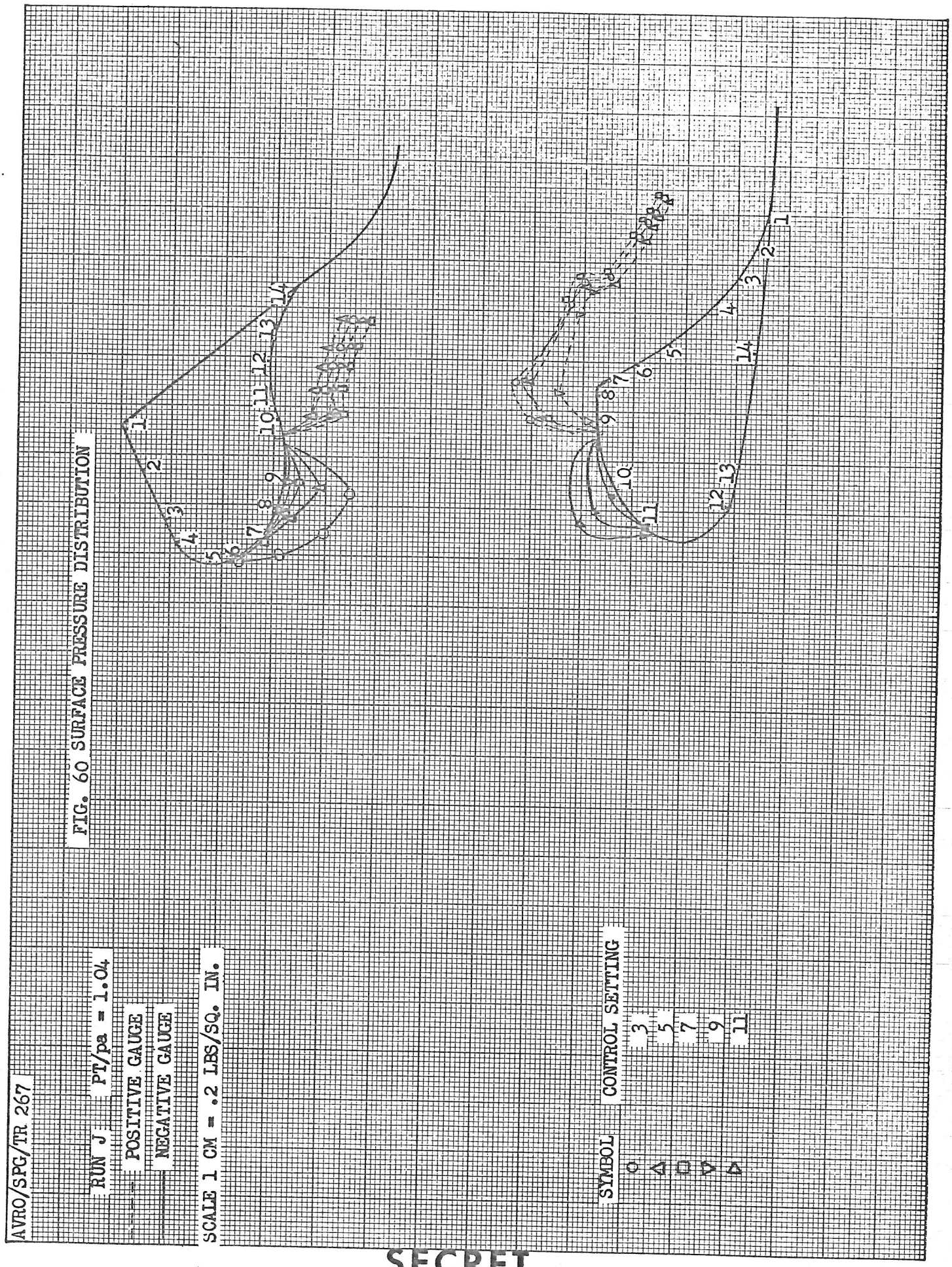

FIG. 60 SURFACE PRESSURE DISTRIBUTION

FIG. 61 Discharge Coefficient vs Control Setting.
For the Pneumatic Transition Spoiler Configuration.
NO OUTER VANES Vent Closed.

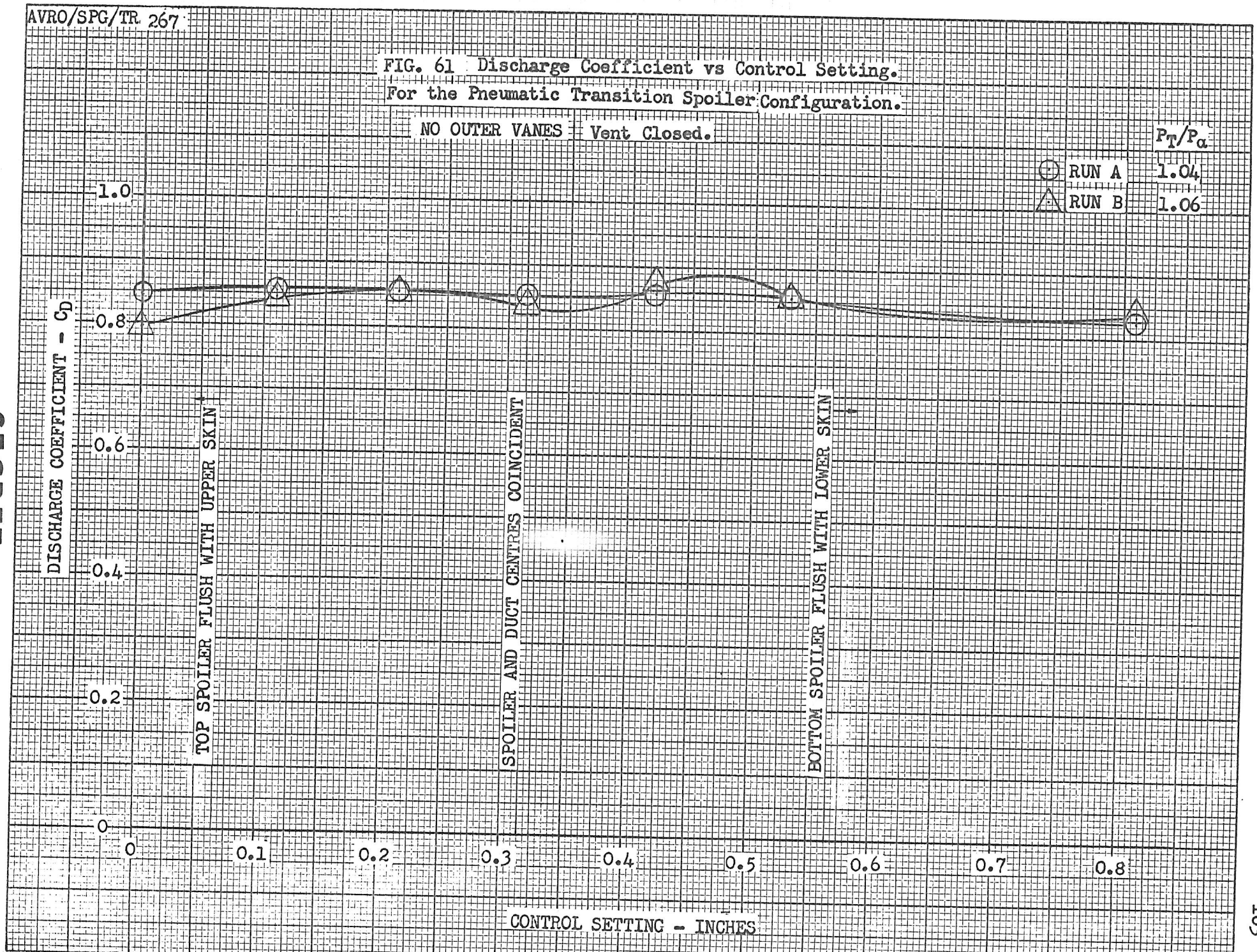

SECRET
SECRET

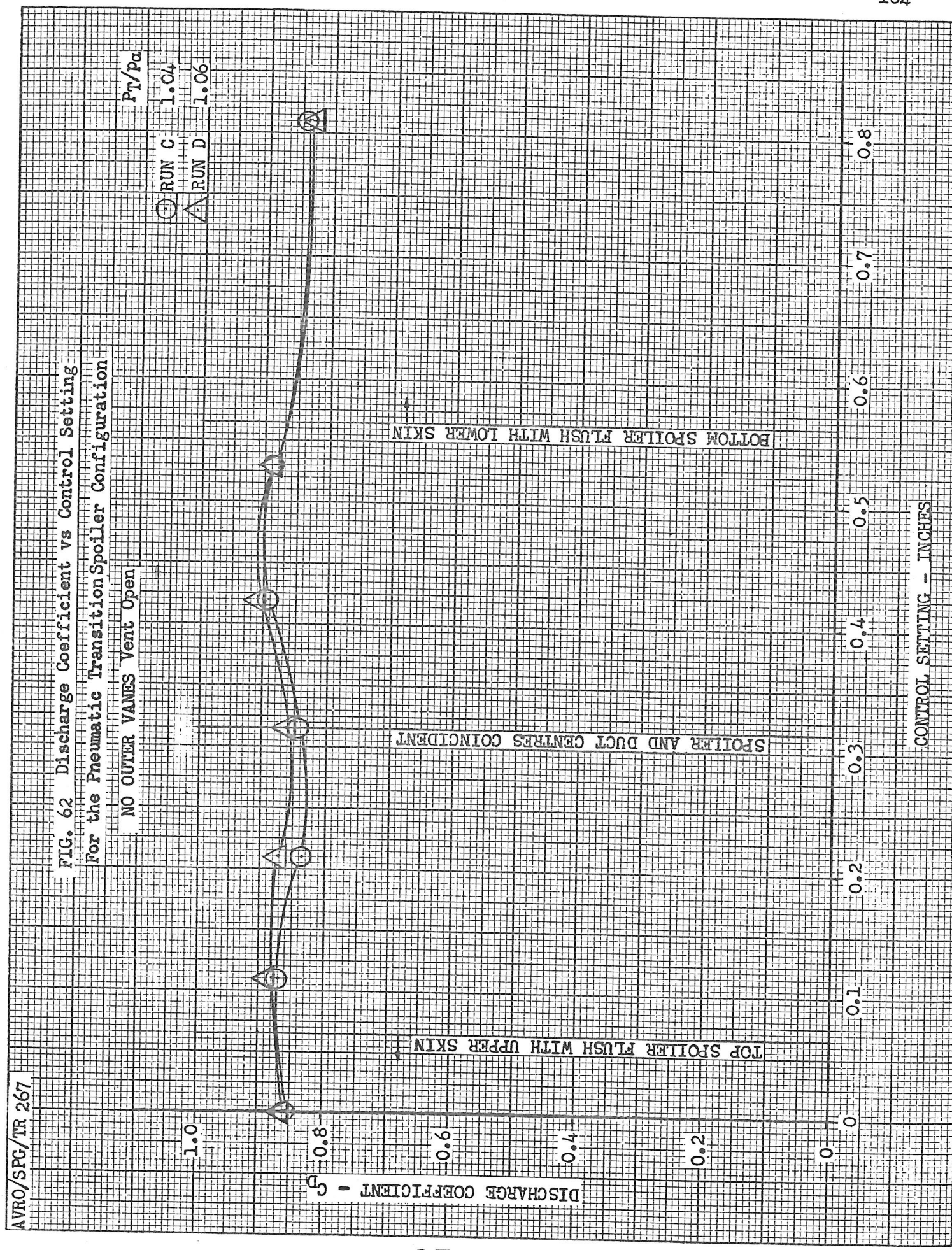
AVRO/SPG/TR 267
FIG. 62 Discharge Coefficient vs Control Setting
For the Pneumatic Transition Spoiler Configuration
NO OUTER VANES Vent Open
P_T/P_a
RUN C 1.04
RUN D 1.06
DISCHARGE COEFFICIENT - C_D
-1.0
-0.8
-0.6
-0.4
-0.2
0
0.1
0.2
0.3
0.4
0.5
0.6
0.7
0.8
CONTROL SETTING - INCHES
TOP SPOILER FLUSH WITH UPPER SKIN
SPOILER AND DUCT CENTRES COINCIDENT
BOTTOM SPOILER FLUSH WITH LOWER SKIN

FIG. 63 Discharge Coefficient vs Control Setting
For Mechanical Transition Spoiler Configuration
NO OUTER VANES P_T/P_a - 1.06

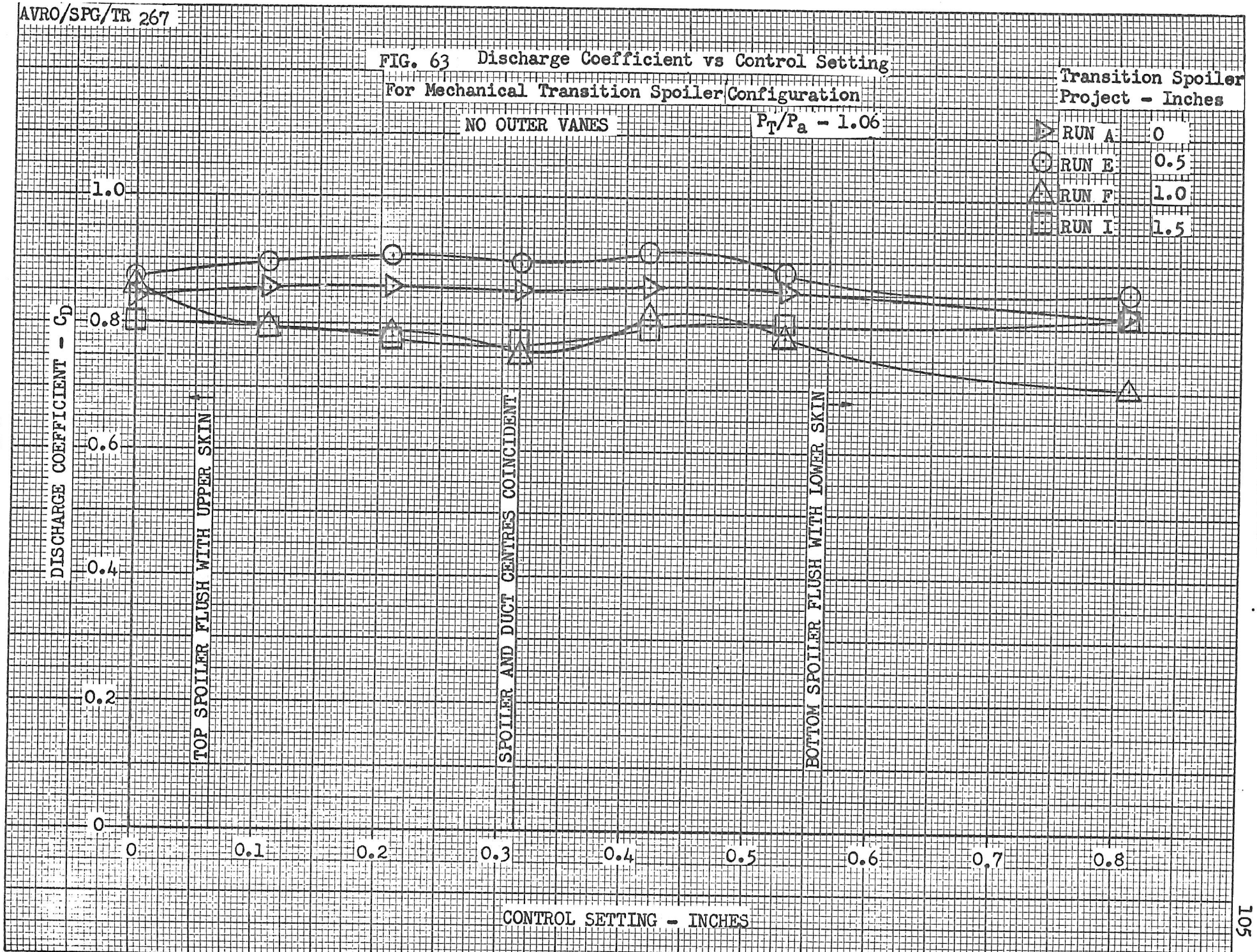

SECRET
SECRET

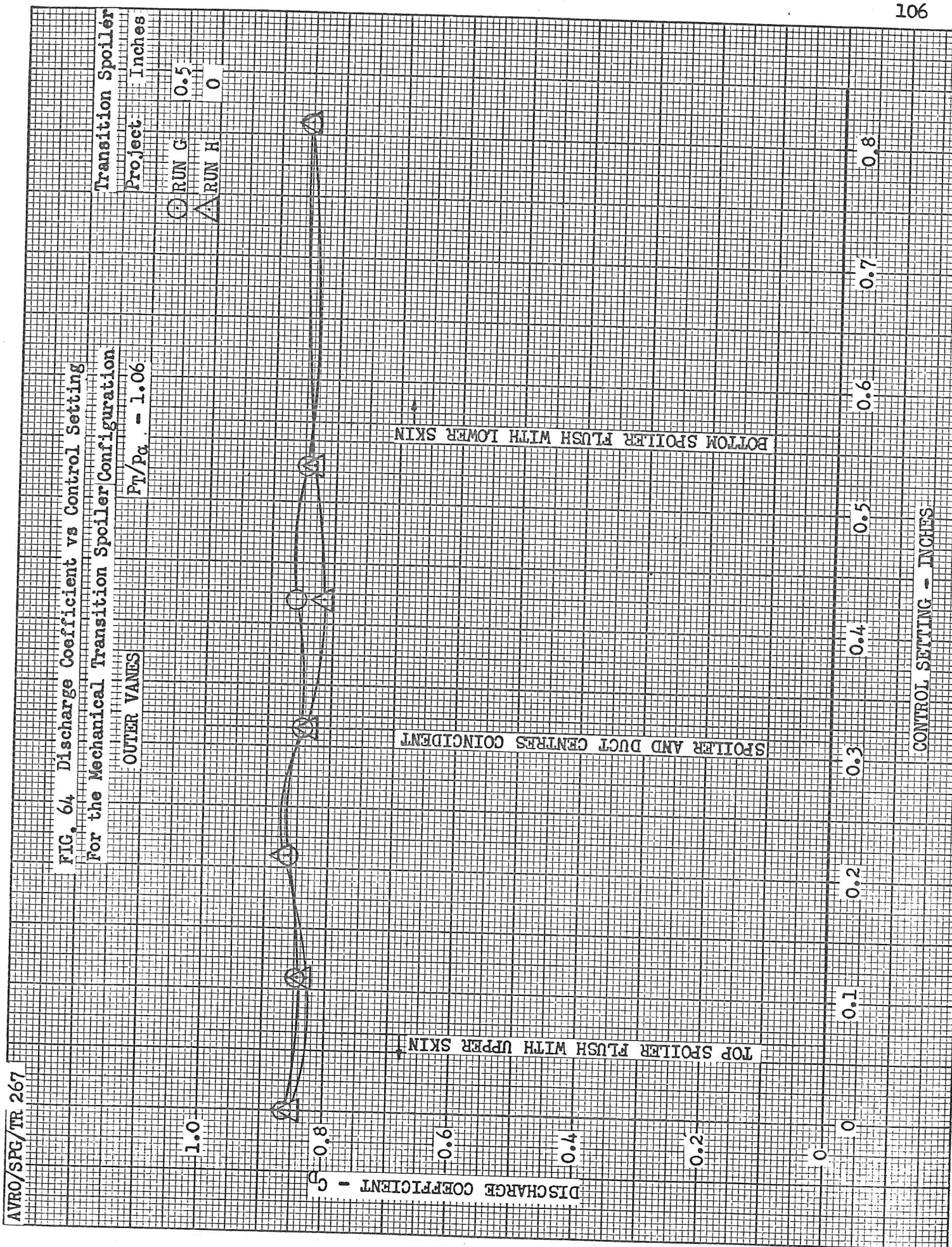
AVRO/SPG/TR 267
FIG. 64 Discharge Coefficient vs Control Setting
For the Mechanical Transition Spoiler Configuration
OUTER VANES
P_T/P_α = 1.06
Transition Spoiler Project Inches
RUN G 0.5
RUN H 0
TOP SPOILER FLUSH WITH UPPER SKIN
SPOILER AND DUCT CENTRES COINCIDENT
BOTTOM SPOILER FLUSH WITH LOWER SKIN
DISCHARGE COEFFICIENT - C_D
CONTROL SETTING - INCHES
1.0
0.8
0.6
0.4
0.2
0
0.1
0.2
0.3
0.4
0.5
0.6
0.7
0.8

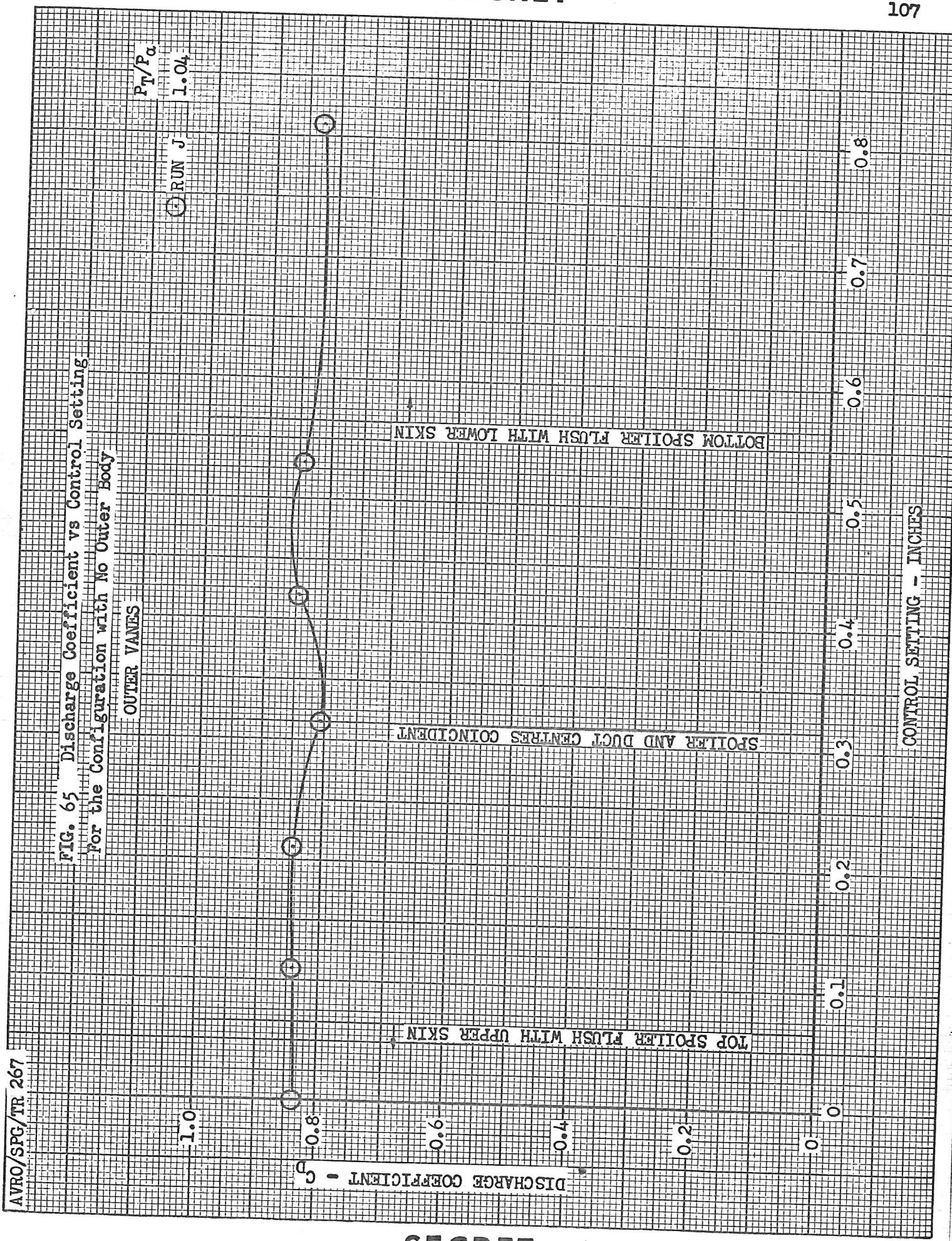

FIG. 65 Discharge Coefficient vs Control Setting For the Configuration with No Outer Body OUTER VANES

AVRO/SPG/TR 267

FIG. 66 DISCHARGE COEFFICIENT VS CONTROL SETTING
MECHANICAL TRANSITION SPOILER CONFIGURATION
OUTER VANES
RUN P PT/pa = 1.04
TRANSITION SPOILER
PROJECTION 0.5 INCHES
RUN Q PT/pa = 1.04
TRANSITION SPOILER
PROJECTION 0 INCHES
BOTTOM SPOILER FLUSH WITH LOWER SKIN
SPOILER AND DUCT CENTRE COINCIDENT
TOP SPOILER FLUSH WITH UPPER SKIN
DISCHARGE COEFFICIENT - C_D
CONTROL SETTING - INCHES
AVRO/SPG/TR 267
1.0
0.8
0.6
0.4
0.2
0
0.1
0.2
0.3
0.4
0.5
0.6
0.7
0.8

AVRO/SPG/TR 267
FIG. 67 DISCHARGE COEFFICIENT VS CONTROL SETTING
MECHANICAL TRANSITION SPOILER CONFIGURATION
OUTER VANES
RUN T PT/pa = 1.04
TRANSITION SPOILER
PROJECTION 0.25 INCHES
RUN V PT/pa = 1.04
TRANSITION SPOILER
PROJECTION 0 INCHES
TOP SPOILER FLUSH WITH UPPER SKIN
SPOILER AND DUCT CENTRE COINCIDENT
BOTTOM SPOILER FLUSH WITH LOWER SKIN
DISCHARGE COEFFICIENT - Cd
CONTROL SETTING - INCHES
1.0
0.8
0.6
0.4
0.2
0
0.1
0.2
0.3
0.4
0.5
0.6
0.7
0.8

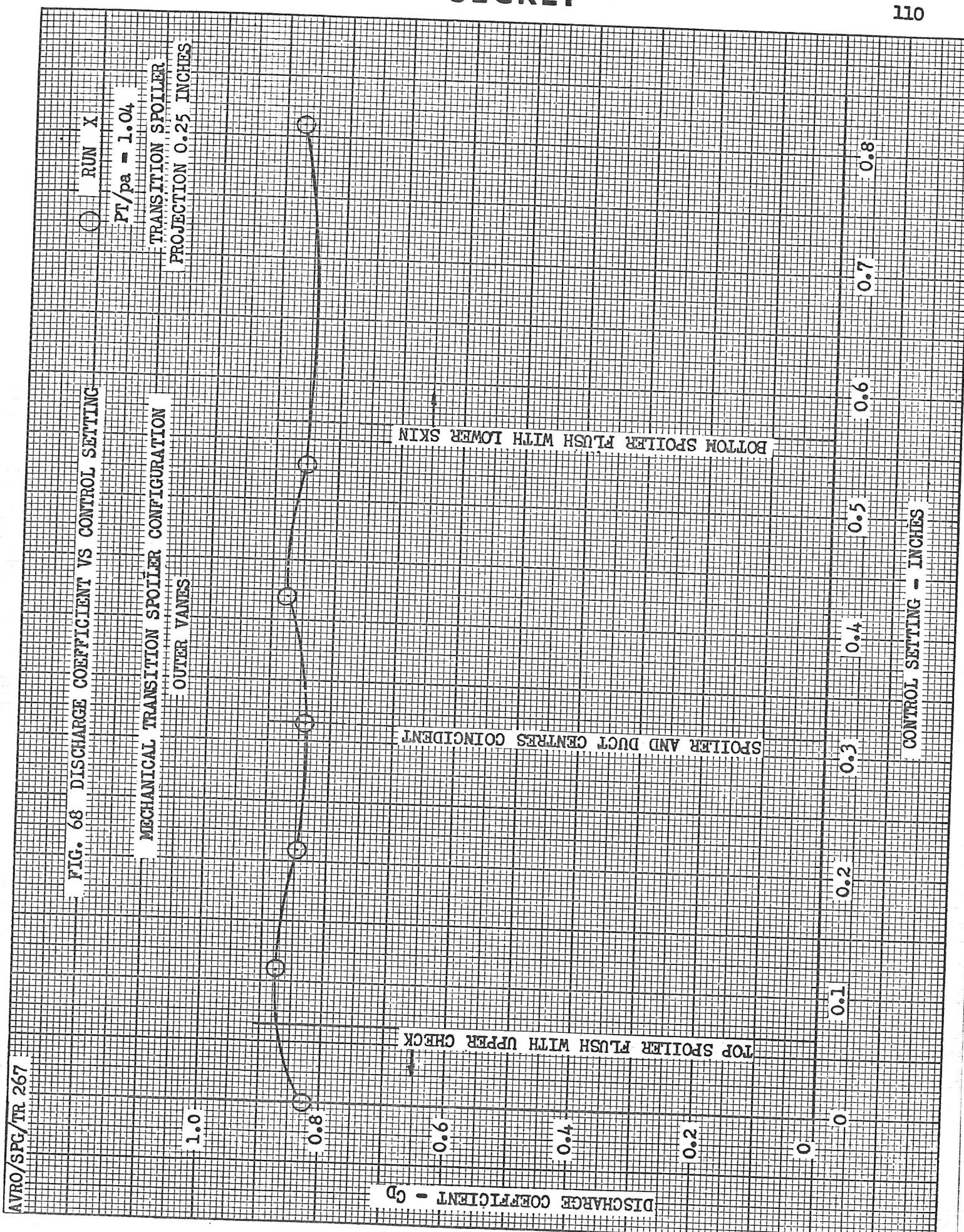
AVRO/SPG/TR 267
FIG. 68 DISCHARGE COEFFICIENT VS CONTROL SETTING
MECHANICAL TRANSITION SPOILER CONFIGURATION
OUTER VANES
TRANSITION SPOILER PROJECTION 0.25 INCHES
RUN X
PT/pa = 1.04
BOTTOM SPOILER FLUSH WITH LOWER SKIN
SPOILER AND DUCT CENTRES COINCIDENT
TOP SPOILER FLUSH WITH UPPER CHECK
DISCHARGE COEFFICIENT - Cd
CONTROL SETTING - INCHES
1.0
0.8
0.6
0.4
0.2
0
0.1
0.2
0.3
0.4
0.5
0.6
0.7
0.8

AVRO/SPG/TR 267

FIG. 69 Pressure Loss Coefficient Between Inner Duct and Spoiler Stations vs Control Setting

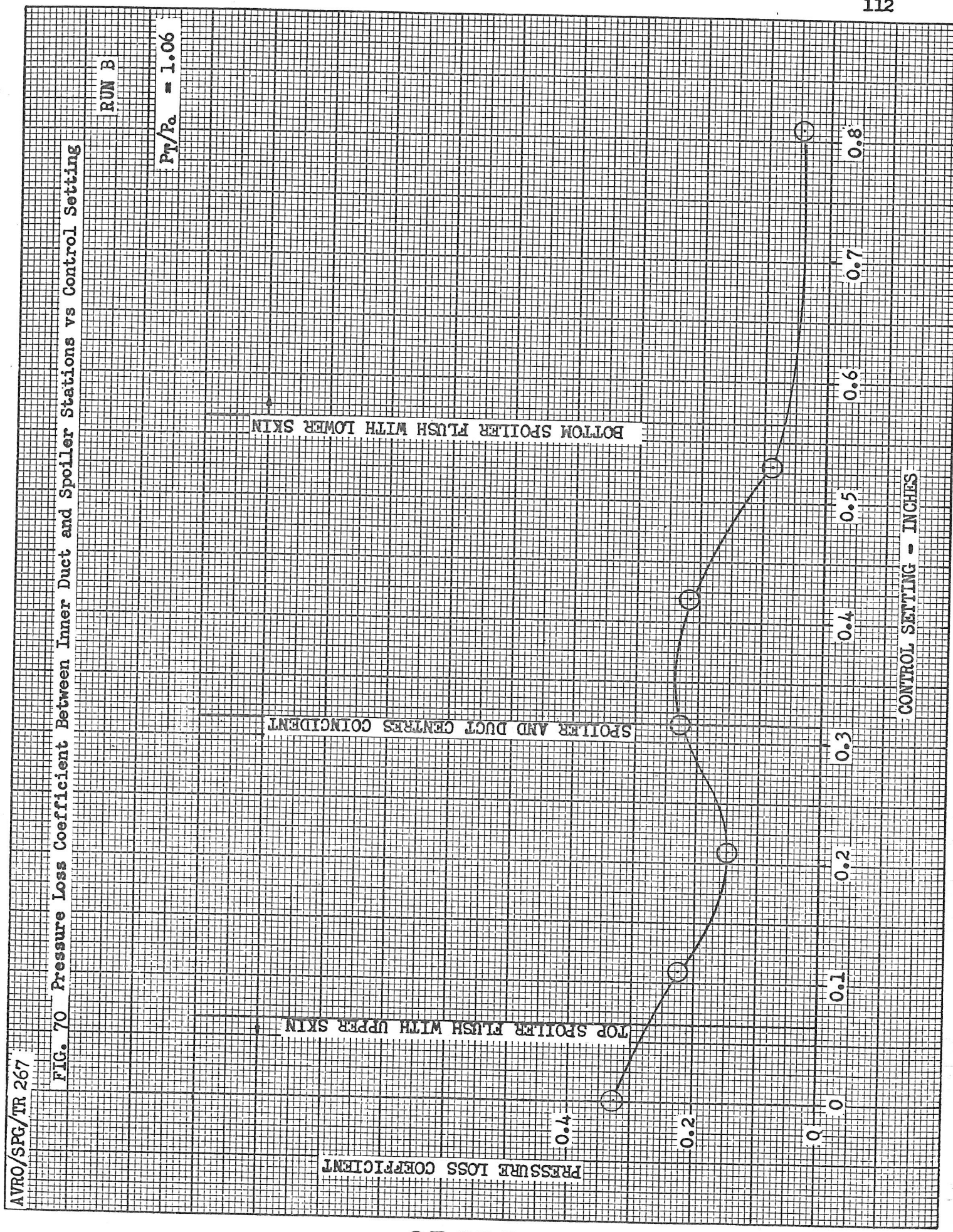

AVRO/SPG/TR 267

FIG. 70 Pressure Loss Coefficient Between Inner Duct and Spoiler Stations vs Control Setting

FIG. 71 Pressure Loss Coefficient Between Inner Duct and Spoiler Stations vs Control Setting

P_T/P_a = 1.06

RUN E

TRANSITION SPOILER PROJECT

INCHES

0.5

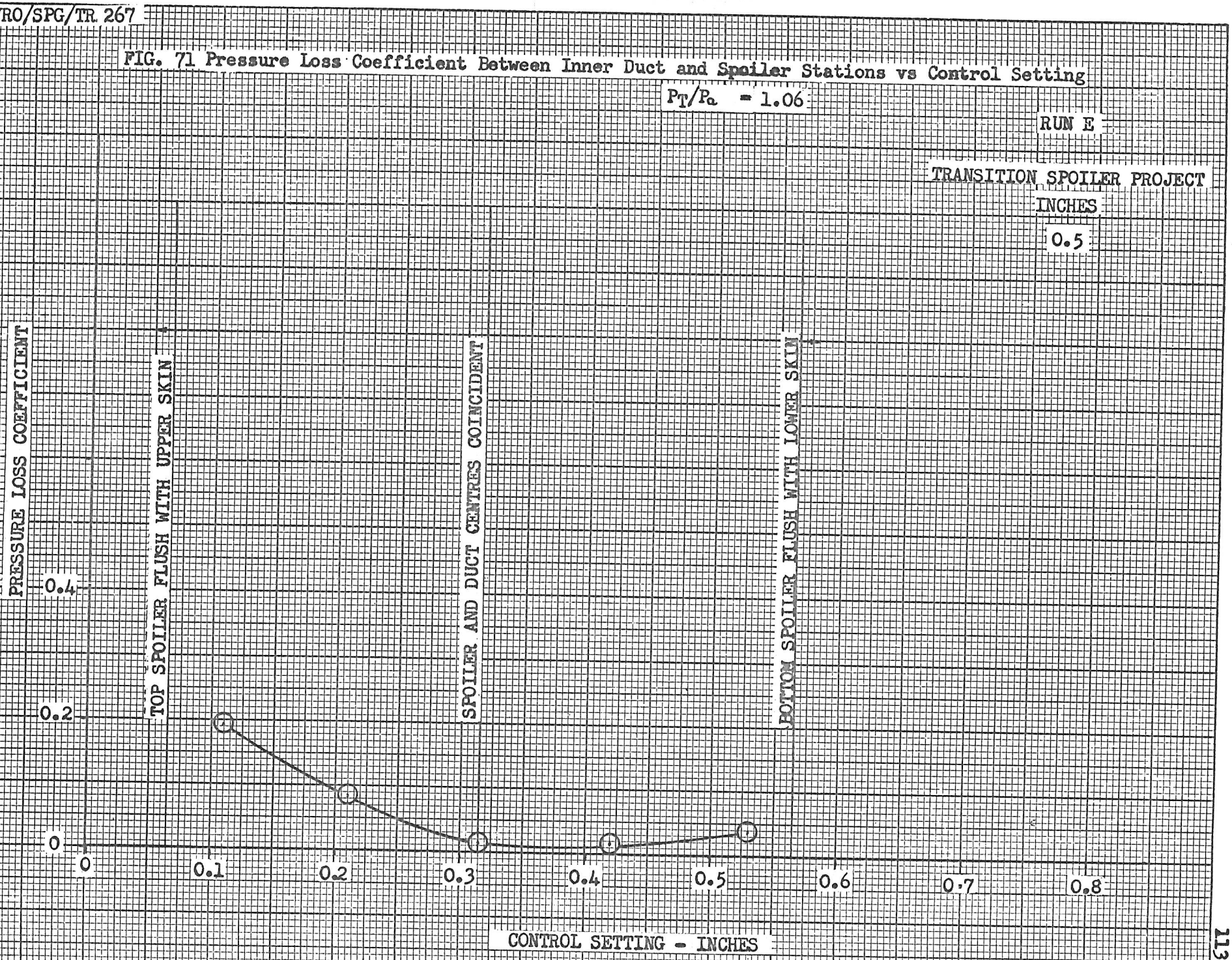

SECRET

SECRET

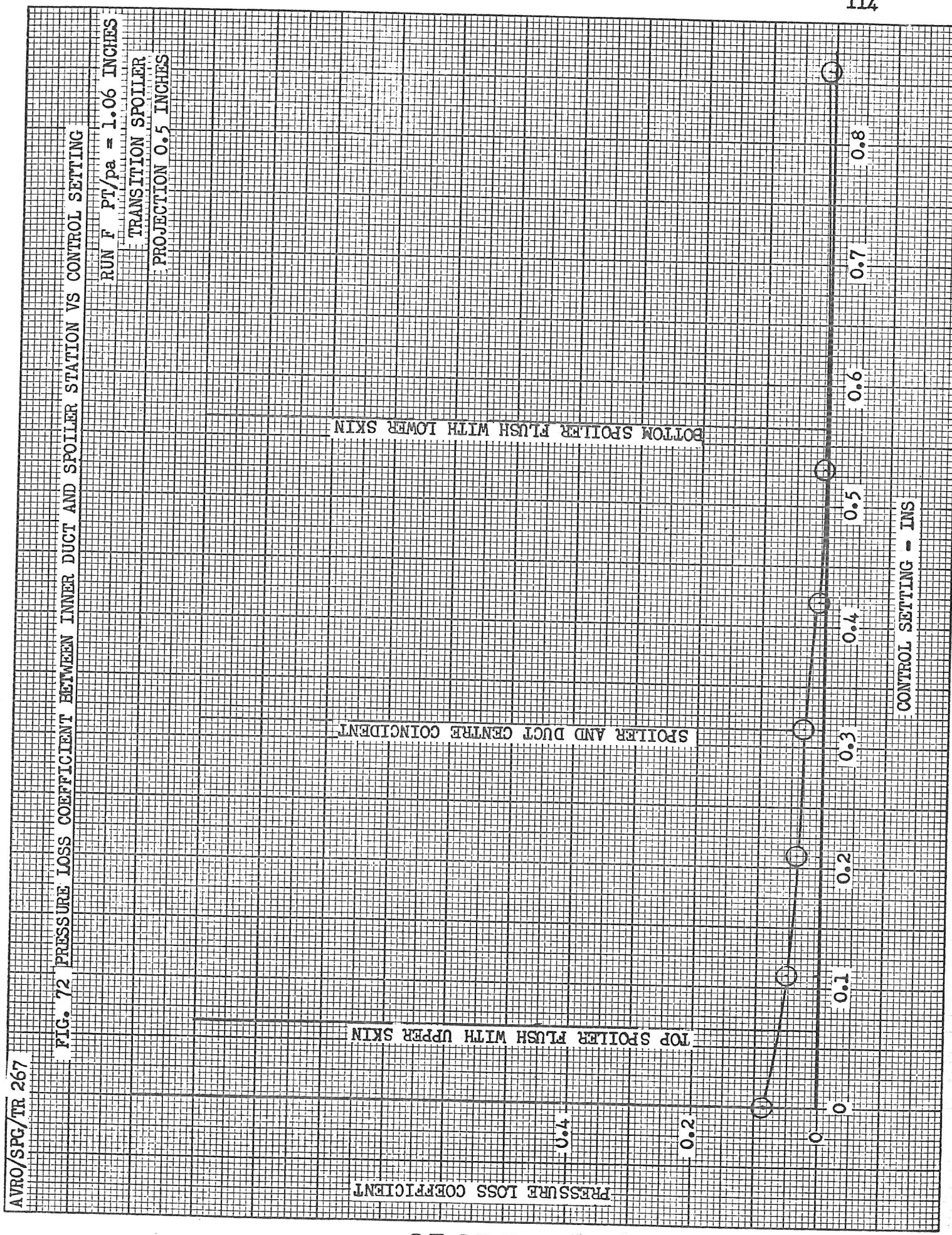
AVRO/SPG/TR 267
FIG. 72 PRESSURE LOSS COEFFICIENT BETWEEN INNER DUCT AND SPOILER STATION VS CONTROL SETTING
RUN F PT/pa = 1.06 INCHES
TRANSITION SPOILER
PROJECTION 0.5 INCHES
BOTTOM SPOILER FLUSH WITH LOWER SKIN
SPOILER AND DUCT CENTRE COINCIDENT
TOP SPOILER FLUSH WITH UPPER SKIN
PRESSURE LOSS COEFFICIENT
0.4
0.2
0
0
0.1
0.2
0.3
0.4
0.5
0.6
0.7
0.8
CONTROL SETTING - INS

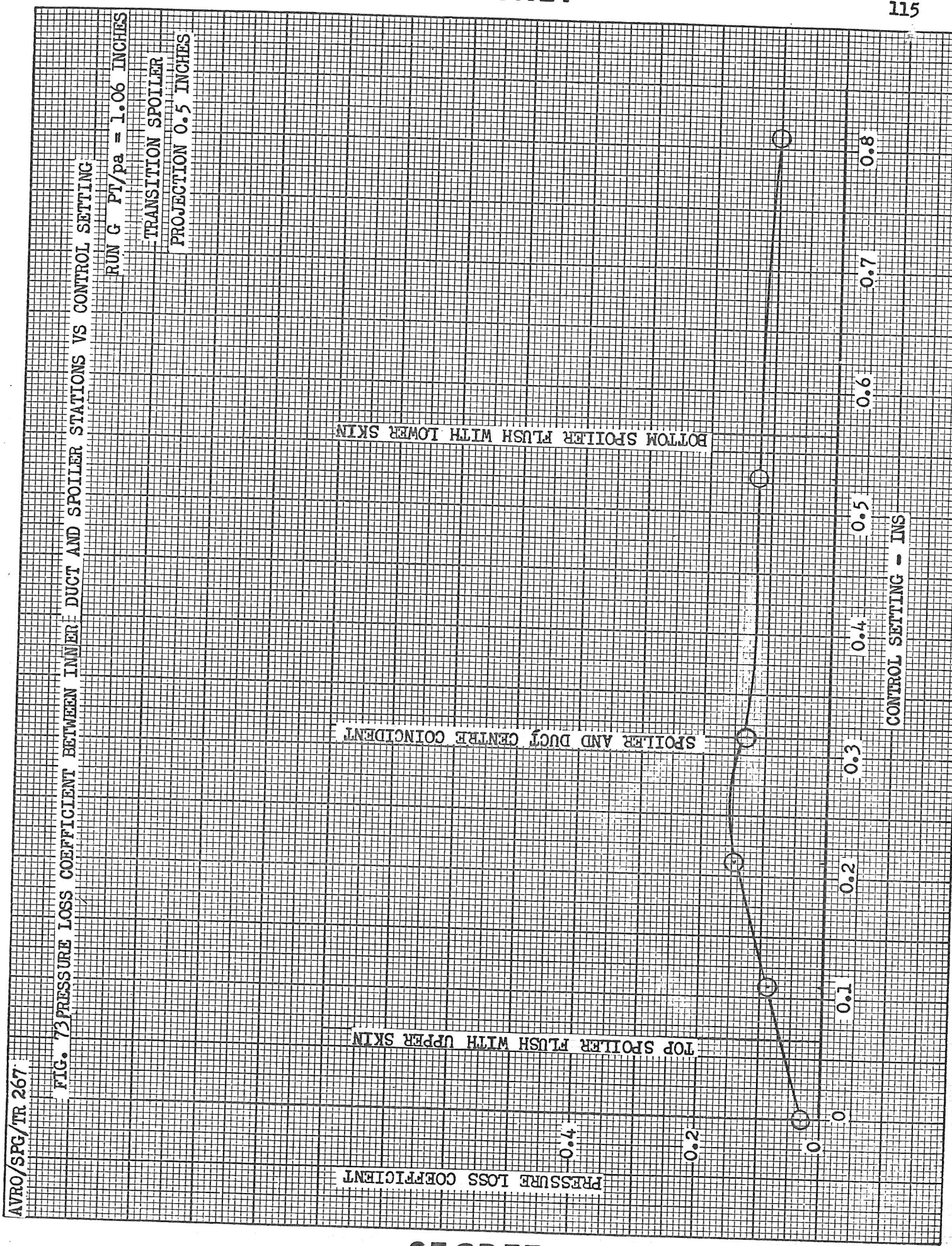
AVRO/SPG/TR 267
FIG. 73 PRESSURE LOSS COEFFICIENT BETWEEN INNER DUCT AND SPOILER STATIONS VS CONTROL SETTING
RUN G PT/pa = 1.06 INCHES
TRANSITION SPOILER
PROJECTION 0.5 INCHES
BOTTOM SPOILER FLUSH WITH LOWER SKIN
SPOILER AND DUCT CENTRE COINCIDENT
TOP SPOILER FLUSH WITH UPPER SKIN
PRESSURE LOSS COEFFICIENT
CONTROL SETTING - INS
0.4
0.2
0
0.1
0.2
0.3
0.4
0.5
0.6
0.7
0.8

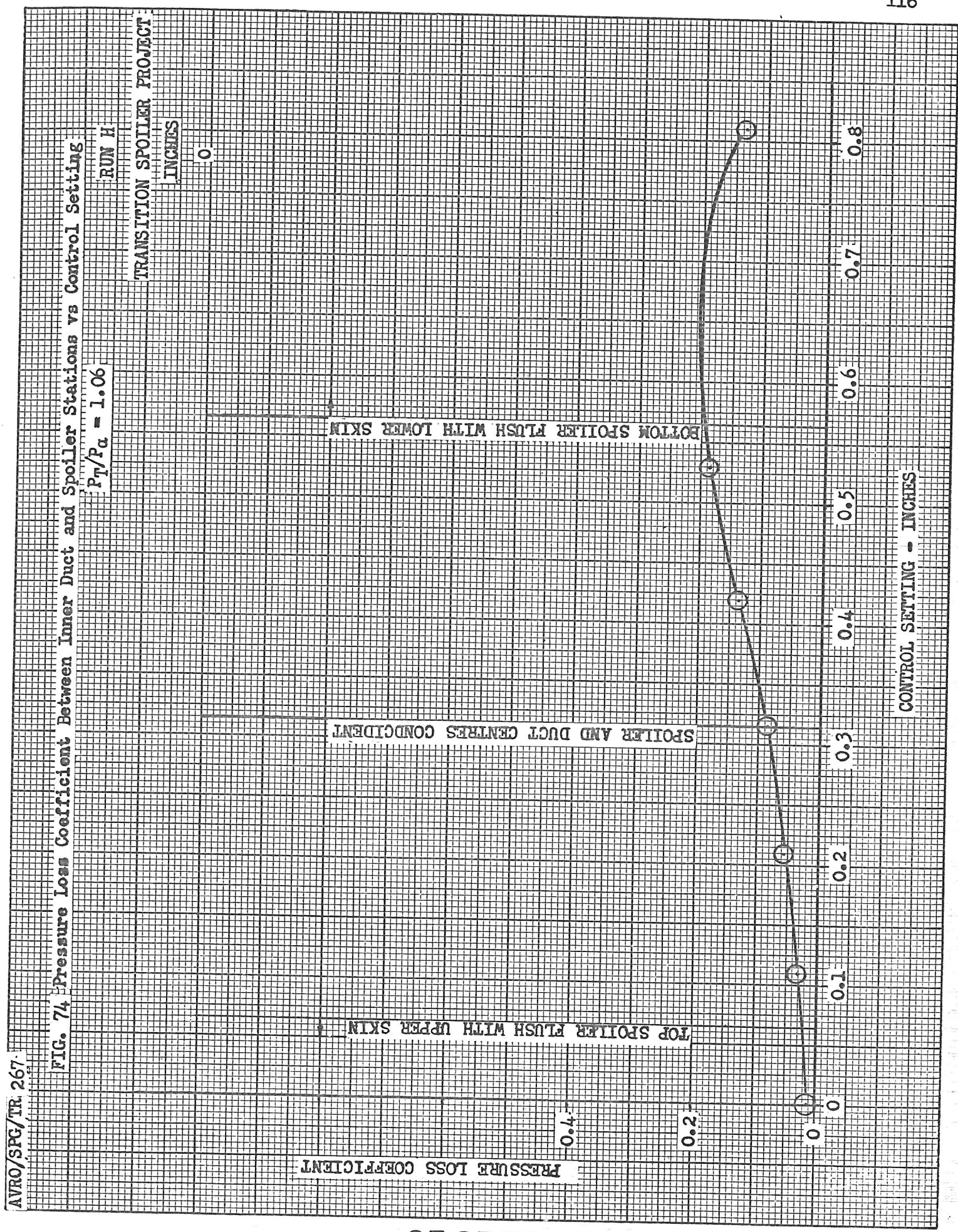
AVRO/SPG/TR 267
FIG. 74 Pressure Loss Coefficient Between Inner Duct and Spoiler Stations vs Control Setting
P_T/P_a = 1.06
RUN H
TRANSITION SPOILER PROJECT
INCHES
0
BOTTOM SPOILER FLUSH WITH LOWER SKIN
SPOILER AND DUCT CENTRES CONCIDENT
TOP SPOILER FLUSH WITH UPPER SKIN
PRESSURE LOSS COEFFICIENT
0.4
0.2
0
0.1
0.2
0.3
0.4
0.5
0.6
0.7
0.8
CONTROL SETTING - INCHES

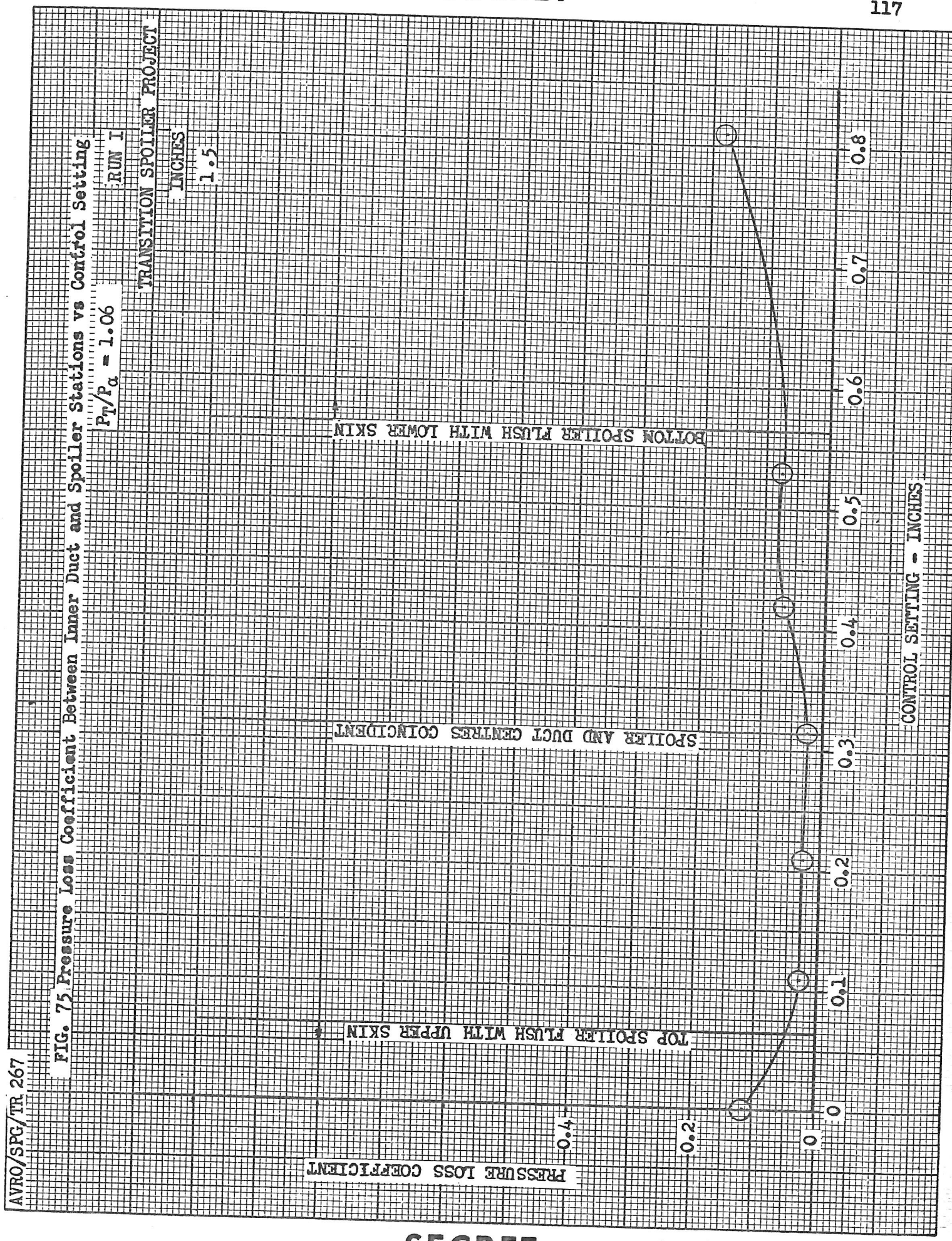

AVRO/SPG/TR 267

FIG. 75 Pressure Loss Coefficient Between Inner Duct and Spoiler Stations vs Control Setting

RUN I

$P_T/P_\alpha = 1.06$

TRANSITION SPOILER PROJECT

INCHES

1.5

AVRO/SPG/TR 267

FIG. 76 Pressure Loss Coefficient Between Inner Duct and Spoiler Stations vs Control Setting

AVRO/SPG/TR 267

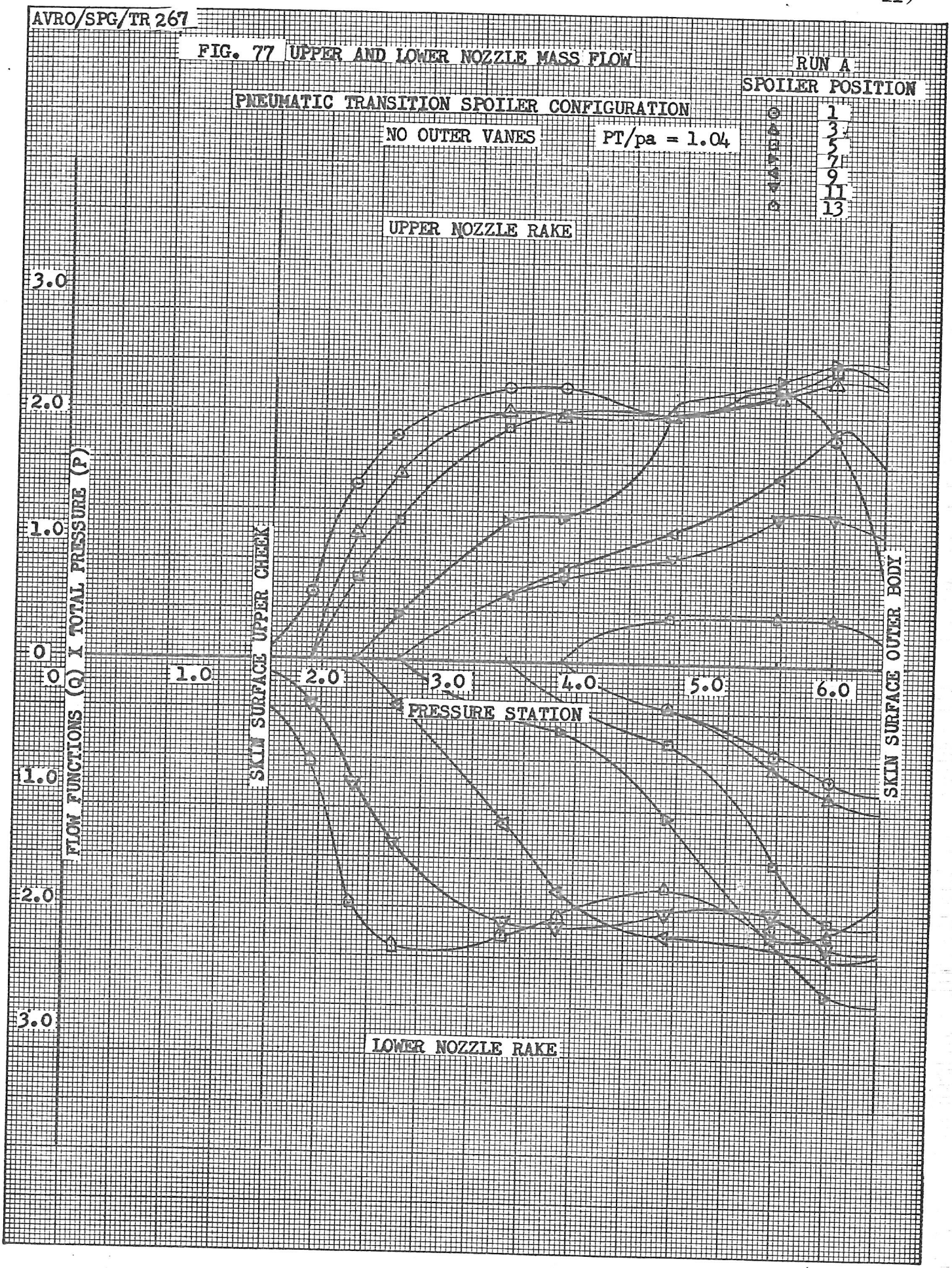

AVRO/SPG/TR 267

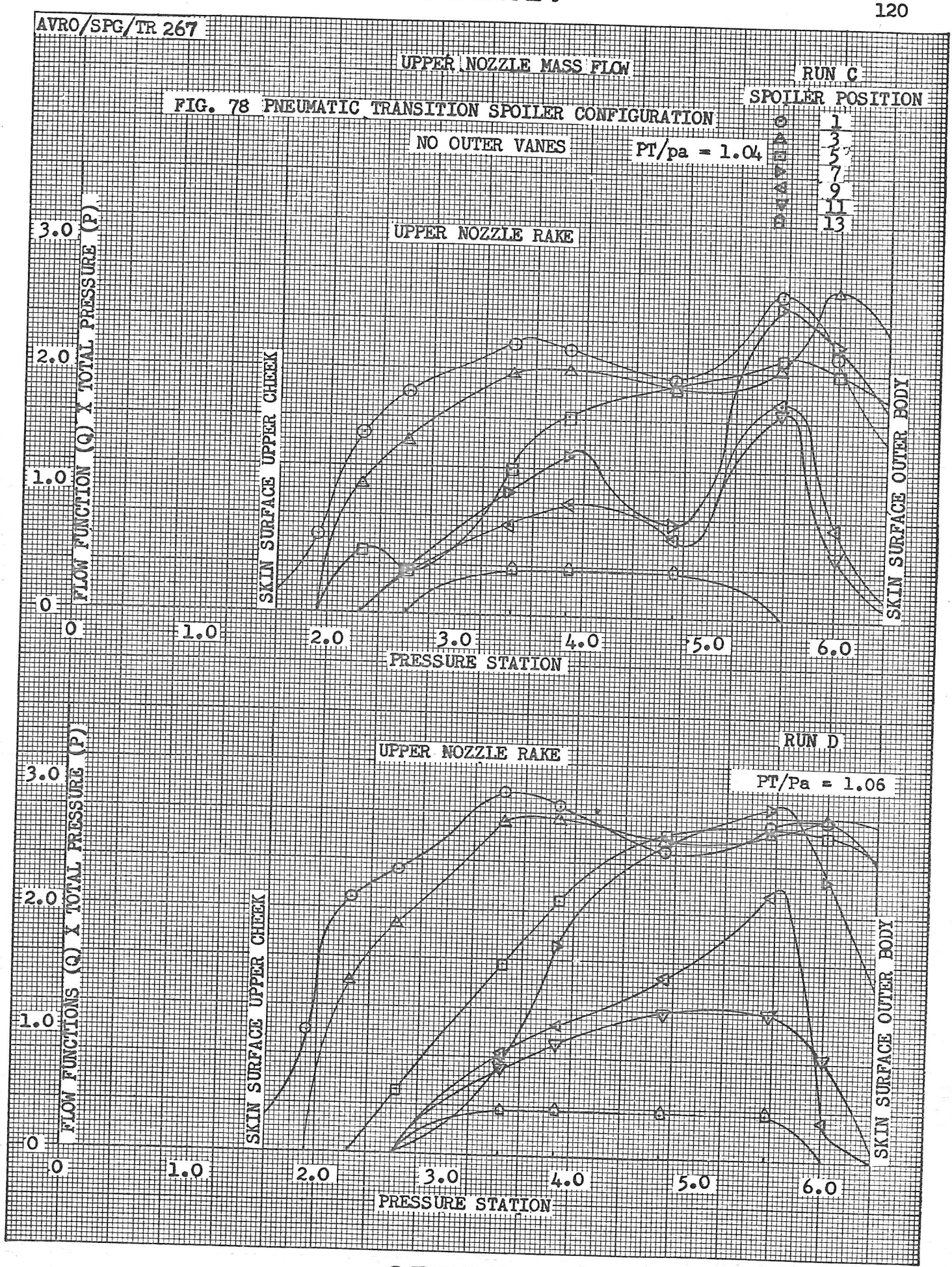

FIG. 78 PNEUMATIC TRANSITION SPOILER CONFIGURATION

AVRO/SPG/TR 267

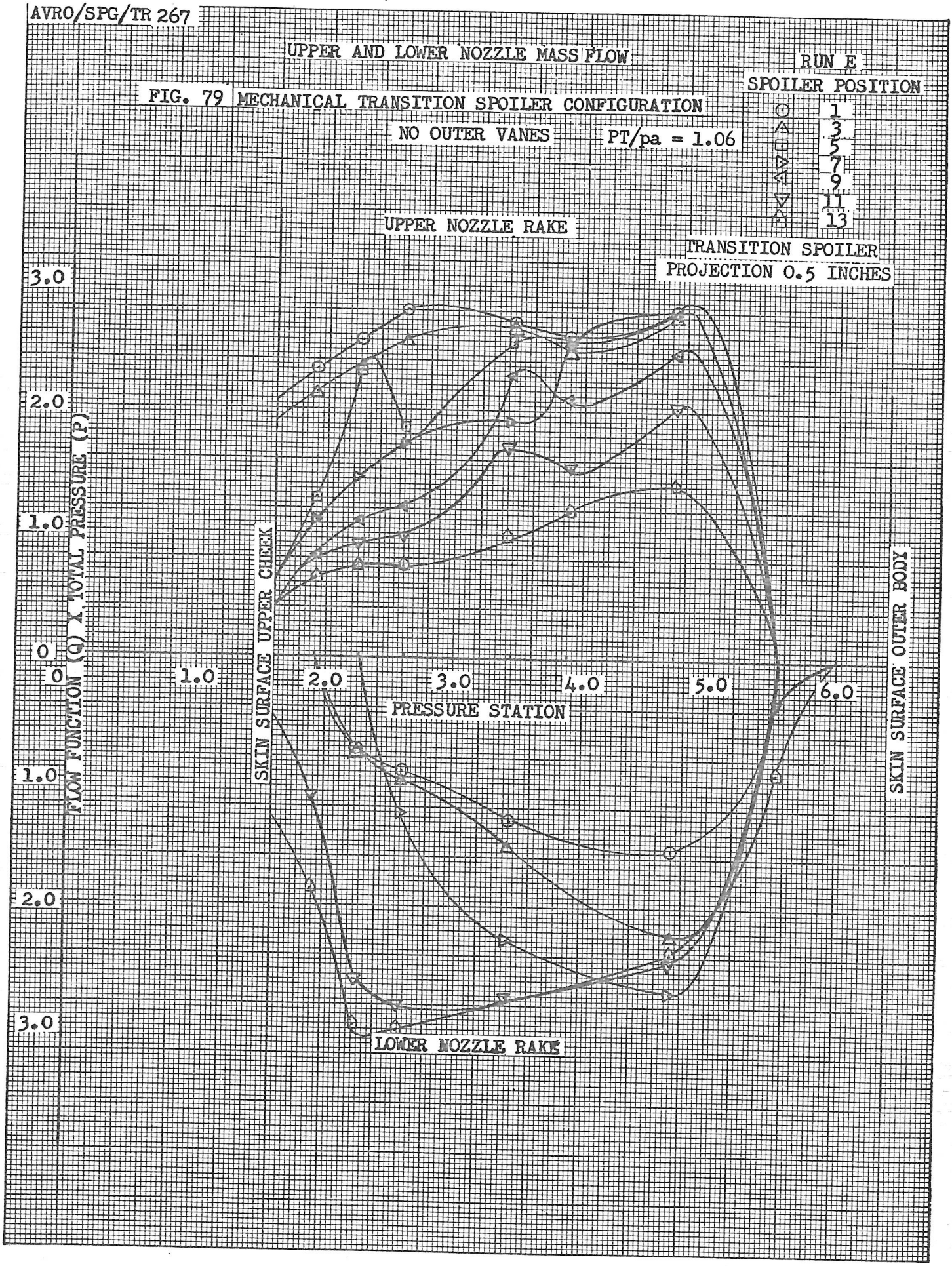

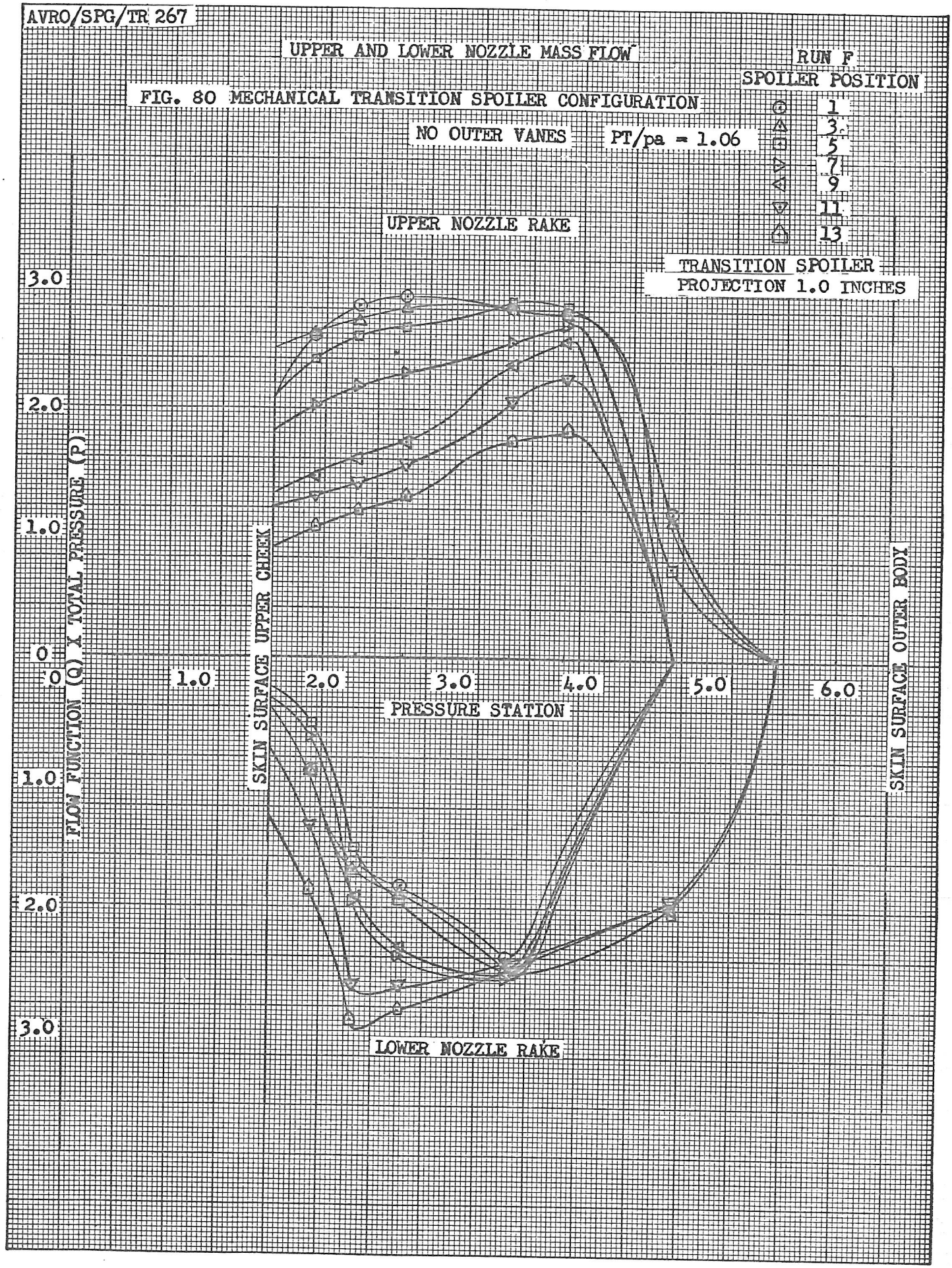
AVRO/SPG/TR 267
UPPER AND LOWER NOZZLE MASS FLOW
RUN F
SPOILER POSITION
1
3
5
7
9
11
13
FIG. 80 MECHANICAL TRANSITION SPOILER CONFIGURATION
NO OUTER VANES
PT/pa = 1.06
UPPER NOZZLE RAKE
TRANSITION SPOILER
PROJECTION 1.0 INCHES
3.0
2.0
1.0
0
0
1.0
2.0
3.0
4.0
5.0
6.0
PRESSURE STATION
FLOW FUNCTION (Q) X TOTAL PRESSURE (P)
SKIN SURFACE UPPER CHEEK
SKIN SURFACE OUTER BODY
LOWER NOZZLE RAKE

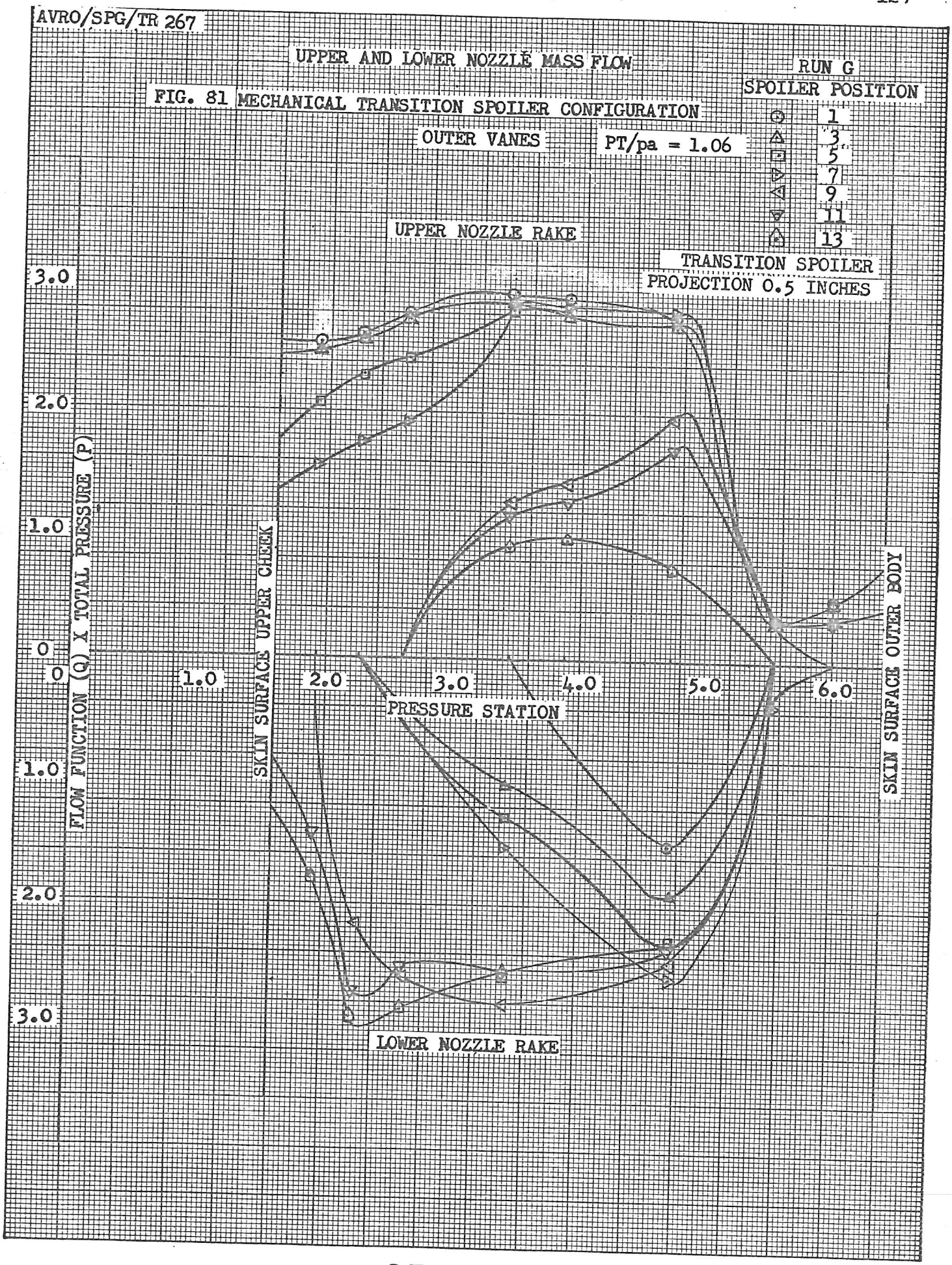
AVRO/SPG/TR 267
UPPER AND LOWER NOZZLE MASS FLOW
FIG. 81 MECHANICAL TRANSITION SPOILER CONFIGURATION
OUTER VANES
PT/pa = 1.06
RUN G
SPOILER POSITION
1
3
5
7
9
11
13
UPPER NOZZLE RAKE
TRANSITION SPOILER
PROJECTION 0.5 INCHES
3.0
2.0
1.0
0
0
1.0
2.0
3.0
1.0
2.0
3.0
FLOW FUNCTION (Q) X TOTAL PRESSURE (P)
SKIN SURFACE UPPER CHECK
1.0
2.0
3.0
4.0
5.0
6.0
PRESSURE STATION
SKIN SURFACE OUTER BODY
LOWER NOZZLE RAKE

AVRO/SPG/TR 267

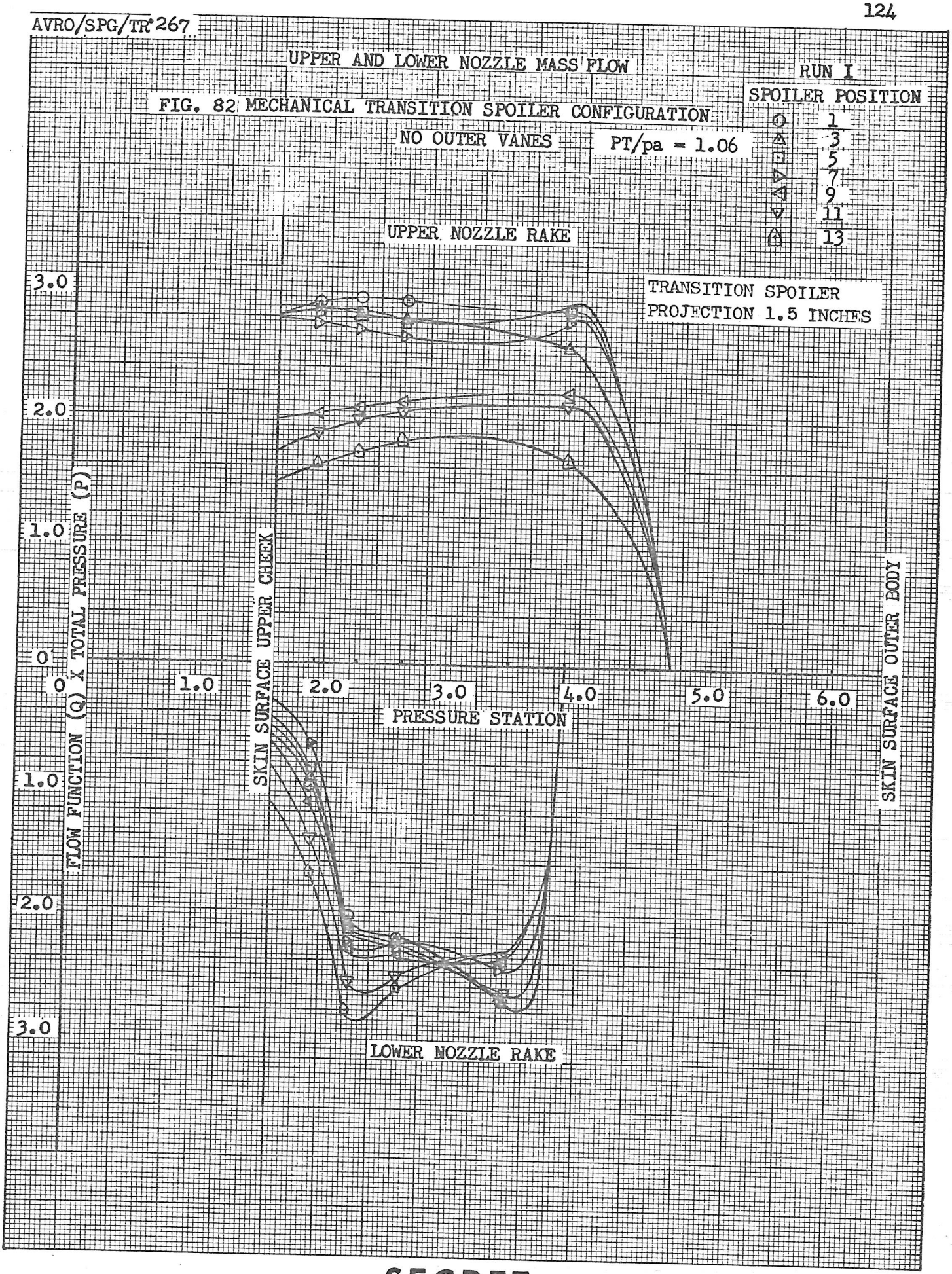

AVRO/SPG/TR 267

FIG. 83 UPPER AND LOWER NOZZLE MASS FLOW

RUN K

SPOILER POSITION

○	1
△	2
□	4
▷	6
◁	8
▽	10
⬠	12

OUTER VANES

PT/pa = 1.04

TRANSITION SPOILER PROJECTION 0.5 INCHES

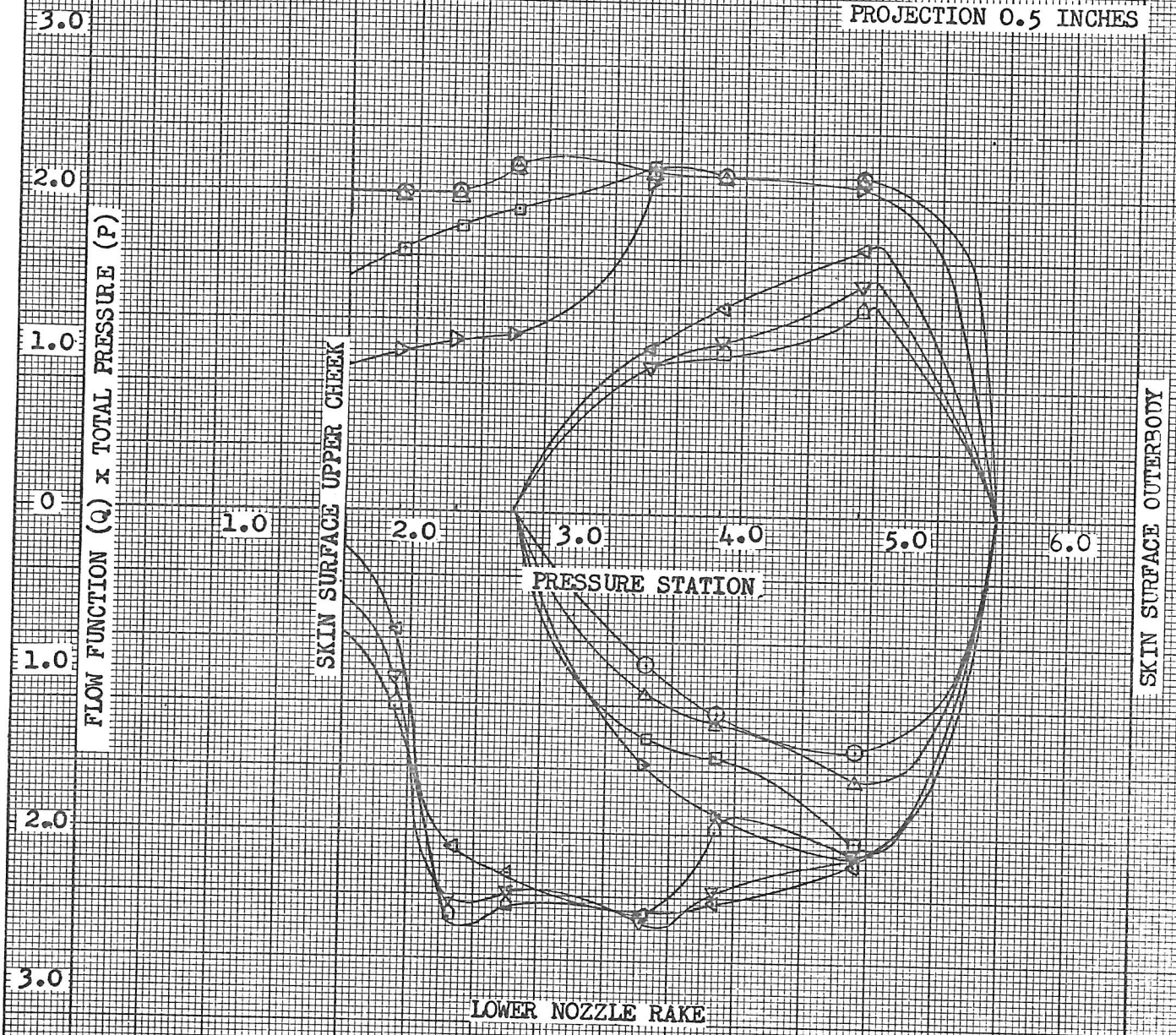

AVRO/SPG/TR 267

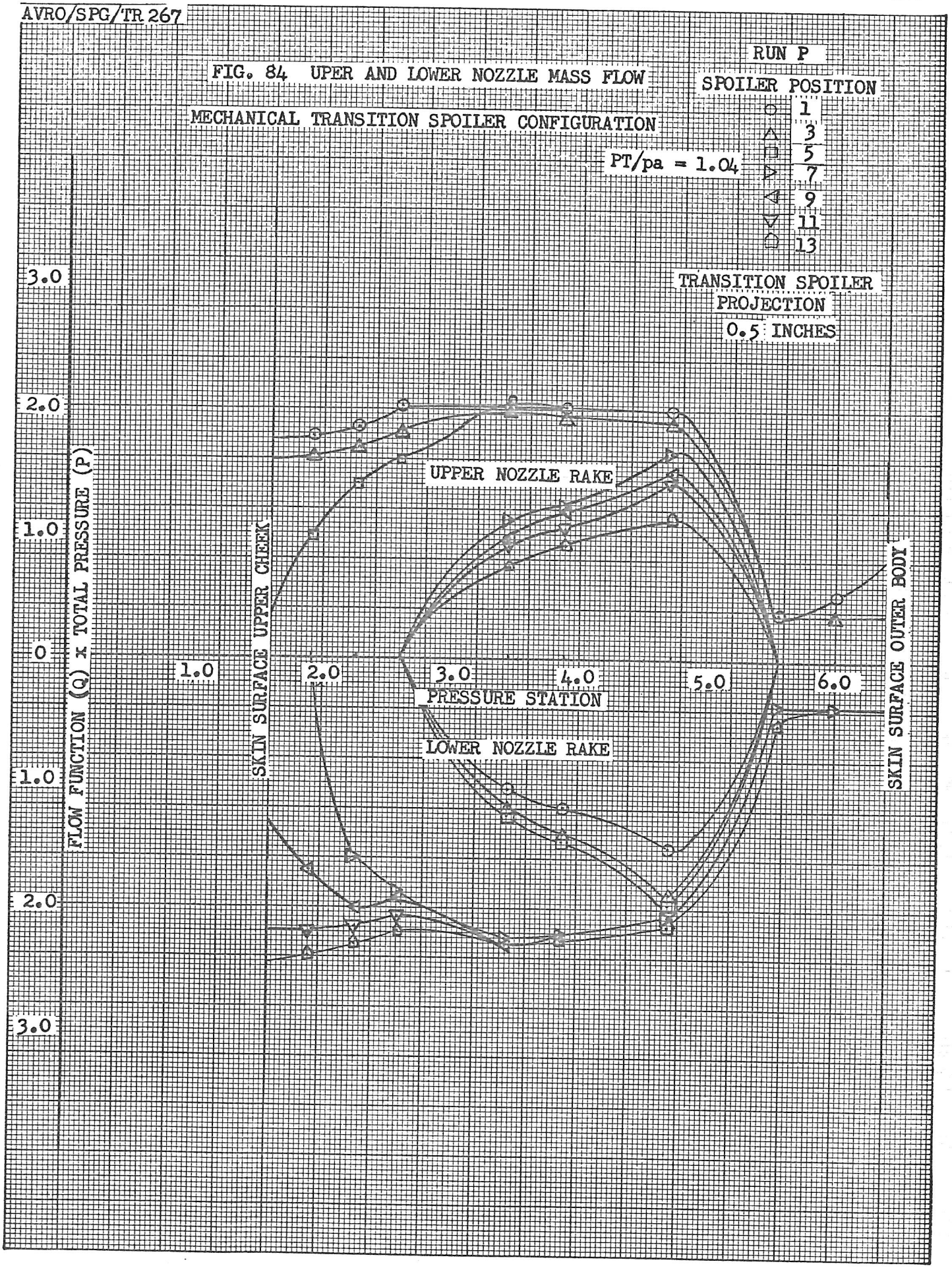

AVRO/SPG/TR 267

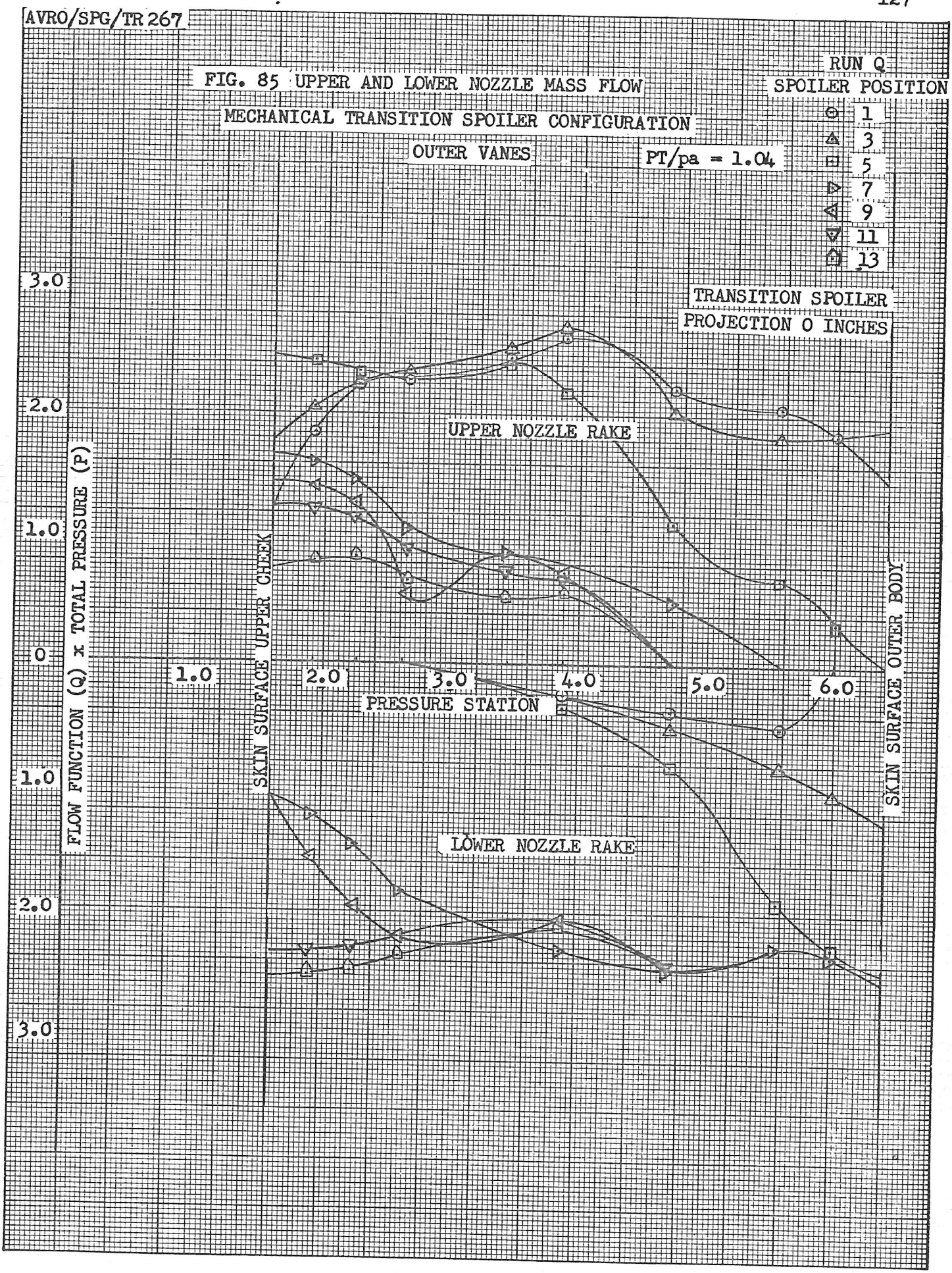

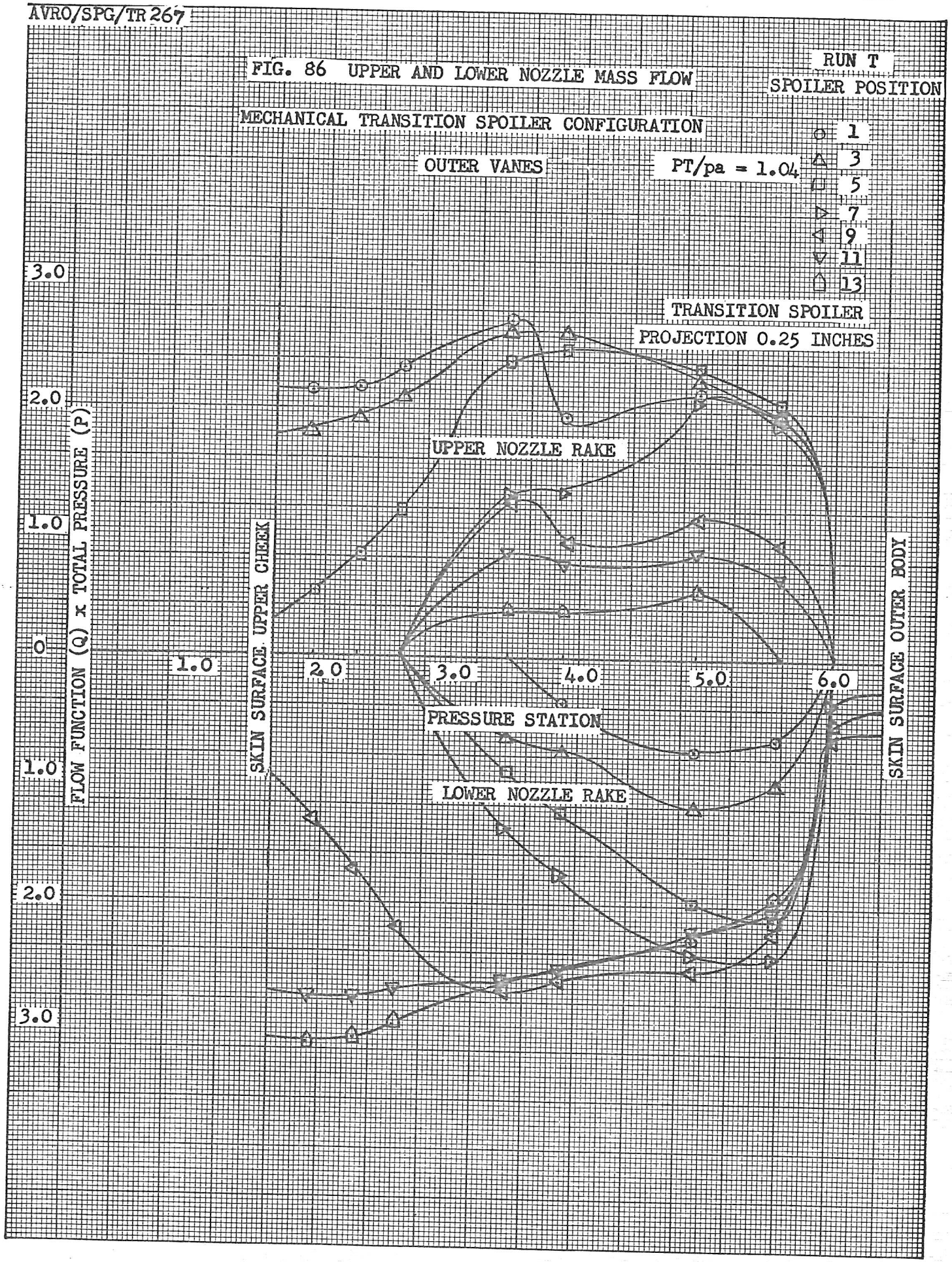
FIG. 86 UPPER AND LOWER NOZZLE MASS FLOW
RUN T
SPOILER POSITION
MECHANICAL TRANSITION SPOILER CONFIGURATION
OUTER VANES
PT/pa = 1.04
1
3
5
7
9
11
13
TRANSITION SPOILER
PROJECTION 0.25 INCHES
UPPER NOZZLE RAKE
LOWER NOZZLE RAKE
PRESSURE STATION
FLOW FUNCTION (Q) x TOTAL PRESSURE (P)
3.0
2.0
1.0
0
1.0
2.0
3.0
SKIN SURFACE UPPER CHEEK
SKIN SURFACE OUTER BODY
2.0
3.0
4.0
5.0
6.0

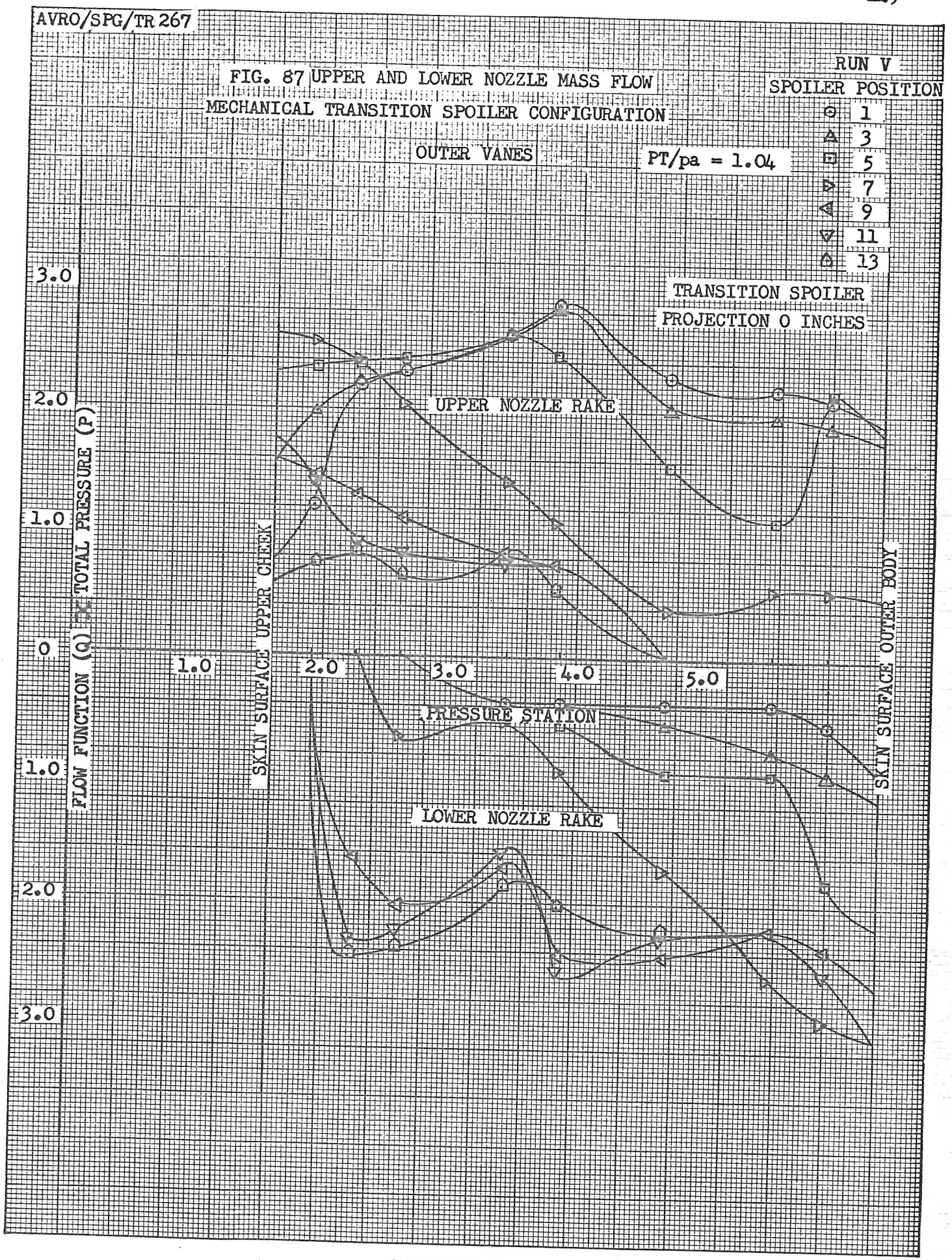
AVRO/SPG/TR 267
FIG. 87 UPPER AND LOWER NOZZLE MASS FLOW
MECHANICAL TRANSITION SPOILER CONFIGURATION
OUTER VANES
PT/pa = 1.04
RUN V
SPOILER POSITION
1
3
5
7
9
11
13
TRANSITION SPOILER
PROJECTION 0 INCHES
UPPER NOZZLE RAKE
LOWER NOZZLE RAKE
FLOW FUNCTION (Q) TOTAL PRESSURE (P)
3.0
2.0
1.0
0
1.0
2.0
3.0
SKIN SURFACE UPPER CHEEK
SKIN SURFACE OUTER BODY
1.0
2.0
3.0
4.0
5.0
PRESSURE STATION

AVRO/SPG/TR 267

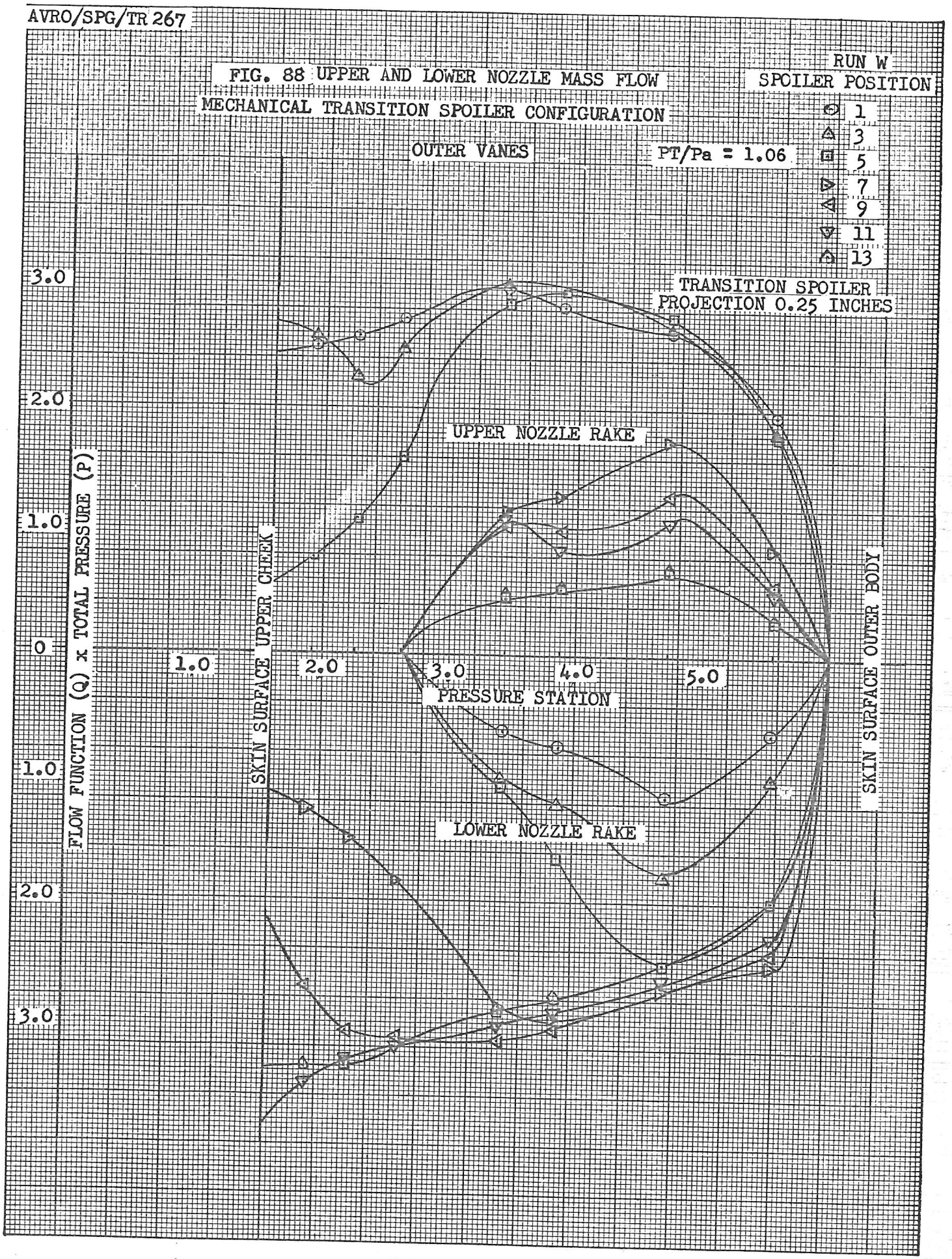

AVRO/SPG/TR 267

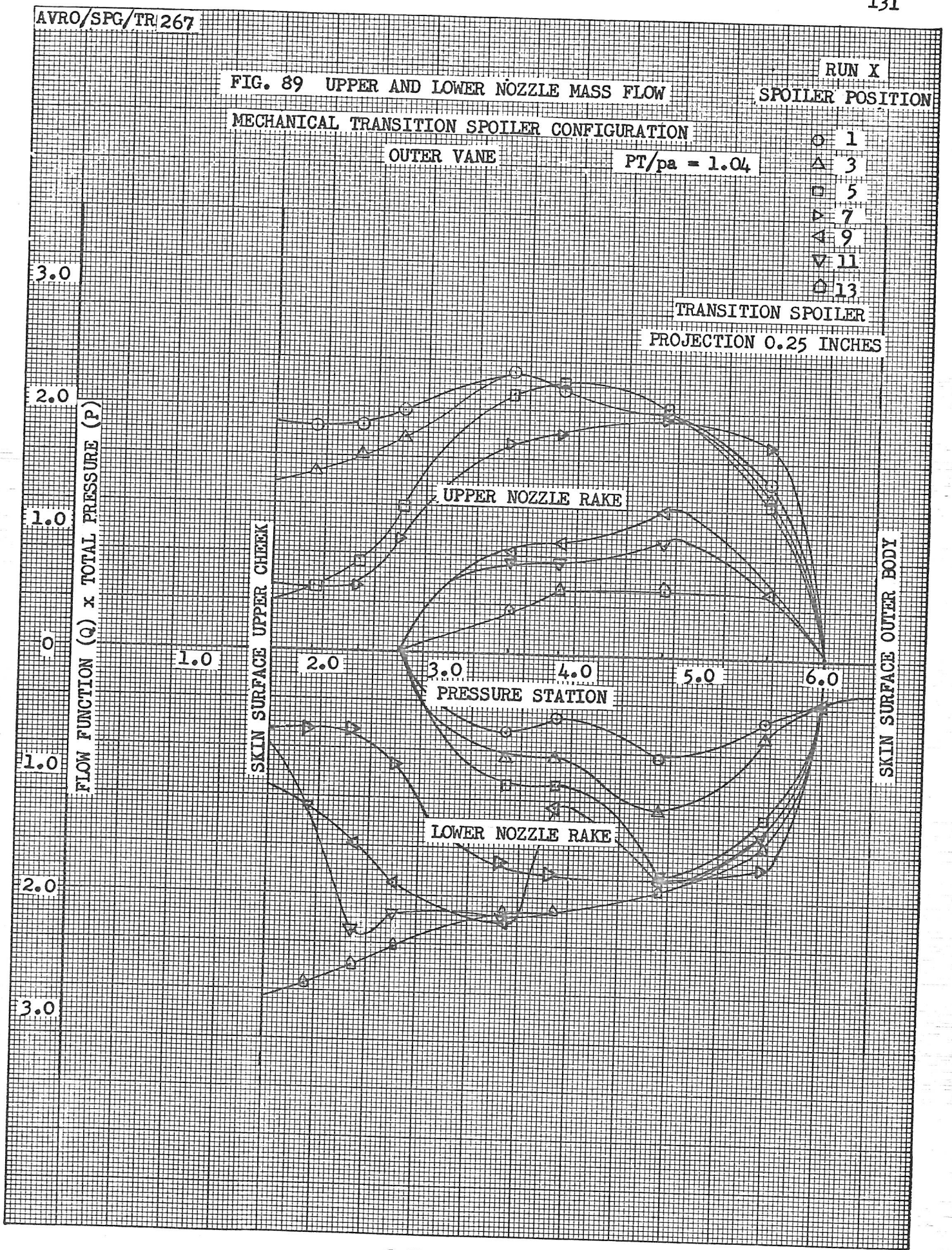

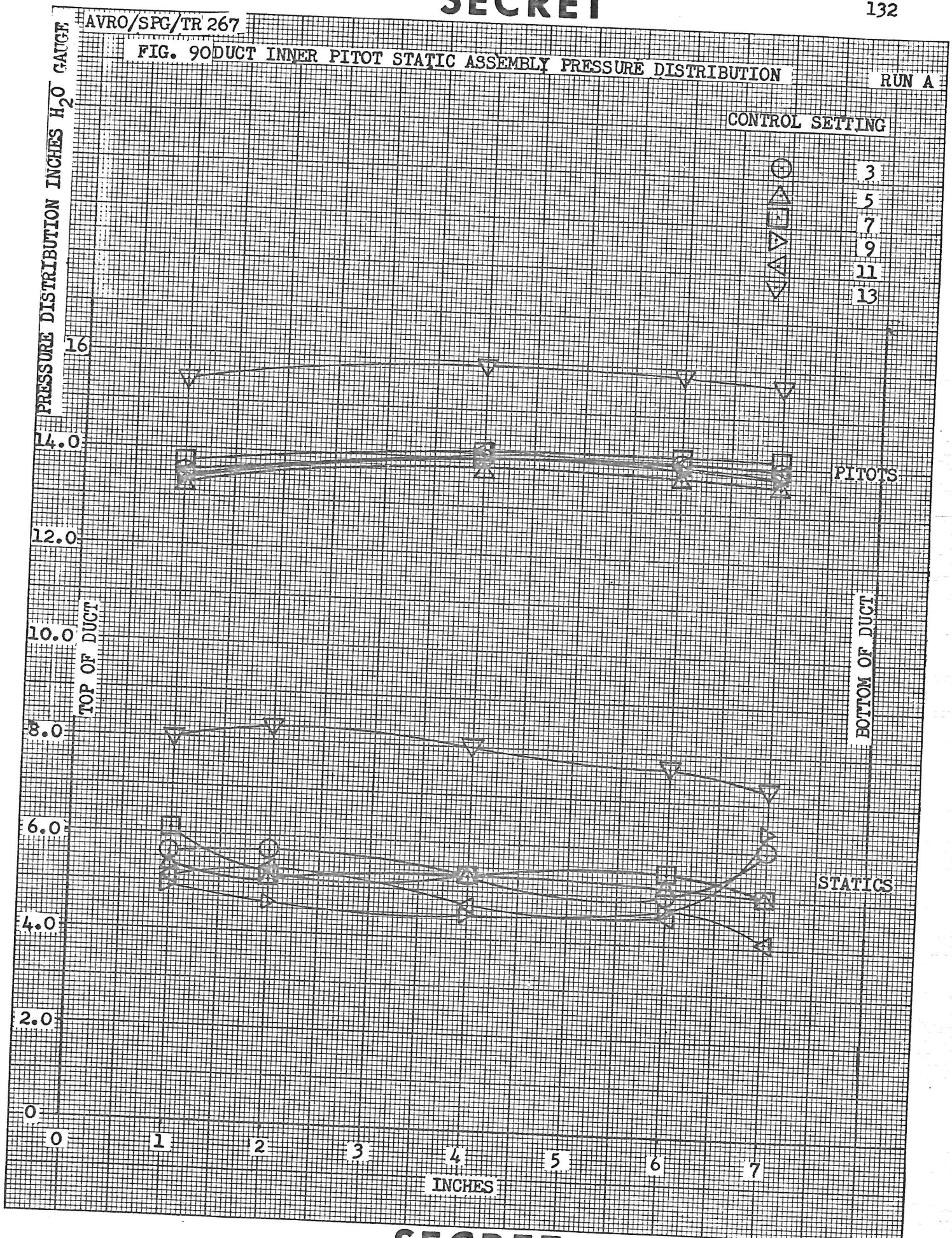
AVRO/SPG/TR 267
FIG. 90 DUCT INNER PITOT STATIC ASSEMBLY PRESSURE DISTRIBUTION
RUN A
CONTROL SETTING
3
5
7
9
11
13
PRESSURE DISTRIBUTION INCHES H_2O GAUGE
16
14.0
12.0
10.0
8.0
6.0
4.0
2.0
0
PITOTS
STATICS
TOP OF DUCT
BOTTOM OF DUCT
0
1
2
3
4
5
6
7
INCHES

AVRO/SPG/TR 267

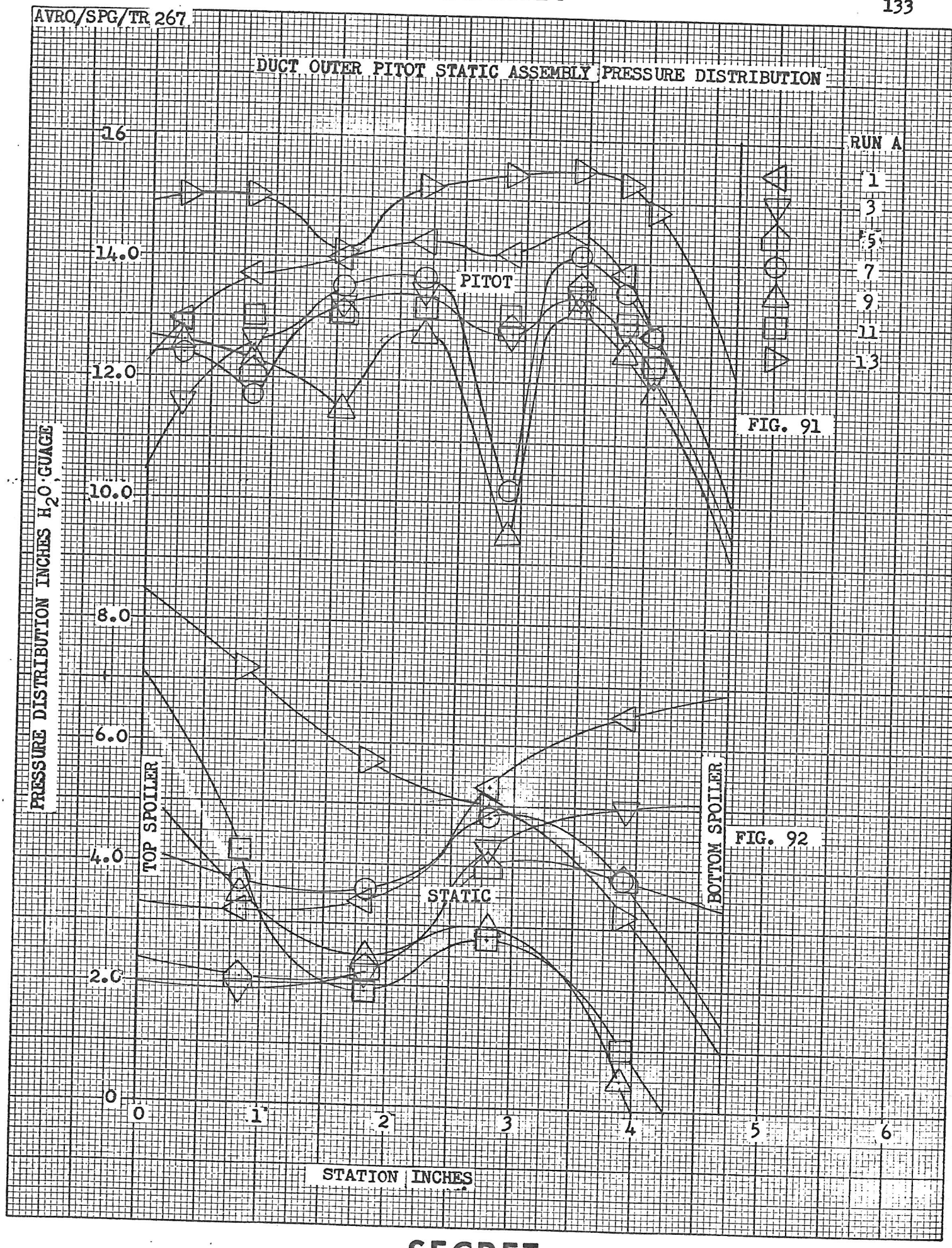

AVRO/SPG/TR 267

FIG. 93 FULL SCALE 20° SEGMENT TESTS

RUN X

UPPER NOZZLE TOTAL PRESSURE DISTRIBUTION

SPOILER POSITION

FULLY DOWN -.238 BELOW CHEEK

PROJECTING BELOW BY - 0.050

SPOILER FLUSH

PROJECTING ABOVE BY - 0.050

FLOW DETACHES AT - 0.080 ABOVE

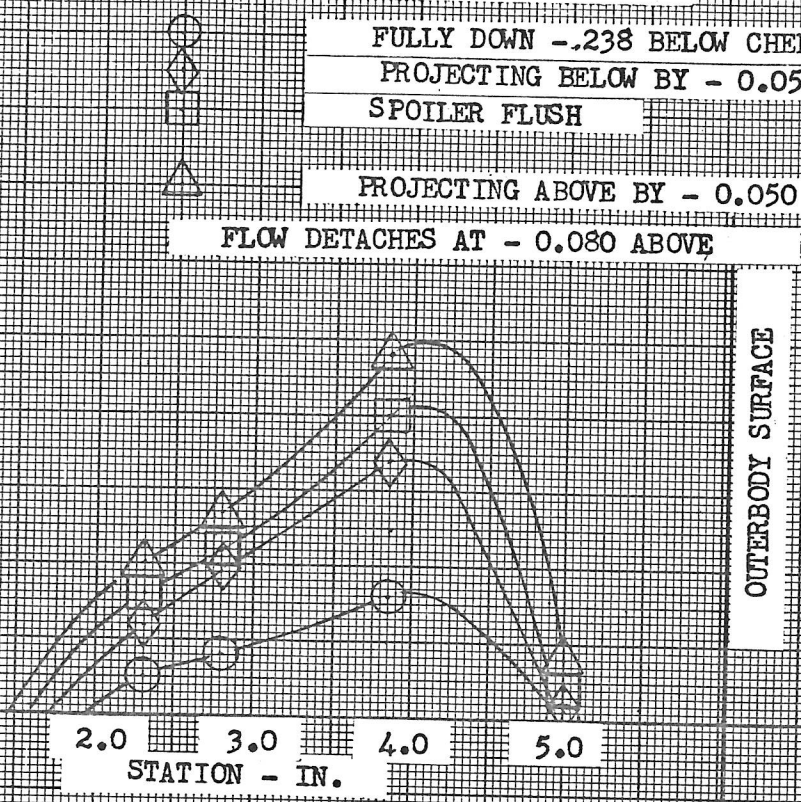

APPENDIX 'C'

(EQUATIONS DERIVATIONS AND SAMPLE CALCULATIONS)

1. Thrust Vector

The section thrust vector can be obtained by performing a graphical integration of surface pressures and momentum flows on lines parallel and normal to the aircraft longitudinal axis. Three different control surfaces were available. A Schematic of each is given below.

4290-802-1

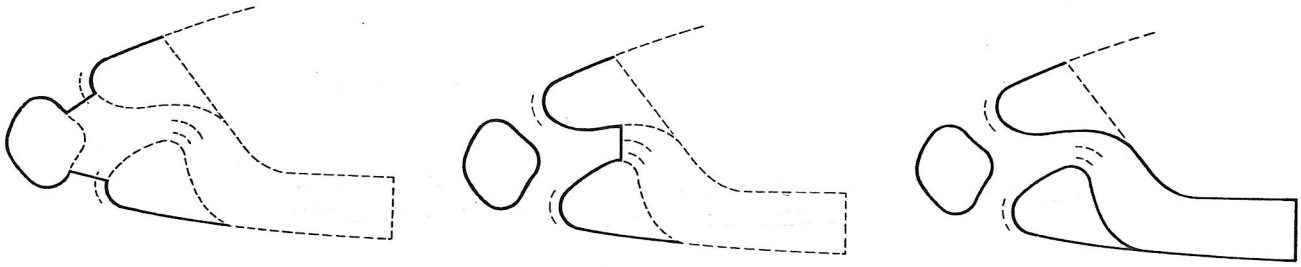

(i) (ii) (iii)

CONTROL SURFACES FOR THRUST EVALUATION

General mathematical expressions for force integration are of the form

$$f_Z = \int_0^R p\,dR + (mV)_Z$$

and

$$f_R = \int_0^Z p\,dZ - (mV)_R$$

For control surfaces (iii) and (ii) $(mV)_Z$ is about zero. For control surface (i) the momentum flux in both directions can be appreciable whereas the surface pressure contributions are usually negligible.

The total section force is calculated as

$$\bar{f} = (f_R^2 + f_Z^2)^{\frac{1}{2}}$$

The angular position of the thrust vector in relation to the longitudinal axis is

$$\tau = \arctan Z/R$$

1. Thrust Vector (Continued)

Gross thrust F for the test segment may be obtained by multiplying the section force by the length of the arc passing through the section centre at pressure and subtending the test segment angle (20°). Employing graphical integration location of the centre of pressure is a tedious process. However movements as so slight that evaluation by inspection is sufficiently accurate for present purposes. Normally the centre of pressure falls at a radial station about midway between upper and lower nozzle centre lines.

2. Section Control Force

Using control surface (iii) only surface pressure integration on the upper and lower cheeks and outerbody was required. The momentum contribution was negligible. Thus:

$$f_Z = \int_0^R p \, dR$$

Using control surface (i) the flow direction was ascertained using the pictures and all relevant pressure data. The momentum flux was calculated for the upper and lower nozzles, and the normal components were evaluated. Integration of exit surface pressures along the longitudinal axis was performed.

The total control force was obtained by summing these parts.

3. Total Mass Flow

The mass flow was calculated as laid out in Ref. 6 for an orifice plate using both types of pressure tappings.

The equation is given below:

$$W = 359.1 \, C \, Z \, d^2 \, E \, (h\rho_1)^{\frac{1}{2}} \, N$$

values of the constants are tabulated as follows:

Orifice Diameter	d (in)	12.400 ± 0.005
Pipe Diameter	D (in)	16.000 ± 0.010
Velocity of Approach Factor $1/(1-m^2)^{\frac{1}{2}}$	E	1.2507
Discharge Coefficient with corner taps	C	0.5925
Discharge Coefficient with D & D/2 Taps.	C	0.6060

3. Total Mass Flow (Continued)

Both Reynold's number and diameter correction factors were unity. The resulting equations for the respective taps are:

Corner Taps

$$W\sqrt{T} = (18.682)\ \varepsilon\ (hp_1)^{\frac{1}{2}N}$$

D & D/2 Taps

$$W\sqrt{T} = (19.107)\ \varepsilon\ (hp_1)^{\frac{1}{2}N}$$

From B.S. 1042.

$$\varepsilon = 0.6 - 0.4\ \frac{p2}{p1} \quad \text{for } 0.8 < \frac{p2}{P1} < 1.0$$

The moisture correction factor was not generally calculated and was taken as unity.

4. Thrust Efficiency

Thrust efficiency was defined as the ratio of the integrated thrust F to the ideal Fi.

The ideal thrust was derived from two dimensional compressible flow theory for a convergent nozzle. It was based on measured mass flow and ambient to nozzle box pressure ratio. The equation is:

$$Fi = W\sqrt{T}\ \left[\frac{2\gamma R}{\gamma-1}\right]^{\frac{1}{2}}\left[1 - \left(\frac{p_a}{P_T}\right)^{\frac{(\gamma-1)}{\gamma}}\right]^{\frac{1}{2}}.$$

Using NACA Standards in Ref. 7 $\gamma = 1.4$

$$Fi = W\sqrt{T}\ (4.571)\ \left[1 - \left(\frac{p_a}{PT}\right)^{1/3.5}\right]^{\frac{1}{2}}$$

P_T was calculated as an arithmetic average of the inner duct total pressure distribution (at inlet to model).

5. Pressure Coefficient

The duct pressure loss was defined as the loss between the average upstream duct total pressure (at inlet to model) and the total pressure at the spoiler station. Arithmetic averages at both stations were employed.

The pressure loss coefficient was calculated as the ratio of the pressure loss to the average upstream duct dynamic pressure.

5. Pressure Coefficient (Continued)

Thus:

$$\frac{\triangle P}{q} = \frac{PT - Ps}{PT - pT}$$

6. Effective Exhaust Area and Discharge Coefficient

The effective exhaust area was defined as the nozzle area required to pass the measured mass flow at the ambient to duct total pressure ratio using two dimensional isentropic flow theory. The mathematical expression is given below.

$$Ae = \frac{W\sqrt{T}}{Q_N P_T}$$

P_T was calculated as before (see para. 4)

The discharge coefficient was taken as the ratio of the effective area to geometric area of the control spoiler gate.

7. Control and Differential Mass Flows

The control mass flows were obtained by performing graphical integration across the upper and lower nozzle plane. To be more explicit the pressure ratios pU/PU and pL/PL were evaluated at each station. The corresponding flow functions Q_U and Q_L were taken from flow tables. Each was multiplied by the appropriate total pressure and plotted against upper and lower nozzle stations.

Their differences resulted in the differential mass flows.

Their summ resulted in total mass flows, including local entrainment.

APPENDIX 'D'

Instrument and Rig Calibrations

The following calibrations were carried out in preparation for the test program:

1. Mass flow.
2. Yawmeter
3. Control spoiler

1.0 Mass Flow Calibration

A preliminary run was conducted on the installation excluding the test specimen to check whether or not the ejector could provide the desired mass flow, and to check out the mass flow instrumentation. The test consisted of successive increments of primary mass flow with notation of corresponding total mass flow orifice plate pressures and temperatures. Data from both corner and D and D/2 taps was taken. The results are presented in Fig. 20. The corner tap data yield consistently higher mass flow figures in the order of 5%. These results appeared to be more reliable than the D and D/2 tap data since the latter instrumentation was not as carefully installed. The maximum measured mass flow was 36 lbs./sec. and the exhaust flow distribution was fairly uniform.

A calibration of primary mass flow vs. total mass flow with the test specimen included was obtained in a similar manner following completion of the main body of tests and is shown in Fig. 21.

2.0 Yawmeter Calibration

The 16 tube static rake assemblies shown in Fig. 13 were the subject of the yawmeter calibration. It was desireable that the static pressure distribution be accurately known at the upper and lower nozzle stations. Therefore static rakes were designed to be insensitive to yaw. Calibrations were concerned with the effect of yaw on static pressure measurement. The calibration consisted of noting the static pressures at each station of the yawmeter for various angular settings with freestream at Mach Numbers of 0.15 and 0.4. Both yawmeters were tested. A typical calibration is shown in Fig. 23. It will be observed that the effect of yawed flow on static pressure measurements is of negligible order. Hence correction to static pressure measurements was not necessary, particularly since the observed yaw angles during specimen tests were not appreciable.

3.0 Control Spoiler Calibration

The spoiler movement was sensed by linear motion potentiometers and recorded by ammeters. The calibration was concerned with relating spoiler movement to ammeter deflection. To obtain the required curve two dial indicator micrometer gauges were mounted at each end of the spoiler, and the readings on these and the respective ammeters were noted at successive spoiler positions. The complete travel was covered yielding the calibration curves, for the two sides, shown in Fig. 22. Small differences between the two curves can be observed, however these are in the order of surface irregularities and it was therefore considered satisfactory to use a mean. This approximation simplified setting of the spoiler positions during tests since both ammeters could then set to the same value on each occasion.

APPENDIX 'E'

STRUCTURAL INTEGRITY

Structural Integrity

No serious structural difficulties were encountered for the range of pressure ratios tested, in spite of the fact that the skin thickness was some 20% less than that employed for the aircraft. However, certain minor regions of weakness which could be remedied by relatively simple means were detected. The components affected and the relevant details are presented and discussed in the following paragraphs.

Upper and Lower Nozzle Guide Vanes

Near the end of Phase II tests after logging some 7 hours on the specimen, the upper and lower nozzle guide vanes worked themselves free of the binding posts and failed. Photographs of the respective failures may be found in Figs. 25 and 26. The top guide vane failure was slightly more advanced than the lower vane failure. The apparent sequence of events was as follows:

1. Pull through and shear through of the binding post screws near the vane leading edge accompanied by tearing commencing at the hole.

2. Fatigue and cracking of the vane leading edge at the instrumentation cut out station.

3. Tearing of the vane end fitting.

4. Final failure at the trailing edge of the cut out station and near binding post.

The failure was due to selection of binding post washers which were too small in diameter, and weakening of the guide vanes due to instrumentation cut outs. The latter is not characteristic of the aircraft where as the former has already been corrected by substitution of 3/4" O.D. washers.

Lower Duct Flanges

During Phase III tests fatigue type cracks were observed on the lower duct flanges. A sketch of the flange affected is given below

4300-802-1

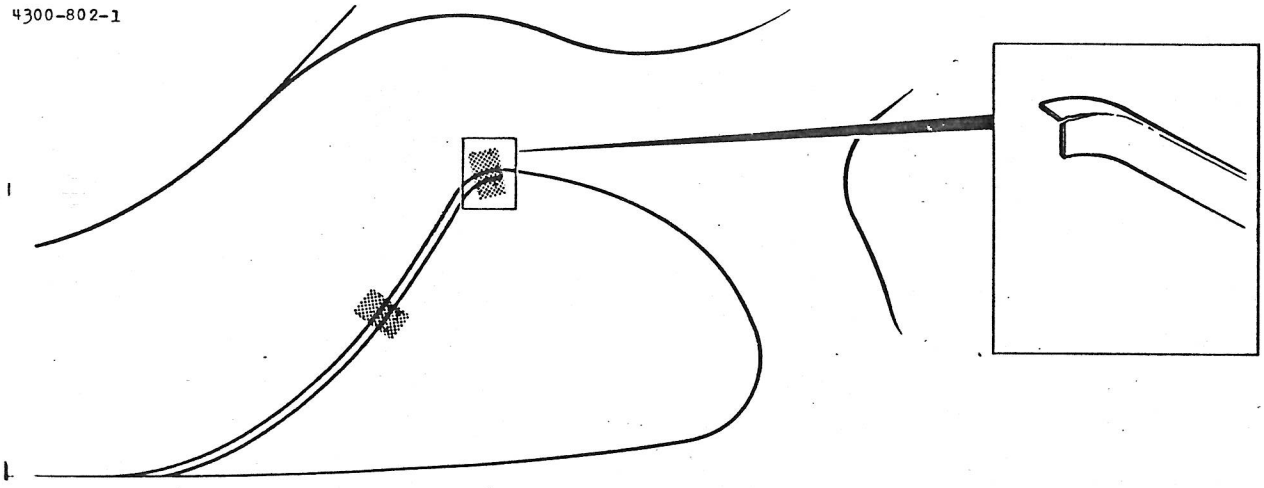

Section A.A.

Lower Duct Flanges (Continued)

The cracks occurred along the flange corners at the ends and middle as shown above. Two of the four flanges had end cracks. One had a long crack (approx. 2") at the middle. This one was replaced before further testing. Vibration of the skin and mild panting appeared to be the causes.

Heavier gauged metal for the flanges, introduction of appropriately spaced intercostals to reduce panting, and heavier gauged skin are some of the remedies considered. The thickness of the aircraft skin is already 20% greater than that on the test specimen.

Rivets

Occasional randomly located and missing rivets were detected. These had no doubt come free due to vibrations and faulty installation. With more care in manufacture they can for practical purposes be eliminated and therefore pose no real problems.